2000-05-05

Intramolecular Energy Transfer in Polychromophores that Utilize Peptide Bridging Groups

David C. Ferguson
Worcester Polytechnic Institute

INTRAMOLECULAR ENERGY TRANSFER IN POLYCHROMOPHORES THAT UTILIZE PEPTIDE BRIDGING GROUPS

By

David C. Ferguson

A Thesis submitted to the Faculty of the

WORCESTER POLYTECHNIC INSTITUTE

In partial fulfillment of the requirements for the

Degree of Master of Science

In

Chemistry

May 2, 2000

Approved:

Dr. W. Grant McGimpsey, Major Advisor

Dr. James P. Dittami, Department Head

Abstract

Efficient singlet-singlet (SSET) and triplet-triplet (TTET) energy transfer between fluorenyl and either phenylbenzoyl or naphthyl chromophores in enantiomerically pure dipeptides occur via through-space intramolecular dipole-induced dipole (Förster-SSET) and electron exchange (Dexter-TTET) mechanisms as demonstrated by, UV-visible absorption, fluorescence, phosphorescence and laser flash photolysis measurements.

Unprotected, optically pure 3-(2-fluorenyl)-L-alanine (**8, Fla**) and its C- and N-protected derivatives were synthesized using a modified Sorensen procedure, and were subsequently used for solution-phase synthesis of the dipeptides (**9, Bpa-Fla** and **10,Npa-Fla**) and solid-phase synthesis of a 15-residue peptide (**7**).

UV absorption spectra of the dipeptides indicate that the chromophores do not interact electronically in the ground state nor do their photophysical characteristics change when incorporated into the peptides. Dipeptide bichromophore fluorescence and phosphorescence results show efficient SSET ($k_{SSET} > 10^9\ s^{-1}$) and TTET ($k_{TTET} > 10^4\ s^{-1}$). Fluorescence and phosphorescence spectra produced by excitation at donor absorbance wavelengths show complete energy transfer in **9** and efficient energy transfer in **10**.

Donor-acceptor separation (transfer separation distance) was calculated from the spectral overlap of the donor fluorescence spectrum and the acceptor UV absorption spectrum using the Förster equation for energy transfer. With the spectral overlap value, assumed orientation of the chromophores in the dipeptide and the fluorescence quantum yield of

the donor, a "critical" Förster transfer distance was calculated for the two dipeptides (**9**, **10**) to be 14.6 Å and 15.1 Å, respectively. The actual distance calculated from dipeptide fluorescence spectra, using an assumed Förster distance was 9.1 Å and 8.7 Å, respectively. HyperChem MM3 modeling of the two dipeptides yielded an average inter-chromophore separation of 11 ±3 Å, comparable to the experimental values.

Laser flash photolysis of the two dipeptides revealed near complete TTET. The spectral analysis of each dipeptide showed essentially 100% acceptor triplet present, although the donor in each case absorbed all or most of the incident light.

Acknowledgements

Several key individuals are responsible for providing me this opportunity and ensuring that I achieved a modicum of success. First is Dr. McGimpsey, by accepting an aged rocket scientist/school teacher into the graduate program and then as a graduate student under his tutelage. He pushed me to my limits. Second is Dr. Weininger who brought me from less than a novice to the skilled pedestrian level on the NMR and in organic synthesis. I have the greatest respect for him because not only does he possess a vast amount of knowledge, he has tremendous compassion for his students, a rare combination.

Having never performed chemical synthesis, my first victim was Dr. Walter Samaniego. Walter, with the disposition of a crocodile and heart of a saint, taught me everything from sep funnels to chiral separations.

My greatest appreciation goes to those whose situation, although dissimilar to mine, possess the same goal, to graduate. Jose Cruz is the most notable. He coached me daily on NMR techniques, synthesis, research and Puerto Rican cooking. Yao Ma, Sal Marchese and Yi Liu filled in for Jose whenever he was out or not sure of the correct answer because they were equally as competent and gracious. My best learning sessions came when all four were there to share their knowledge and lunch. I am also grateful for John Benco and Chris Cooper for enduring my incessant photochemistry questions and teaching me every step. Last, but not least, Rong Zhang, a kind, professional, synthetic chemist. I hope some day to be as persistent and conversant with any subject as Rong.

My inspiration through all of this was my wife and best friend, Cathe and my daughter, Elissa. Nothing matters without them.

Table of Contents

List of Figures

List of Tables

Introduction

Background

The key to the operation of any molecular photonic or electronic device is the selective transfer of energy or charge within the device and communication with the macroscopic world. While links between the molecular and macroscopic regimes remain problematic, recent work suggests that internal device operation can be achieved by using polychromophoric molecules that facilitate rapid, controllable and, when desired, unidirectional energy and charge transfer between chromophores.

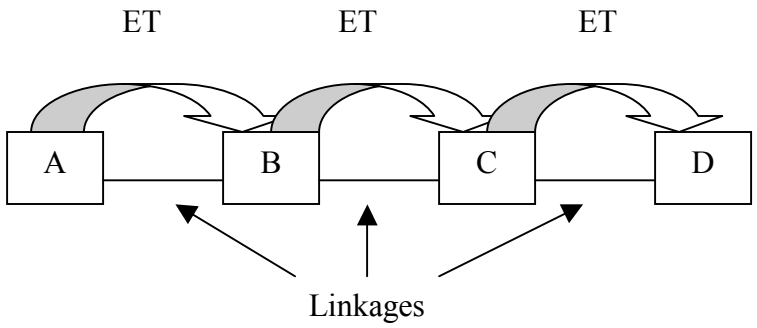

Figure 1. Polychromophoric (A, B, C, D) molecule showing flow of energy (information) from chromophore to chromophore.

One of the keys to efficient operation of molecular photonic or electronic devices is the nature of the molecular architecture that links together the chromophores. Linkers contribute to molecular flexibility or rigidity and can provide structural order to the molecule, which is potentially important to device operation. In some investigations chromophores were coupled covalently with rigid molecules in order to control spacing

and molecular orientation for optimum energy transfer.[1, 2] Rigid spacers control the distance and orientation of the chromophores.[3, 4, 5] Examples of these structures include decalinyl bridges (**1**),[6] polynorbornyl bridges (**2**),[7] the steroidal 5α-androstanyl system (**3**),[8] and adamantyl bridges (**4**).[3]

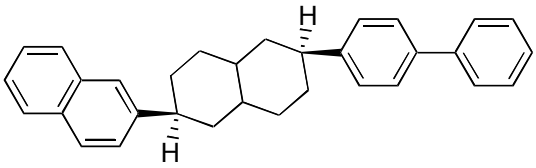

1

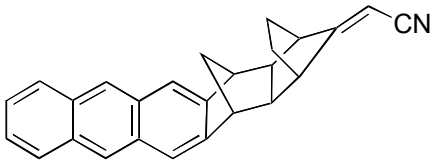

2

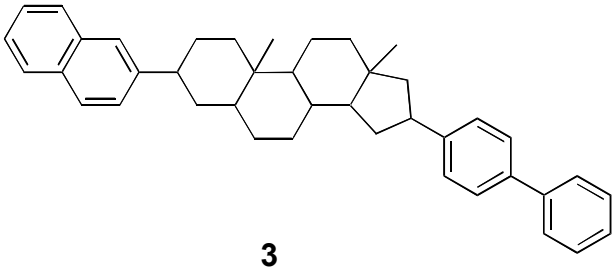

3

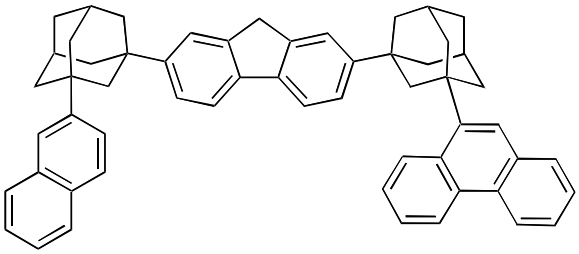

4

These molecules have proven difficult to synthesize and in some cases offer limited flexibility in spacing. Other molecules utilize more flexible coupling arrangements, including methylenic (**5**)[9] and ester (**6**)[10, 11] linkages. Compounds with these spacers, although simpler to synthesize, suffer from reduced transfer efficiency due to variable chromophore orientation and spacing.

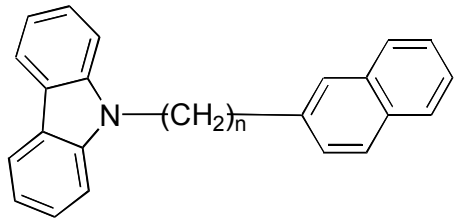

5

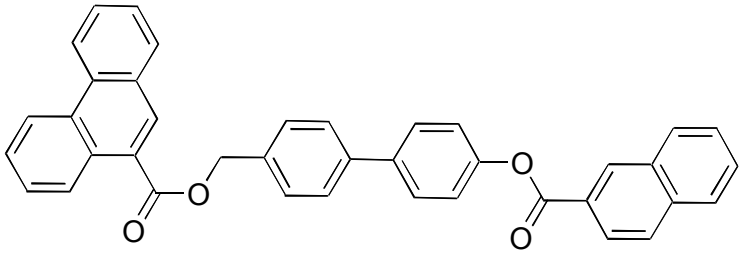

6

More recently, several groups have used polypeptides as the molecular framework or scaffolding for chromophores.[12-18] Polypeptides are synthesized from amino acids that are coupled to form amide bonds and naturally coil to form a stable helix. Pispisa, et al.[17] demonstrated that intramolecular chromophoric energy transfer is maximized when 3 residues separate donor and acceptor. In addition, Galoppini and Fox[12] observed unfolding of the last three residues at the peptide termini, so the minimum polypeptide containing three chromophores with a stable helical orientation should contain 15 residues, three terminal residues and three residues separating each chromophore.

Peptide scaffolds offer several advantages for studying and controlling energy transfer. The amino acid precursors are readily available or reasonably straightforward to synthesize, solid and solution phase synthetic techniques are well developed, automated purification techniques are well established and spacing and orientation are controlled by the helical orientation of the peptides and spacing of the chromophores.

We set about to synthesize and characterize a 15-residue polypeptide (**7**) containing three chromophores: benzophenone (**Bpa**), fluorene (**Fla**) and naphthalene (**Npa**). This arrangement of chromophores and scaffold was chosen for the following characteristics.

1. A fifteen-residue peptide should form a stable helix with equidistant spacing between the chromophores.
2. Triplet energy levels of these chromophores are appropriately spaced for TTET from **Bpa** to **Fla** to **Npa**, an important trait for device applications.
3. Two of the three chromophores can be purchased in the form of a substituted amino acid, enantiomerically pure, simplifying the peptide synthesis.
4. It is possible that the leucine residues in (**7**) will limit the possible orientations of the chromophores by forcing them to be orthogonal to the helix. An orthogonal orientation should make the chromophores co-planar and produce the minimum separation distance between chromophores needed to maximize energy transfer efficiency.

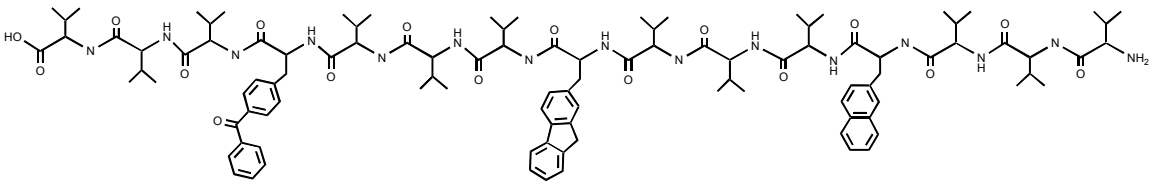

7

Since we visualize the operation of a device based on sequential energy transfer, we review here the fundamental photophysical processes, as they are relevant to energy transfer.

Photoinduced energy transfer

The process of absorption of electromagnetic radiation in the 200-700 nm range by molecules can best be visualized as a change in the occupation of electronic orbitals or energy states. The Jablonski diagram, figure 2, schematically shows how electronic energy is redistributed within a molecule.[19-22] The absorption and emission of photons involves changes in the electronic energy levels. Energy absorption depends on a match between the wavelength of the incident photons and electronic structure of the molecule. Initial photon absorption (Abs) is $S_o \rightarrow S_n$, where n = 1, 2, 3, etc. Electronic energy redistribution follows four general pathways:

1. internal conversion (IC) from a high electronic energy level to a highly vibrationally excited lower electronic energy level, $S_n \rightarrow S_m V_p$, where m < n and p=1,2,3, etc. This vibrational energy can subsequently be lost through vibrational relaxation (VR), $S_m V_p \rightarrow S_m V_0$,
2. fluorescence (Fl), $S_n V_0 \rightarrow S_0 V_p$ (n is usually 1, p = 1, 2, 3, …),
3. triplet formation through intersystem crossing (ISC), $S_n \rightarrow T_m V_p \rightarrow T_1 V_0$ (n is usually 1), T_1 can subsequently phosphoresce

(Ph) to S_0 or undergo energy transfer to another molecule (quenching/sensitization), or

4. molecular rearrangement to form a new structure/molecule.

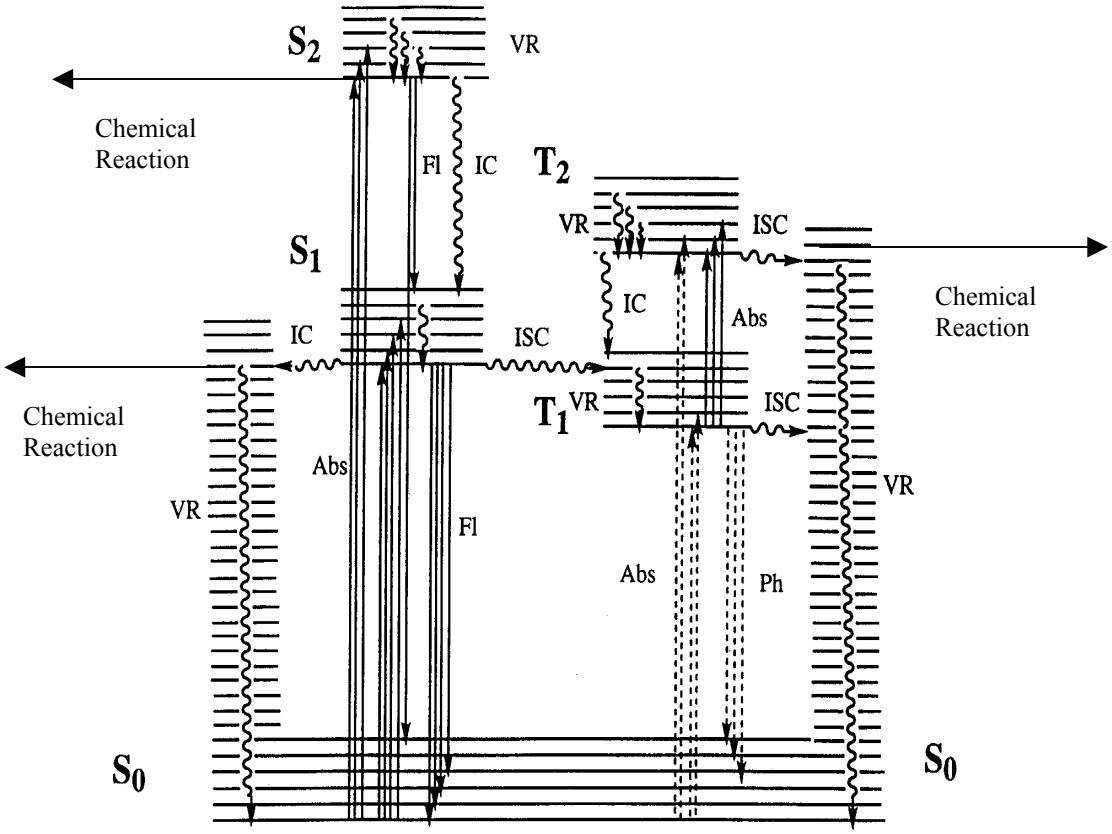

Figure 2. Energy state (Jablonski) diagram illustrating various photophysical events.

Energy transfer between chromophores can either be radiative (also known as trivial) or nonradiative. In the radiative process, one molecule emits a photon of electromagnetic radiation that is absorbed by another molecule. Nonradiative energy transfer can follow two mechanisms, involving either electron exchange or dipole-dipole (Coulombic) interactions. Both mechanisms have the same result (eq 1, 2),

$$D^* + h\nu \rightarrow D^* \quad (1)$$

$$D^* + A \rightarrow A^* + D \quad (2)$$

where D and A represent donor and acceptor molecules and * represents the excited state.[21]

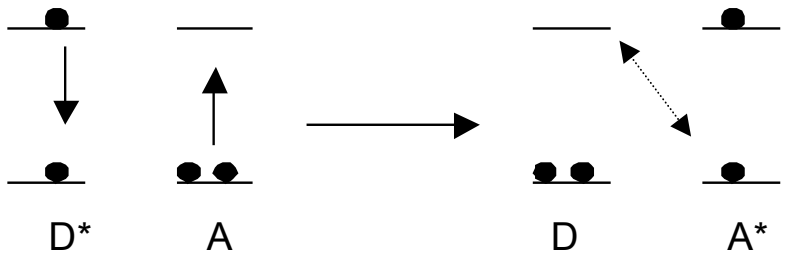

Figure 3. Dipole-induced dipole energy transfer pathway.[16]

In the dipole-induced dipole energy transfer process, figure 3, the energy is lost by the donor and acquired by the acceptor through resonance, much like tuning forks. A vibrating tuning fork of one frequency can induce a vibration in another tuning fork a great distance away if the fundamental frequency of the second tuning fork is in resonance with the fundamental frequency of one of the harmonics of the first. With tuning forks the energy transferred is in the form of vibrations (pressure oscillations)

traveling through the air, which are then absorbed by the acceptor tuning fork, producing vibrational energy at the second fork.

The process of energy transfer in bichromophoric molecules is similar to the tuning forks in that energy is transferred over a distance. In this case though, the excited molecule electronic dipole induces dipole oscillation in the acceptor. This process occurs over fairly large molecular distances, some as great as 50-100Å.[23] The transition occurs through a Coulombic resonance interaction via the electromagnetic field and does not require physical contact of the interacting partners.[21] Only singlet-singlet energy transfer (SSET) provides sufficient spectral overlap for this type of energy transfer process. The calculated rate constant, $\mathbf{k_{ET}}$, for this mechanism is dependent on the lifetime of the excited donor, $\boldsymbol{\tau_D}$, relative orientation of the chromophores, $\boldsymbol{\kappa}$, distance between D and A, $\mathbf{R_{DA}}$ and the critical transfer distance (distance that produces 50% energy transfer), $\mathbf{R_0}$. $\boldsymbol{\kappa^2}$, for randomly oriented donor and acceptor molecules has an estimated value of 2/3.

$$k_{ET} = (3/2)\kappa^2 \tau_D^{-1} (R_0 / R_{DA})^6 \qquad (3)$$

$\mathbf{R_0}$ is determined from the quantum yield of the donor, $\boldsymbol{\Phi_D}$, the refractive index of the solvent, $\boldsymbol{\eta}$, Avogadro's number, $\mathbf{N_A}$, and the spectral overlap integral of donor and acceptor, $\boldsymbol{J}$ (equations 4, 5). The last term includes the extinction coefficient of the acceptor, and emission shape is normalized to unity. For SSET the fluorescence spectrum of the donor must overlap the absorbance spectrum of the acceptor.[21, 23] If no overlap exists energy transfer through this mechanism is not possible.

$$R_0^6 = \frac{9100(\ln 10)\Phi_D \kappa^2}{128\eta^4 \pi^5 \mathrm{N}_A} J \tag{4}$$

$$J = \frac{\int_0^\infty f_D(\nu)\varepsilon_A(\nu)\nu^{-4} d\nu}{\int_0^\infty f_D(\nu)} \tag{5}$$

Electronic energy transfer occurs, not only through the process described above, but also through exchange interactions. Electron exchange is a quantum mechanical process but can be visualized as an exchange of an electron in an upper level orbital of the donor for a low orbital level electron of the acceptor and requires near collisional contact between the interaction partners, figure 4. Electron exchange is a result of the overlap of the wave functions of the two chromophores.

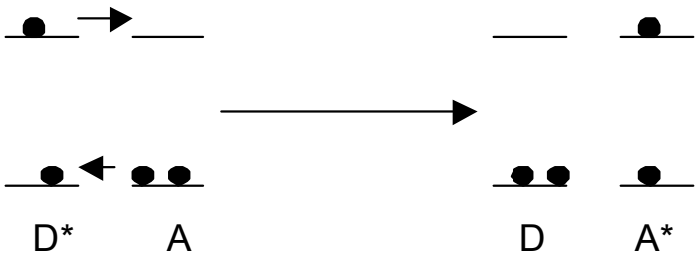

Figure 1. Electron exchange energy transfer pathway.[16]

The exchange, or Dexter, transfer rate is given by equation 6,

$$k = (2\pi / \hbar) KJ \exp(-2R / L) \qquad (6)$$

where **K** and **L** reflect the ease of electron tunneling between donor and acceptor and **ħ** is Planck's constant. The spectral overlap integral, ***J***, is now defined from the emission shape and the absorption shape when both are normalized to unit area. This process works with both SSET and TTET.

Strategy

A molecular device such as a wire operating on the basis of intramolecular energy transfer will undergo a potentially large number of transfer steps. The trichromophoric molecule we have designed will demonstrate that sequential intramolecular energy transfer steps are possible. This then will be a prototypical wire.

The chromophores in the 15-residue peptide (**7**) were selected such that, when exposed to 355nm light, they should efficiently produce the benzophenone triplet, and then transfer the triplet energy through the fluorene triplet to form the naphthalene triplet. The energy level diagram for this mechanism is shown in figure 5.

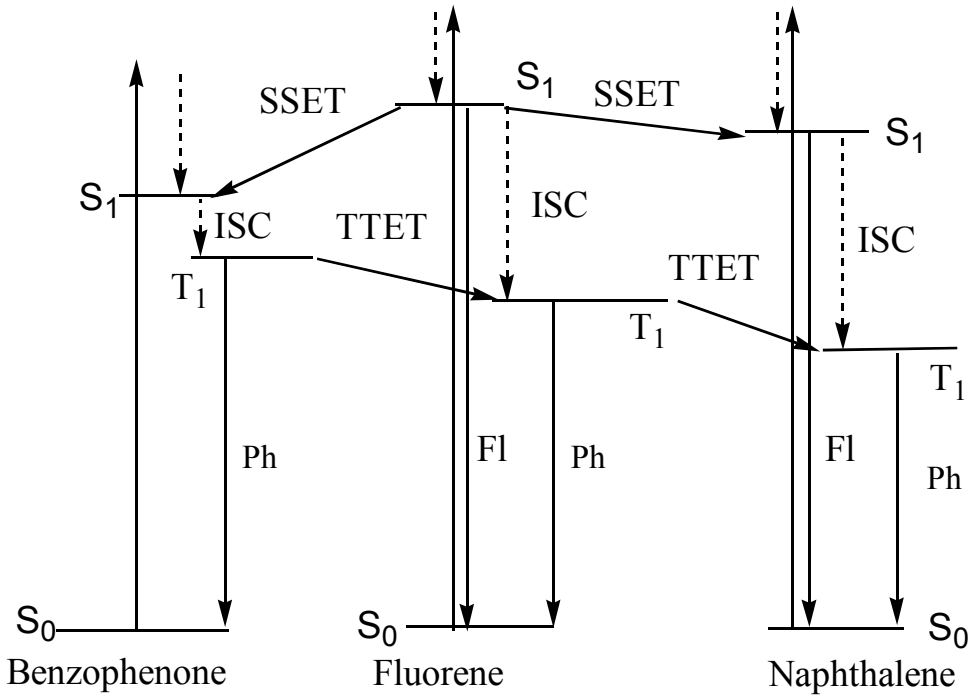

Figure 5**.** Jablonski diagram for benzophenone-fluorene-naphthalene photoinduced energy transfer.

In order to study energy transfer in a trichromophoric peptide, it was necessary first to acquire the building blocks for the peptide, either by purchase or synthesis. As already stated, we chose a poly-L-leucine peptide backbone into which were to be inserted alanine residues containing the appropriate chromophores. In the proposed 15-residue peptide, all of the residues with the exception of **Fla** were available commercially. Thus we undertook the synthesis of the appropriately N-protected **Fla**.

The synthesis and characterization of this polypeptide required the development and demonstration of several critical steps:

1. Synthesis of 3-(2-fluorenyl)-L-alanine (**Fla**, **8**), as an unprotected amino acid, a methyl ester and in amine-protected form. The N-protected moiety was required for the 15-residue polypeptide synthesis and the methyl ester protected moiety was required for the dipeptide model compounds.
2. Photochemical characterization of each chromophore-containing amino acid.
3. Synthesis of dipeptides containing the neighboring chromophore pairs (**Bpa-Fla**, **9**, **Fla-Npa**, **10**) and photochemical characterization of each to verify efficient energy transfer with no deleterious reactions. Chromophores on adjacent amino acids should provide a reasonable indication of how well they will respond in the polypeptide.
4. Development of solid-phase peptide synthetic methods and solvent systems to handle amino acid residues when they are attached to bulky chromophores.
5. Computer modeling of each dipeptide and the 15-residue polypeptide to visualize potential intermolecular distances and orientation of chromophores.

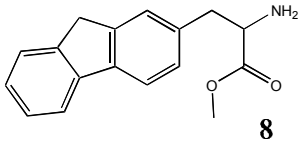

8

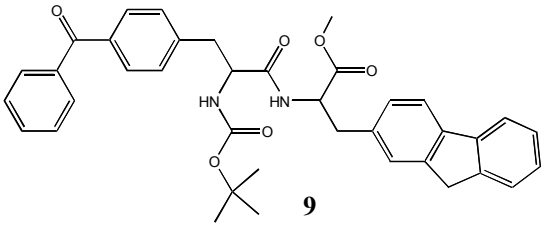

9

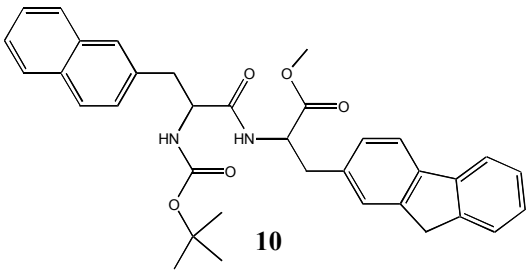

10

Experimental Section

General methods

Proton nuclear magnetic resonance (^{1}H NMR) spectra were obtained on a Bruker AVANCE 400 (400 MHz) NMR spectrometer. Chemical shifts are reported in ppm (δ) relative to internal tetramethylsilane (TMS) at 0.00 ppm. Carbon nuclear magnetic resonance (^{13}C NMR) spectra were recorded at 100 MHz on the spectrometer mentioned above.

Analytical thin layer chromatography was performed using precoated silica gel plates (Whatman 200 μm KCF18 silica gel 60A reverse phase plates or Whatman 250 μm thickness KF6F silica gel 60A normal phase plates), which were visualized under a UV lamp. Flash chromatography was performed on Mallinckrodt Baker 40 μm 60A silica gel under positive air or N_2 pressure. Preparative thin layer chromatography was performed using precoated silica gel plates (1000 μm Whatman K6F silica gel 60A). Melting points were obtained on a Thomas-Hoover capillary melting point apparatus and are uncorrected.

Solvents and reagents

All solvents were Aldrich or VWR Spectrophotometric grade and were used as received. The Chiro-CLEC-BL Subtilisin protease was purchased from Altus Biologics Inc. N-Boc-3-(2-Naphthyl)-L-alanine and N-Boc-(4'-benzoyl)-L-phenylalanine were purchased from both NovaBioChem and Advanced ChemTech and used as received. All chemical

reagents used in the synthesis of the N-(fluorenyl-methoxycarbonyl)-3-(2-fluorenyl)-L-alanine were from Aldrich (98-99+%) and were used as received.

UV Absorption spectroscopy

UV absorption spectra were obtained with a Shimadzu UV2100 UV-visible or Hitachi U2000 spectrophotometer. The wavelength range was typically 200-400 nm. The purpose of these spectral analyses was to produce a plot of extinction coefficient vs. wavelength, and therefore, a range of concentrations was analyzed. In some cases up to 14 solutions were prepared to obtain absorbance values between 0.1 and 1.0 over the entire absorbance range. All solutions were prepared with acetonitrile as solvent.

Fluorescence and phosphorescence spectroscopy

Fluorescence emission, excitation and phosphorescence spectra were obtained with a Perkin-Elmer LS-50 spectrofluorimeter. Excitation and emission fluorescence spectra of all compounds that fluoresce (benzophenone has an extremely low fluorescence quantum yield, 4×10^{-6})[20] were obtained on samples with a maximum absorbance of 0.1, to minimize self-absorption. The wavelength of overlap on the excitation and emission spectra was taken as the S_1 singlet energy of the molecule.

All phosphorescence measurements were made in a quartz Dewar at 77 K (N_2, liq.). Samples were prepared by dissolving the compound in 1:1 methanol/ ethanol, placing the solution in a 10mm x 10mm quartz UV cell, measuring the absorbance at the intended excitation wavelength, adjusting the concentration to obtain an absorbance $A > 1$,

degassing for 10 minutes by bubbling dry N_2 through the sample, transferring the sample by syringe to a 2 mm diameter quartz tube with a septum, and placing the tube in the liquid N_2 dewar in the spectrophotometer.

Laser flash photolysis.

The laser flash photolysis (LFP) system is discussed in detail in other reports.[24, 25] A summary of the technique is reported here. The LFP method is similar to that for obtaining a UV spectrum. A sample is irradiated with a laser pulse and the absorbance of the species generated is recorded at time intervals after the pulse. UV absorbance at selected wavelengths is expressed as a change in optical density, ΔOD. The system consists of laser excitation sources, a detection system and signal processing and control. The lasers utilized for the experiments reported here were a Lumonics EM510 XeCl excimer laser emitting a 308 nm, ~30 mJ/pulse of 8 ns pulse duration, and a Continuum "Surelite" Nd/YAG laser with a fundamental wavelength of 1064 nm. The third harmonic at 355 nm was used.

Samples were prepared for LFP analysis by dissolving the compound in acetonitrile such that an absorbance of ~0.6 at the laser excitation wavelength (308 nm or 355 nm) in a 10 x 10 mm or 7 x 7 mm quartz cell was obtained. Measurements were taken with either a Shimadzu UV2100 UV-visible or Hitachi U2000 spectrophotometer. The solutions (~3mL) were capped with a rubber septum and wrapped with parafilm. The solutions were degassed for 10 min by bubbling dry N_2 through the sample. If irradiation was found to degrade the compound, a flow system was used.

Synthesis of N-fluorenylmethoxycarbonyl-3-(2-fluorenyl-L-alanine

2-Fluorenylmethanol (11, FlOH) [29] Fluorenyl-2-carboxaldehyde (3.0 g, 15.4 mmol) was added to 75 mL of MeOH and heated until the solid dissolved. The solution was allowed to return to room temperature; then 0.25 g (0.4 eq) of $NaBH_4$ was added. The mixture was stirred at 25 ^oC for 20 min. Cold H_2O (15 mL) was added. The mixture was heated to reflux for 30 min. then allowed to return to room temperature. The mixture was poured into 100 mL of cold H_2O and extracted (3 x 20mL) with CH_2Cl_2. The combined organic extracts were washed (2 x 20mL) with sat. $NaHCO_3$, dried over anhydrous Na_2SO_4 and the solvent removed in vacuo to give 2.98 g (98 %) of a white solid, mp 142-143 ^oC, lit.[28] mp 140.5-142.5 ^oC: TLC R_f = 0.25 (CH_2Cl_2, normal phase).

2-Fluorenylmethyl bromide (12, FlBr) [29] Phosphorus tribromide (4.5 mL) was added to a solution of **11** (2.98 g, 15.1 mmol) and 30 mL of dry benzene. The mixture was left, without stirring, for 24 h at 25 ^oC. The solution was, slowly poured into a 60/40 mixture (250 mL) of Et_2O/H_2O. The organic phase was extracted with H_2O (3 x 40 mL), dried over anhydrous Na_2SO_4, and solvent removed in vacuo to give 3.86 g (98%) of a white solid, mp 92-93 ^oC, lit.[28] mp 95-100 ^oC: TLC R_f = 0.50 (10:1 CH_2Cl_2-MeOH, normal phase).

Diethyl (fluorenylmethyl)-2-acetamidomalonate (13, FlAAM)[29] Diethyl acetamidomalonate (3.21 g 14.8 mmol) and NaH (0.39 g, 1.1 eq.) were placed in a dry, N_2 purged flask. The flask was cooled to 0 ^oC and 45 mL of dry THF were slowly added

while the mixture was stirred magnetically. Absolute EtOH (0.42 mL, 0.5 eq.) was added and the mixture allowed to return to room temperature. A solution of **12 (**3.86 g, 14.8 mmol) (dissolved in dry THF, 42 mL), was added to the flask and the mixture was refluxed for 18h. The solvent was removed in vacuo to give a light brown solid (5.86 g, 100%), mp 144-145 ^{o}C, lit[28] mp 149.5-150.5 ^{o}C: TLC R_f = 0.35 (4:1 MeOH-H_2O, normal phase).

N-Acetyl-3-(2-fluorenyl)-D,L-alanine (14, AcFla)[29] A mixture of **13 (**5.86 g, 14.8 mmol) and 10% aqueous NaOH (22.4 mL, 4 eq.) was combined in a flask and heated to reflux 4 h. HCl (3 M, 18.7 mL, 4 eq) was added, and the mixture was heated to reflux an additional 2 h. The mixture was allowed to cool; the pH was adjusted to 4, and the solution extracted with EtOAc (3 x 150 mL). The organic extracts were combined and extracted with 0.2 M aqueous NaOH (3 x 75 mL). The pH of the combined aqueous extracts was adjusted to 4 and the mixture extracted with EtOAc (3 x 150 mL). The three EtOAc extracts were combined and dried over anhydrous Na_2SO_4, and the solvent removed in vacuo to give 3.75 g (86 %) of a white solid, mp 223-226 ^{o}C, lit.[29] mp 225-227 ^{o}C: TLC R_f = 0.75 (4:1 MeOH-H_2O, reverse phase); ^{1}H NMR (DMSO-d_6): δ 1.75 (s, 3H, CH_3), 2.84-3.09 (two dd, 2H, CH_2, J = 4.9 Hz, 4.9 Hz), 3.84 (s, 2H, CH_2), 4.4 (m, 1H, CH), 7.20-7.83 (m, 7H, Ar).

N-Acetyl-3-(2-fluorenyl)-D,L-alanine methyl ester (15, AcFlaMe)[29] Absolute methanol (75 mL) and **14** (3.75 g, 12.7 mmol) were combined in a dry, N_2 purged flask and BF_3OEt_2 (3.79 g, 3.38mL, 2.1eq) was slowly added. The mixture was heated to reflux

for 1h. The solvent was removed under reduced pressure and the solid product was partitioned between EtOAc (200mL) and H_2O (200 mL). The organic phase was washed with 5% $NaHCO_3$, H_2O and sat. NH_4Cl and dried over Na_2SO_4. The solvent was removed in vacuo to give 3.74 g (95%) of a pale yellow solid, mp 154-156 ^oC, lit[29] mp 170-171 ^oC: TLC R_f = 0.30 (4:1 MeOH-H_2O, reverse phase); ^1H NMR (DMSO-d_6): δ 1.76 (s, 3H, CH_3), 2.87-3.06 (two dd, 2H, CH_2, J = 5.6 Hz, 5.6 Hz), 3.56 (s, 3H, CH_3), 3.84 (s, 2H, CH_2), 4.4 (m, 1H, CH), 7.18-7.83 (m, 7H, Ar); ^{13}C-NMR ($CDCl_3$): δ 23.46 (NCH), 37.22 (CH_2), 38.37 (CH_2), 52.83 (CH_3), 53.84 (CH_3), 120.23, 120.31, 125.45, 126.28, 127.16, 127.20, 128.21, 134.58, 141.26, 141.66, 143.53, 144.13, 170.64 (CO), 172.49 (CO); ^{13}C-NMR ($CDCl_3$ DEPT): δ 23.46 (NCH), 37.22 (CH_2), 38.37 (CH_2), 52.83(CH_3), 53.84 (-OCH_3), 120.23 (CH), 120.31 (CH), 125.45 (CH), 126.28 (CH), 127.16 (CH), 127.20 (CH), 128.21 (CH).

N-acetyl-3-(2-fluorenyl)-L-alanine hydrochloride (16, L-AcFla)[29] A solution of **15** (3.74 g, 12.1 mmol) in acetone (120 mL) was combined with phosphate buffer (120 mL, 0.2 M pH 7.8). Protease enzyme (55 mg, CLEC-BL, crystallized Subtilisin Carlsberg Type VIII) was added. The mixture was agitated on an orbital shaker at 200 rpm at 37 ^oC for 24 h. To monitor reaction progress, a small aliquot was removed and the acetone evaporated under reduced pressure. The pH of the aqueous residue was reduced to 3 and extracted with EtOAc. The organic phase was dried over sodium sulfate and the solvent removed in vacuo. The NMR spectrum of the dry product was analyzed to determine the ratio of the methyl CH_3 and the fluorenyl CH_2 peak areas. When the ratio reached 3:4, all the L-isomer had been hydrolyzed. The remaining solution was centrifuged to recover the

CLEC-BL protease. The solid CLEC-BL was washed twice with acetone and dried in vacuo.

The supernatant contained the hydrolysis product, **16,** and the unreacted N-acetyl-3-(2-fluorenyl)-D-alanine methyl ester (**17**, **D-AcFlaMe**). To recover and separate the two products, the acetone in the supernatant was removed under reduced pressure. The pH was adjusted to 3 with 1 M HCl and the products were extracted with EtOAc (3 x 75 mL). The organic phase was then extracted with 0.2 N NaOH (3 x 50 mL). The organic phase was dried over Na_2SO_4 and solvent removed in vacuo to give 1.83 g (98%) of a light yellow solid, mp 154-156 ^oC, lit[29] mp 170-171 ^oC (racemate): TLC R_f = 0.30 (4:1 MeOH-H_2O, reverse phase); ^1H NMR (DMSO-d_6): δ 1.76 (s, 3H, CH_3), 2.87-3.06 (two dd, 2H, CH_2, J = 4.4Hz, 9.2 Hz), 3.56 (s, 3H, CH_3), 3.84 (s, 2H, CH_2), 4.4 (m, 1H, CH), 7.18-7.83 (m, 7H, Ar).

The basic aqueous phase was adjusted to pH 4 with HCl (3 M) and extracted with EtOAc (3 x 75 mL). The EtOAc extracts were dried over Na_2SO_4 and the solvent removed in vacuo to give 1.61 g (90%) of a pale yellow solid, mp 223-226 ^oC, lit[29] mp 225-227 ^oC (racemate): TLC R_f = 0.80 (4:1 MeOH-H_2O, reverse phase); ^1H NMR (DMSO-d_6): δ 1.75 (s, 3H, CH_3), 2.84-3.09 (two dd, 2H, CH_2, J = 4.9 Hz, 4.9 Hz), 3.84 (s, 2H, CH_2), 4.4 (m, 1H, CH), 7.20-7.83 (m, 7H, Ar), 12.66 (s, 1H, COOH).

3-(2-Fluorenyl)-L-alanine hydrochloride (18, FlaHCl)[29] A mixture of **16 (**1.61 g, 5.5 mmol) and 6 M HCl (60 mL) was heated to reflux for 18 h. The HCl was removed under

reduced pressure and the product dried in vacuo to give 1.56 g (99%) of a white solid, mp 262-266 °C, lit[29] mp 264-269 °C: TLC R_f = 0.35 (4:1 MeOH-H_2O, reverse phase); ^1H NMR (DMSO-d_6): δ 3.19 (d, 2H, CH_2, J = 4 Hz), 3.86 (s, 2H, CH_2), 4.16 (m, 1H, CH), 7.25-7.86 (m, 7H, Ar) 13.85 (s, 1H, COOH).

N-Fluorenylmethoxycarbonyl(Fmoc)-3-(2-fluorenyl)-L-alanine (19, Fmoc-Fla) A solution of **18** (1.56 g, 5.39 mmol) in dioxane (100 mL) and 10% aq Na_2CO_3 (200 mL) was cooled to 0 °C and 9-fluorenylmethoxychloroformate (5.64 g, 4 eq, dissolved in 15 mL of dioxane) was added very slowly. The mixture was stirred 4 h at 0 °C and 18 h at 25 °C. The reaction mixture was poured into 500 mL of H_2O and refrigerated 4 h. The solid product was filtered and washed, first with Na_2CO_3/10% dioxane solution (pH 11 aq), then H_2O. The aq. phase was adjusted to pH 2 with 6 M HCl and the solution refrigerated 18 h. The precipitate, which was unreacted **Fla**, was recovered by extraction with EtOAc (2 x 50 mL).

The solid from the first filtration was dried in vacuo and then triturated with Et_2O. The suspension was centrifuged for 5 min at 4000 rpm, and the Et_2O was decanted. The solid product was washed with Et_2O (2 x 30 mL) and again centrifuged after each washing. The Et_2O wash removed the excess Fmoc reagent as 9-fluorenylmethanol. TLC (4:1 MeOH-H_2O, reverse phase) was used to track the removal of the 9-fluorenylmethanol. The dried product was partitioned between 1.5 M HCl (25 mL) and EtOAc (75 mL). The organic phase was washed with sat. NaCl, dried over Na_2SO_4 and the solvent was removed in vacuo to give 2.07 g (81%) of a white solid, mp 190-200 °C: TLC R_f =

0.40 (4:1 MeOH-H_2O, reverse phase); ^{1}H NMR (DMSO-d_6): δ 2.86-3.11 (2dd, 2H, CH_2, *J* = 4.7 Hz, 4.9 Hz), 3.72 (s, 2H, CH_2), 4.08 (m, 1H, CH), 4.15 (t, 1H, CH, Fmoc), 4.26 (m, 1H, NH), 4.06-4.19 (dt, 2H, CH_2), 7.08-7.85 (m, 15H, Ar).

Preparation of precursors for peptide synthesis and dipeptides

3-(2-Fluorenyl)-L-alanine methyl ester (20, Fla) A solution of **18** (0.212 g 0.73 mmol) in anh. MeOH (5.1 mL) was placed in a dry, N_2-purged flask. BF_3OEt_2 (195 μL, 2.1 eq) was added and the solution was heated to reflux for 2 h at 80 ^{o}C. The solvent was removed under reduced pressure to form a brown oil. $NaHCO_3$ (5%, 30 mL) was added to the flask. A white precipitate formed, which was isolated by filtration, washed with H_2O and dried in vacuo to give 0.172 g (88%) of a white solid, m.p.109-110.5^{o}C: TLC R_f = 0.70 (4:1 MeOH-H_2O reverse phase); ^{1}H NMR (400MHz, DMSO-d_6) δ 1.84 (s, 2H, NH_2), 2.80-2.93 (2dd, 2H, CH_2, *J* = 6.1 Hz, 6.2 Hz), 3.55 (s, 3H, -OCH_3), 3.6 (m, 1H, CH), 3.84 (s, 2H, CH_2), 7.13-7.82 (m, 7H, Ar); ^{13}C-NMR (DMSO-d_6): δ 36.6 (CH_2), 41.29 (CH_2), 51.7 ($COOCH_3$), 56.3 (CH), 120.00, 120.13, 125.46, 126.36, 126.84, 127.06, 128.17, 137.07, 139.71, 141.37, 143.24, 143.34, 175.83 (CO); ^{13}C-NMR (DMSO-d_6 DEPT): δ 36.6 (CH_2), 41.28 (CH_2), 51.7 (CH_3), 56.3 (CH) 120.00 (CH), 120.13 (CH), 125.46 (CH), 126.36 (CH), 126.85 (CH), 127.06 (CH), 128.17 (CH).

N-Butoxycarbonyl(Boc)-3-(2-naphthyl)-L-N-alanyl-3-(2-fluorenyl)-L-alanine methyl ester (10, Npa-Fla) A suspension of **20** (0.114 g, 0.426 mmol) in $CHCl_3$ (1.7 mL) in a dry, N_2 purged flask was cooled to 0 ^{o}C. Dry Et_3N (0.33 mL, 2.13 mmol), 1-hydroxy-

1*H*-benzotriazole (0.077 g, 0.51 mmol), a solution of N-Boc-3-(2-naphthyl)-L-alanine (0.149 g, 0.469 mmol) in $CHCl_3$ (1.9 mL), and 1-[3-dimethylamino)propyl]-3-ethylcarbodiimide hydrochloride (0.109 g, 0.51 mmol) were successively added to the initial suspension under continuous N_2 flow.[44] The mixture was allowed to reach room temperature, and stirred for 18 h. TLC (24:1 CH_2Cl_2-MeOH, normal phase) indicated incomplete reaction. TLC showed that the reaction had gone to completion after an additional 30 h. The solution was then diluted with $CHCl_3$ (50 ml) and washed with 6 M HCl, sat. aq $NaHCO_3$, and brine. The organic phase was dried over Na_2SO_4, and the solvent removed in vacuo to give 0.232 g (96%) of a white solid. The crude product (**10**) was purified by flash chromatography (260:1 CH_2Cl_2-MeOH, normal phase) to give 0.195 g (81%). mp 172-173 ^oC: ^1H-NMR ($CDCl_3$): δ 1.36 (s 9H, t-Bu), 3.08-3.16 (m, 4H, 2 CH_2), 3.19 (d, 2H, CH_2, J = 7.1 Hz), 3.55 (s, 3H, OCH_3), 3.70 (d, 2H, CH_2, J = 3.8 Hz), 4.42 (m, 1H, CH), 4.79 (m, 1H, CH), 7.26-7.65 (m, 14H, Ar). ^{13}C-NMR ($CDCl_3$ DEPT): 28.57 (t-Bu), 37.06 (CH_2), 38.47 (CH_2), 38.97 (CH_2), 52.61 (CH_3), 53.84 (CH), 55.68 (CH), 120.19 (CH), 125.39 (CH), 126.16 (CH), 126.24 (CH), 127.06 (CH), 127.12 (CH), 127.96 (CH), 128.04 (CH), 128.54 (CH).

N-Boc-3[(4'-benzoyl)-phenyl]-L-alanyl-N-3-(2-fluorenyl)-L-alanine methyl ester (11, Bpa-Fla) A suspension of **20** (0.191 g, 0.72 mmol) in $CHCl_3$ (3.0 mL) in a dry, N_2 purged flask was cooled to 0 ^oC. Dry Et_3N (0.50 mL, 3.6 mmol), 1-hydroxy-1*H*-benzotriazole (0.117 g, 0.86 mmol), a solution of N-Boc-3-[(4'-benzoyl)-pheny]-L-alanine (0.266 g, .72 0 mmol) in $CHCl_3$ (2.9 mL), and 1-[3-dimethylamino)propyl]-3-ethylcarbodiimide hydrochloride (0.166 g, 0.86 mmol) were successively added to the

initial solution under continuous N_2 flow. The mixture was allowed to reach room temperature, and stirred for 18 h. The reaction was monitored with TLC (24:1 CH_2Cl_2-MeOH, normal phase). The solution was then diluted with $CHCl_3$ (100 mL), and washed with 6 M HCl, sat. aq $NaHCO_3$, and brine. The organic phase was dried over Na_2SO_4, and the solvent removed in vacuo to give 0.359 g (81%) of a white solid. The crude product was purified through flash chromatography on silica gel (260:1 CH_2Cl_2-MeOH) to give 0.0982 g (22%) of a white solid, mp 166-167.5 ^oC. ^{1}H-NMR ($CDCl_3$): δ 1.36 (s. 9H, t-Bu), 3.06-3.16 (m, 4H, 2 CH_2), 3.66 (s, 3H, OCH_3), 3.80 (s, 2H, CH_2), 4.82 (dd, 1H, CH, J = 6.0 Hz, 6.1 Hz), 5.11 (d, 1H, CH, J = 7.5 Hz), 7.01 (d, 1H, Ar, J = 7.8 Hz), 7.20-7.75 (m, 16H, Ar). ^{13}C-NMR ($CDCl_3$): δ 28.63 (t-Bu), 36.76 (CH_2), 38.10 (CH_2), 38.28 (CH_2), 52.36 (CH_3), 53.91 (CH) 55.42 (CH), 120.23, 120.31, 125.44, 126.35, 127.14, 127.18, 128.21, 128.68, 129.74, 130.39, 130.84, 132.81, 134.49, 136.63, 137.99, 141.25, 141.68, 142.06, 143.55, 144.09, 155.69 (CO), 170.97 (CO), 171.93 (t-BuO<u>C</u>O), 196.73 (Ph-<u>C</u>O-Ph); ^{13}C-NMR ($CDCl_3$ DEPT): δ 28.20 (CH_3), 36.76 (CH_2), 38.10 (CH_2), 38.28 (CH_2), 52.36 (CH_3), 53.75 (CH) 55.42 (CH), 119.79 (CH), 119.87 (CH), 125.00 (CH), 125.92 (CH), 126.70 (CH), 127.77 (CH), 128.25 (CH), 129.30 (CH), 129.96 (CH), 130.41(CH) , 132.38 (CH).

Results and Discussion

A major portion of this research effort consisted of the synthesis and characterization of **Fla** and it's C and N-protected analogs. The discussion includes a review of the literature and our results. The last section of the synthesis discussion includes a brief review of the synthesis methods for dipeptides, which were prepared with little deviation from the

reported procedure.[44] The 15-residue polypeptide was synthesized by John Benco and its synthesis will not be discussed here.

The order of the photochemistry results and discussion section follows the flow chart sequence in figure 8.

Synthesis

Synthesis of amino acid derivatives – Literature Summary

Snyder et al.[27] have developed a modification of the Sorenson procedure,[26] (in which phthalimidomalonic ester is alkylated) that utilizes acetamidomalonic ester to produce alanine derivatives. This general procedure, with modifications, has been used by Morrison[28] in the preparation of 3-(2-Fluorenyl)-D/L-alanine and by Nestor et al.[29] with aryl alkyl halides to produce a host of optically pure alanine derivatives for subsequent peptide synthesis. The racemic N-acetyl methyl ester products were resolved with Subtilisin Carlsberg Type VIII protease enzyme as described by Bosshard and Berger and others.[30-33] The general procedure is shown in figure 6.

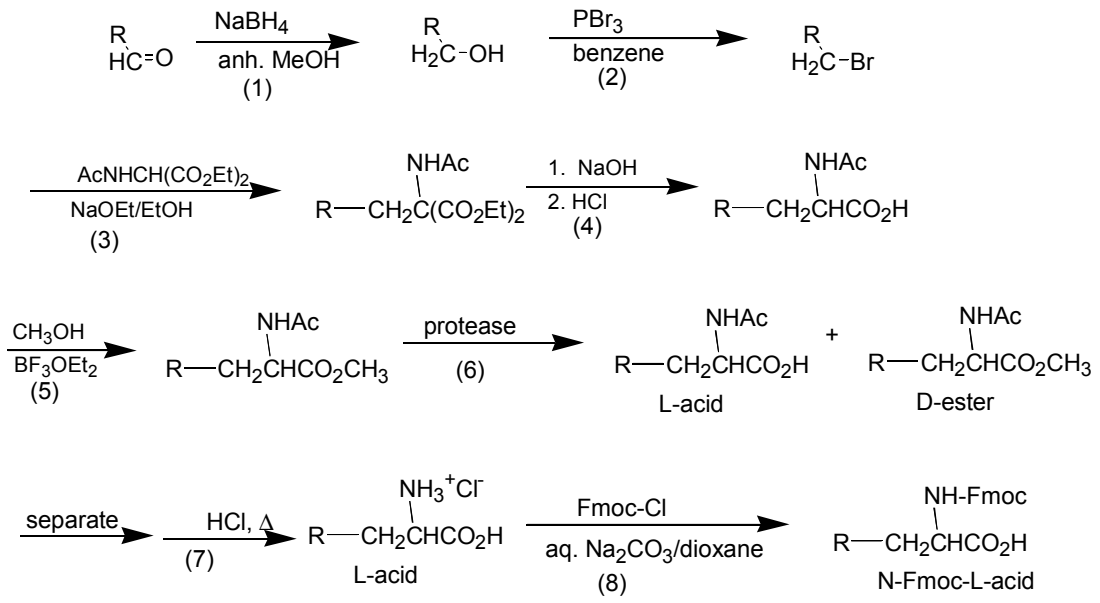

Figure 6**.** Synthetic route to N-Fmoc-L-alanine derivatives.

Synthesis of N-Fmoc-3-(2-fluorenyl)-L-alanine – Results

Synthesis of amino acid derivatives necessary for the photochemical investigations began with review of the procedure described by Nestor, et al.[29] A summary of the synthetic method followed for **Fmoc-Fla** is given in figure 7.

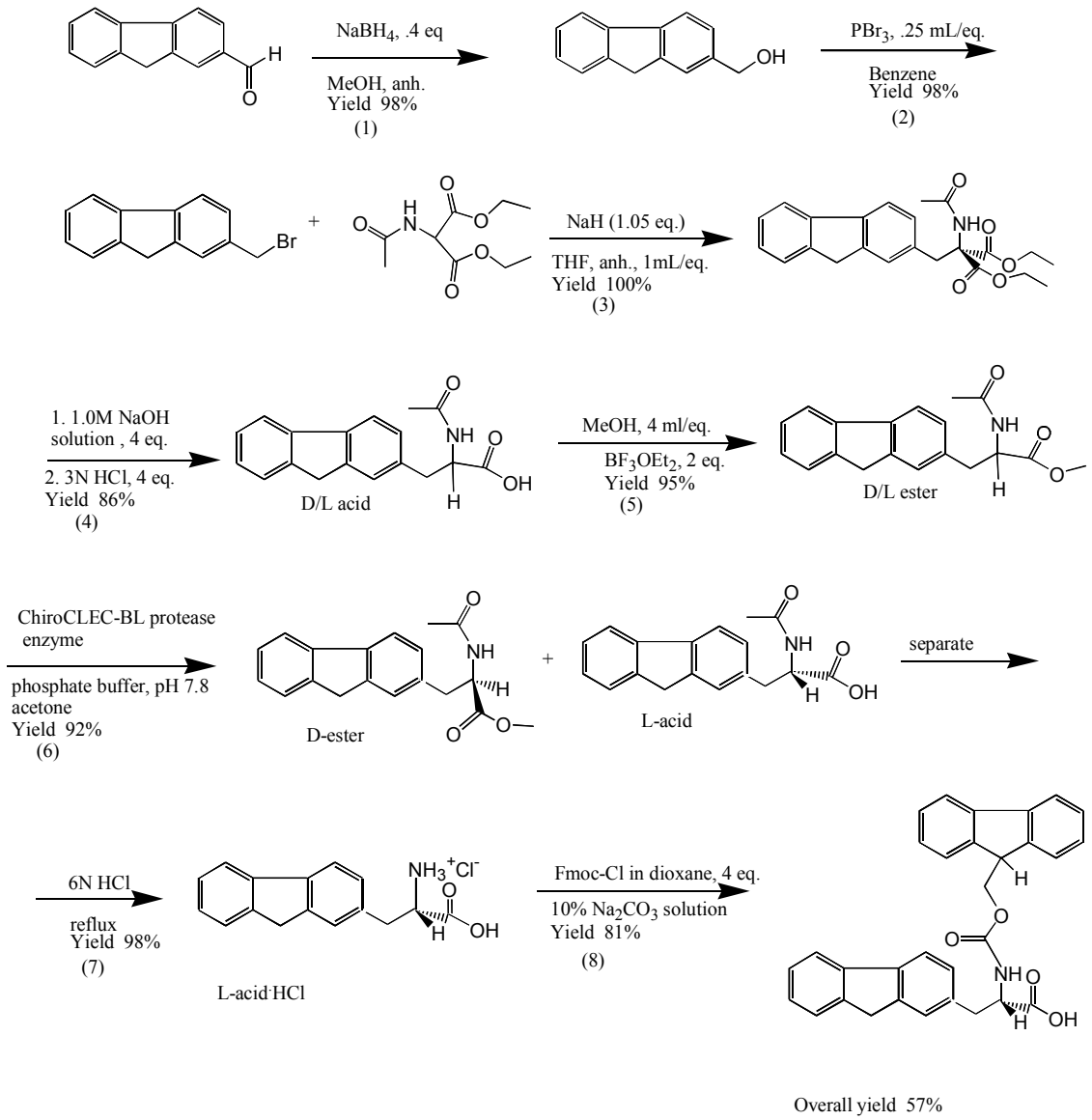

Figure 7. Synthesis of N-Fmoc-3-(2-fluorenyl)-L-alanine, **Fmoc-Fla**.

The first 5 steps of the synthesis were completed in much the same manner as those of Morrison[28], Snyder et.al.[27] and Sorensen.[26] Morrison used lithium aluminum hydride in the first step, while sodium borohydride was used here for improved yield and safety. For the third step, Morrison and Snyder used sodium metal in anhydrous ethanol to make sodium ethoxide which then deprotonated the diethylacetamidomalonate; sodium hydride offers improved handling and safety and was utilized for our reaction. Snyder's procedure for synthesis of the DL-N-acetyl amino acid was used without change. The methyl ester synthesis in step 5 was identical to that described by Nestor et al.[29] The enzymatic separation of the DL-methyl ester proved to be difficult, most likely due to the hydrophobic nature of the fluorenyl group. At this point several options were investigated, including the use of mandelic acid,[49] acylase[50-52] and a variety of protease methods.[29-32] Mandelic acid forms diastereoisomeric salts with slightly different solubilities. The racemic mixture is separated through recrystallization. Initial protease experiments produced limited success, 10-35 % (optical yield) conversion of the L-amino acid ester to the acid. These experiments were conducted in aqueous, phosphate-buffered solutions with and without small amounts of acetone to improve solubility. Protease is easily denatured and nonreactive in most solvents. Protease II-Fungus Orgyae, obtained from Alpha Beta, was also evaluated and gave only 3-5% optical yield.

A one-pot procedure was investigated utilizing Subtilisin protease, type VIII and acylase to produce the Fmoc-protected amino acid was also attempted but was abandoned at the protease step due to poor yield (maximum conversion 24%).[31] Although this approach was not further investigated, the modifications described below could make the one-pot

approach more viable. Production of the amino acid ethyl ester directly from the malonate in the one-pot process saved a great amount of time by eliminating two purification steps and the methylation step.

The enzyme ChiroCLEC^{TM}-BL (Subtilisin protease, type VIII, Altus Biologics, Inc.) is reported to be successful in resolving a wide array of amino acids in buffered aqueous DMF and acetone as well as in neat isooctane, alcohols, acetone, toluene, THF, acetonitrile, DMF and pyridine.[34] CLEC (Cross-Linked Enzyme Crystals) is manufactured from protease that has been cross-linked with glutaraldehyde, similarly to a procedure reported by Tüchsen and Ottesen.[53] Other CLEC enzymess can also be used to form optically pure peptides from racemic mixtures. Our first attempt with CLEC protease gave a hydrolytic yield of 46.4% (optical yield 92.8% of L-isomer). Subsequent reactions produced near stoichiometric optical yields.

Reaction progress was measured utilizing ^{1}H NMR spectroscopy. Thin layer chromatography, TLC, is inappropriate for tracking reaction progress because the reaction is complete when 50% of the starting material is still present and the size of the TLC spots cannot be quantified. Fluorenylalanine methyl ester generates clearly discernable (in the NMR) fluorenyl CH_2 and ester CH_3 signals. Initially, the methyl/methylene proton ratio is 3:2 but, when the reaction is complete, the ratio in the product mixture should be 3:4. Due to clarity of these two peaks and the ease with which a sample can be purified, integrating these two peaks and calculating the ratio produces a

more quantitative measure of reaction progress. Table 1 summarizes the results of several protease reactions.

Table 1. Results of protease reactions comparing percent reaction using NMR calculated values with actual (actual yields are the amounts obtained when the sample was purified).

Sample	Optical yield, NMR	Optical yield, Actual
DCF-26 Subtilisin protease	54	61
DCF-27 Subtilisin protease	68	50
DCF-33 Subtilisin protease	52	52
DCF-45 protease II	14	10
DCF-50 CLEC protease	98	92
DCF-82 CLEC protease	98	98

Concurrent with the enzyme investigation, attempts were made to attach the Fmoc protecting group using fluorenylmethoxy chloroformate (Fmoc-Cl) in aqueous base and dioxane.[31, 33, 35, 37-43, 48] Attempts at Fmoc protection, using the one-pot synthesis described above, were unsuccessful. We attributed this to the poor yield of the ester.[35, 36]

Another obstacle in the Fmoc process is the formation of side products. The use of Fmoc-N-hydroxyl succinimide ester rather than Fmoc-Cl was attempted as a possible method for reducing dipeptide formation.[33, 49, 54-56] The method worked extremely well with phenanthrylalanine, but marginal results were obtained with fluorenylalanine.

Use of trimethylsilyl chloride (TMS-Cl) is reported by Bolin[48] also to prevent formation of dipeptide and tripeptide contaminants. The TMS acts as a blocking agent for the carboxylate site but is extremely labile for removal later. An additional goal of using TMS was to alter the polarity of the fluorenylalanine, improving its solubility in aqueous base/dioxane. Solubility improved, but the yield was reduced. Further improvements in the original Fmoc-Cl/Na_2CO_3/dioxane method produced the desired product, reproducibly, with acceptable yield, > 80%. To accomplish this, the ether wash to remove the fluorenylmethanol from the reaction mixture was delayed until the crude product had been precipitated, filtered and washed with a dioxane/Na_2CO_3 solution and dried. The solid product was then triturated with ether and centrifuged to recover the insoluble **Fmoc-Fla**.

Dipeptide Synthesis

Dipeptides formed by combining either N-Boc-3-(2-naphthyl)-L-alanine (**22, Npa**) or N-Boc-3-[(4'-benzoyl)pheny]-L-alanine (**21, Bpa**) with 3-(2-fluorenyl)-L-alanine methyl ester (**20, Fla**) were synthesized in solution using **Fla** and the Boc (t-butoxycarbonyl) protected form of the second amino acid. The Boc N-protection is used in the dipeptide synthesis rather than Fmoc because it does not interfere with photochemical analysis.[9]

Spectroscopy

As outlined in the introduction, intramolecular charge and energy transfer in polychromophores that utilize peptide bridges is the area of primary emphasis in this report. The three model compounds, **Bpa**, **Npa** and **Fla** and the two dipeptides, N-Boc-3-(2-naphthyl)-L-N-alanyl-3-(2-fluorenyl-L-alanine methyl ester (**10, Npa-Fla**) N-Boc-3[(4'-benzoyl)-phenyl]-L-alanyl-N-3-(2-fluorenyl)-L-alanine methyl ester (**11, Bpa-Fla**) were synthesized and/or procured to elucidate the mechanism of energy/charge transfer between chromophores. The results obtained here will provide valuable insight into the transfer mechanisms of much larger polypeptides. We have chosen to study these molecules for several reasons including: their relative ease of synthesis, their well-characterized photophysics and their potential application in nanoscale devices.

Singlet-singlet energy transfer (SSET) readily occurs between the above chromophores allowing for accurate calculation of interchromophore distance and transfer efficiency and rates. After the distances are determined, triplet-triplet energy transfer (TTET) efficiency is evaluated through phosphorescence and laser flash photolysis experiments.

The photophysical characterization of each bichromophore followed the steps elucidated in Figure 8.

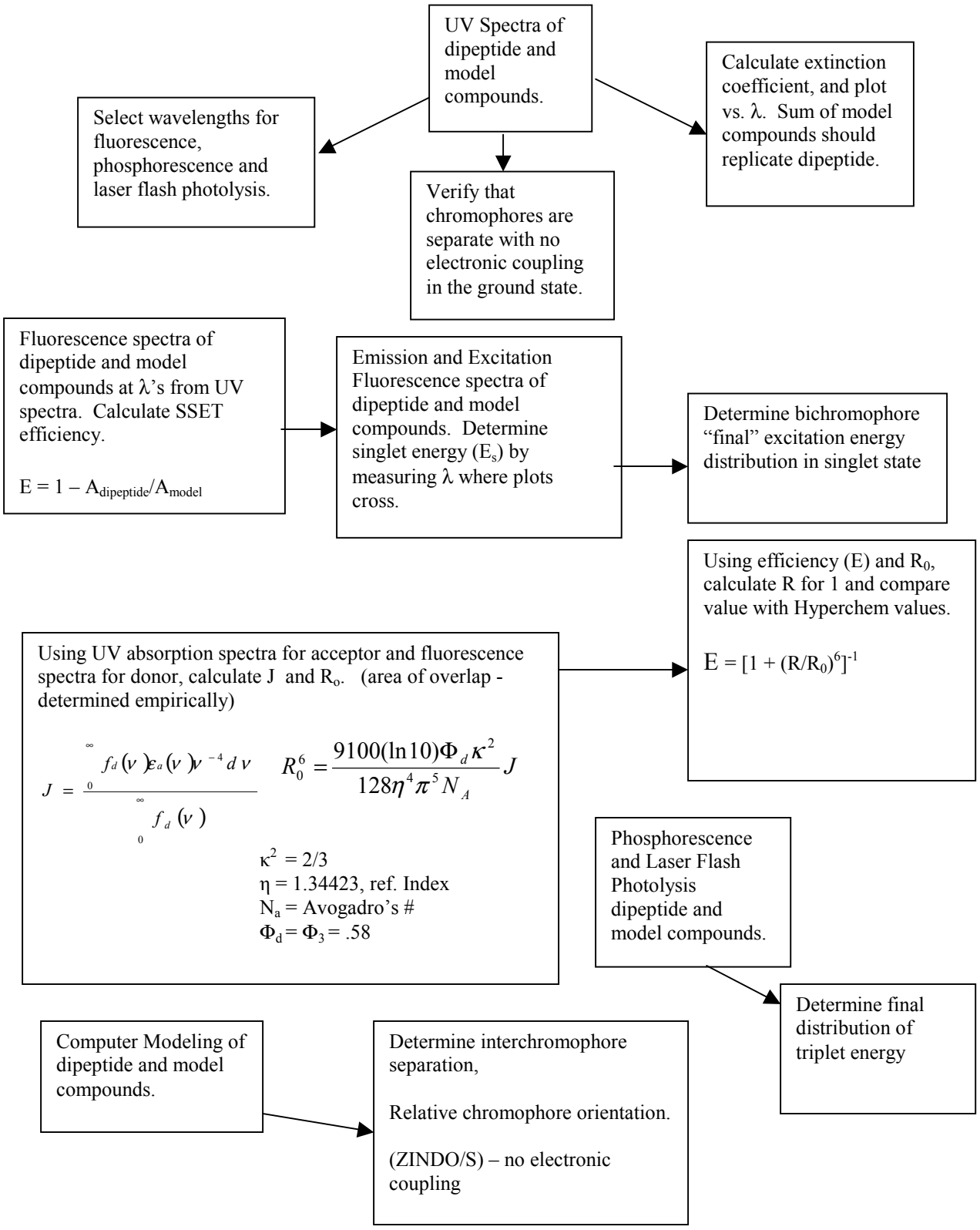

Figure 8**.** Spectroscopy flow chart.

UV Absorption Measurements

UV spectra were obtained for the three model compounds (**Npa, Bpa and Fla**) over a range of concentrations necessary to produce reasonable absorbance over the entire spectrum of each, figures 9, 10 and 11.

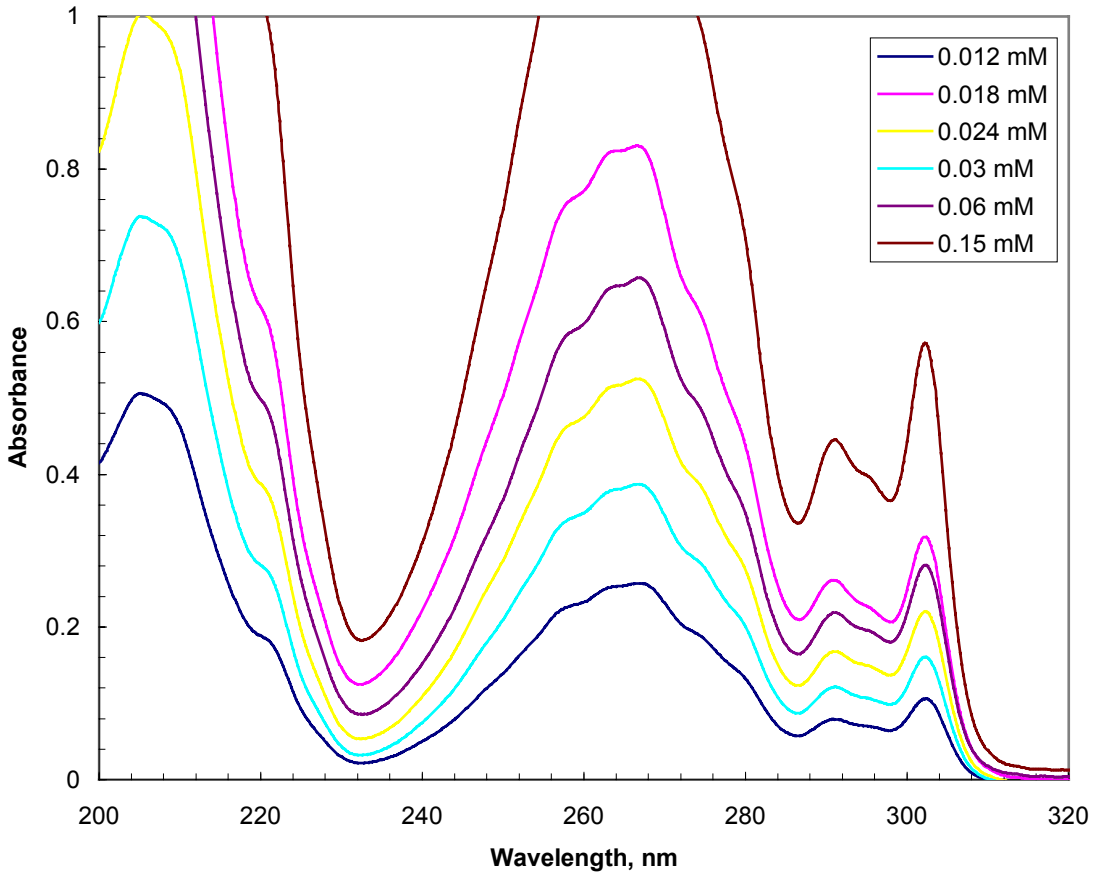

Figure 9**.** **Fla** UV spectra at different concentrations.

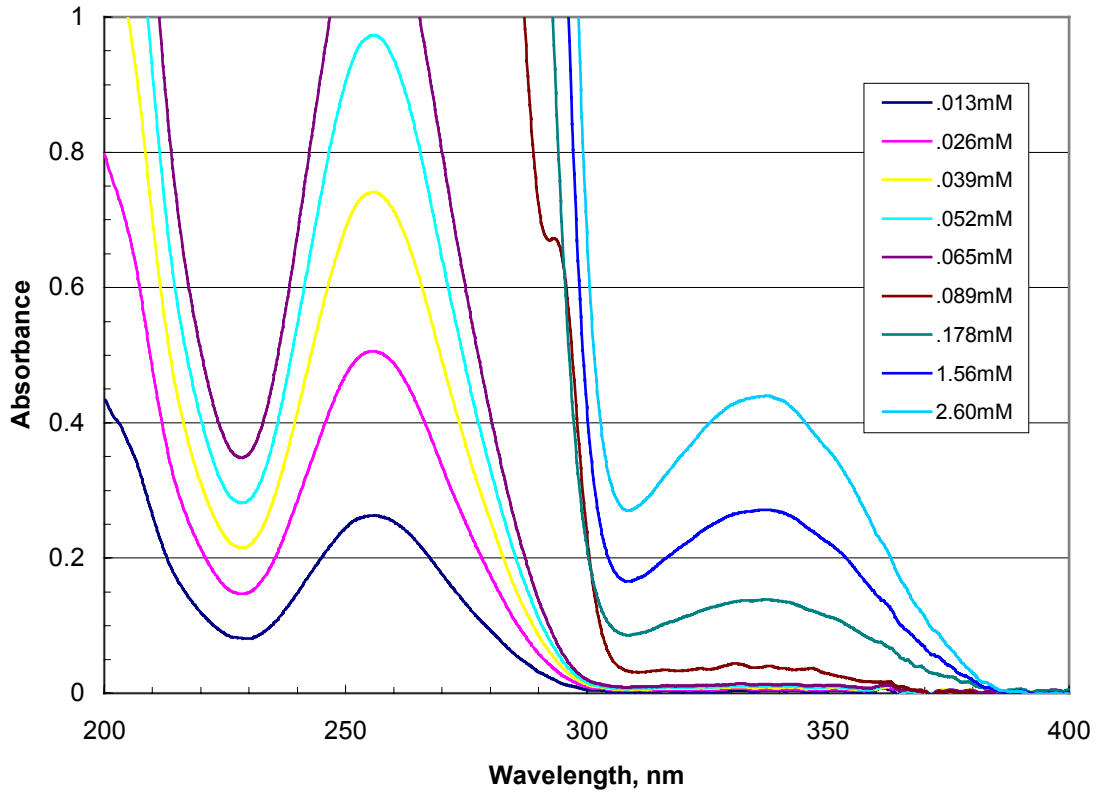

Figure 10. **Bpa** UV spectra at different concentrations.

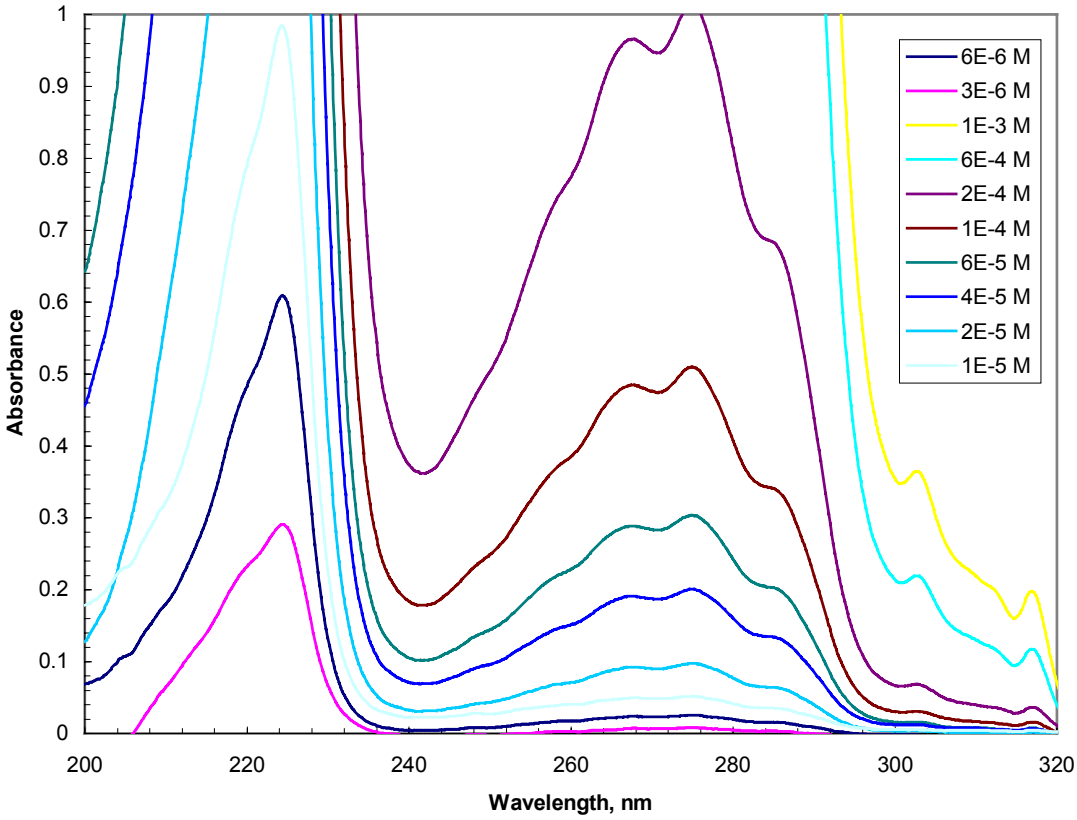

Figure 11. **Npa** UV spectra at different concentrations.

Analogous spectra were obtained for **Bpa-Fla** and **Npa-Fla** dipeptides, figures 12 and 13.

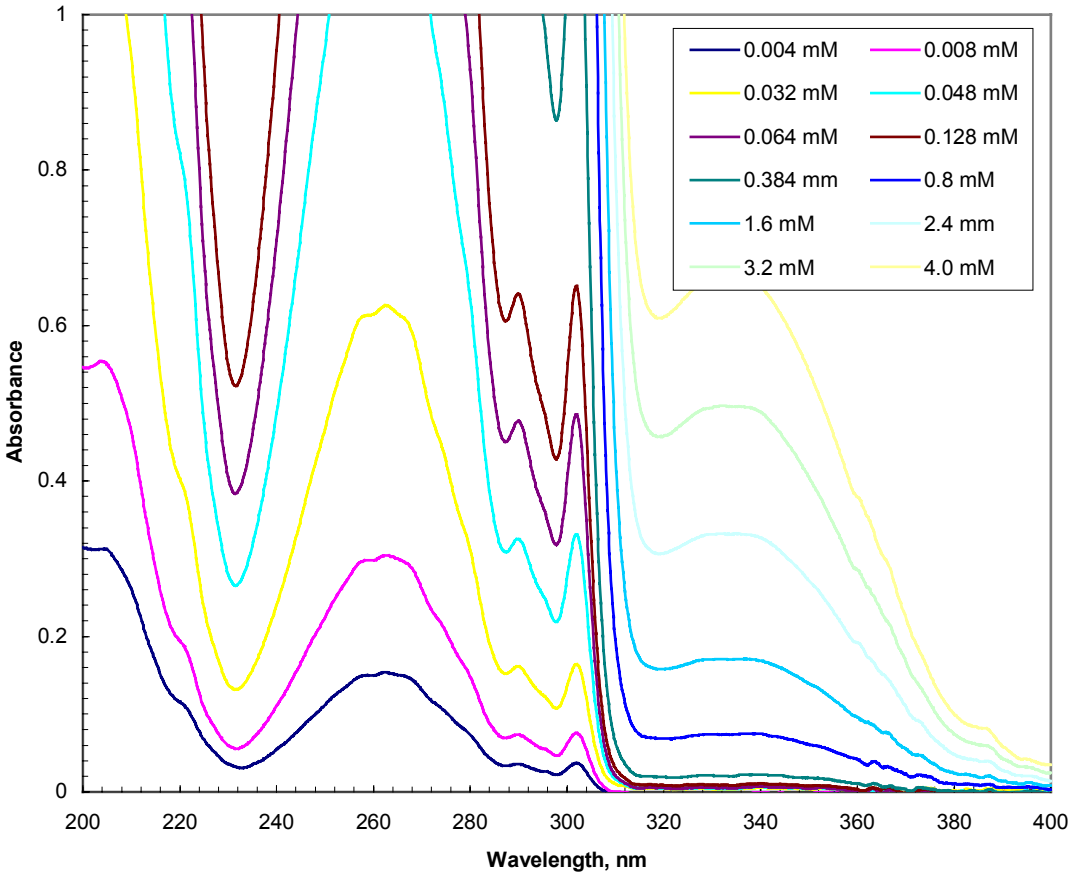

Figure 12**.** **Bpa-Fla** dipeptide UV spectral analysis.

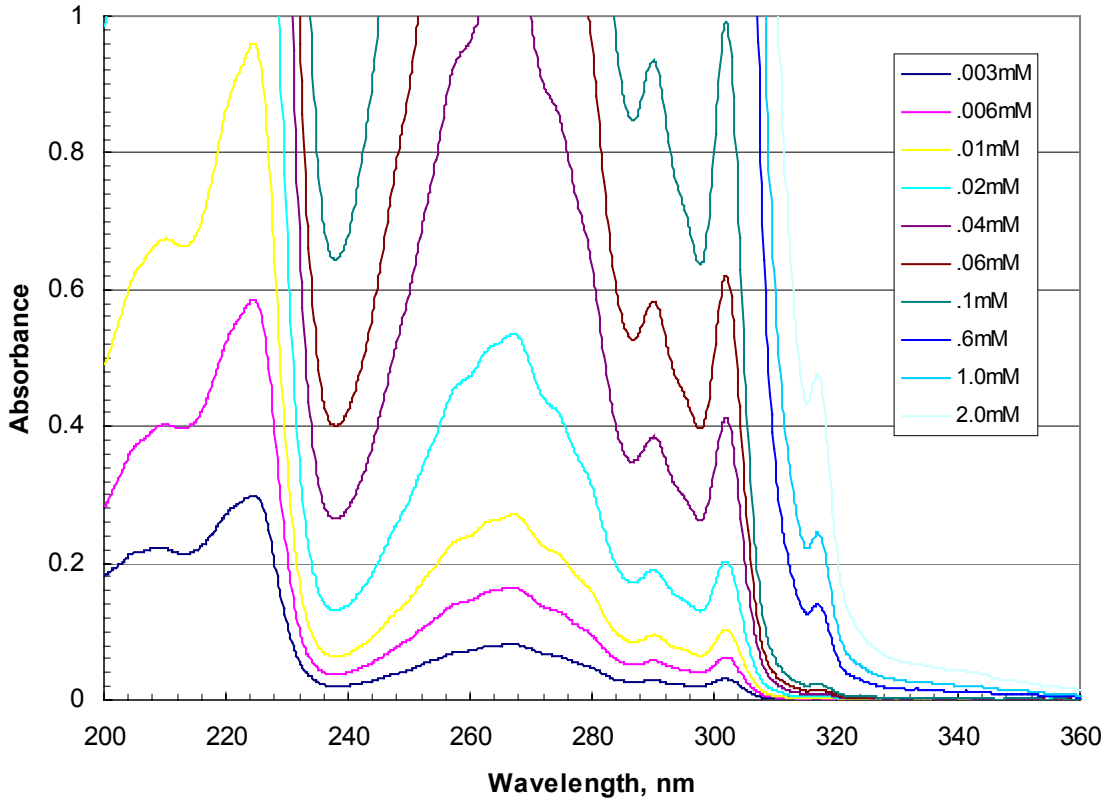

Figure 13. **Npa-Fla** dipeptide UV spectra at different concentrations.

Ground state extinction coefficients for model compounds **Npa**, **Fla** and **Bpa** and both dipeptides were determined from the above spectra. Extinction coefficient plots of the dipeptides are virtually identical to the composite plots from the model compounds indicating that there is little interaction in the ground state between the chromophores. Figure 14 contains the extinction coefficient data for **Bpa**, **Fla**, the sum of the their spectra and for the **Bpa-Fla** dipeptide. Figure 15 shows the same information for the **Fla-Npa** system.

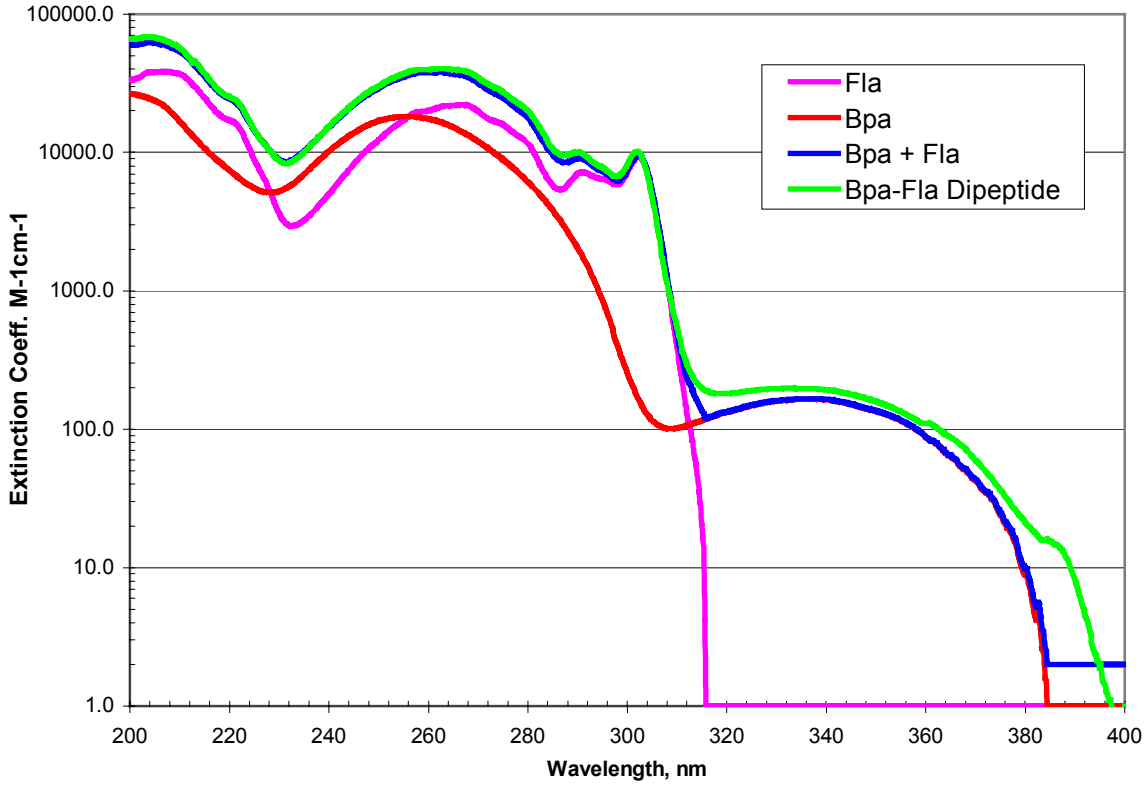

Figure 14**.** Extinction coefficient vs. wavelength for **Bpa-Fla** dipeptide and model compounds.

ZINDO/S calculations on dipeptides with similar chromophore moieties indicated that the highest six occupied molecular orbitals and the lowest six unoccupied molecular orbitals were localized in the individual chromophores. Therefore it was unlikely that excitation of the localized ground state of one chromophore would result in the production of an excited state in another chromophore. As a result, the extinction coefficients of the model compounds at each wavelength were used to estimate how the initial excitation

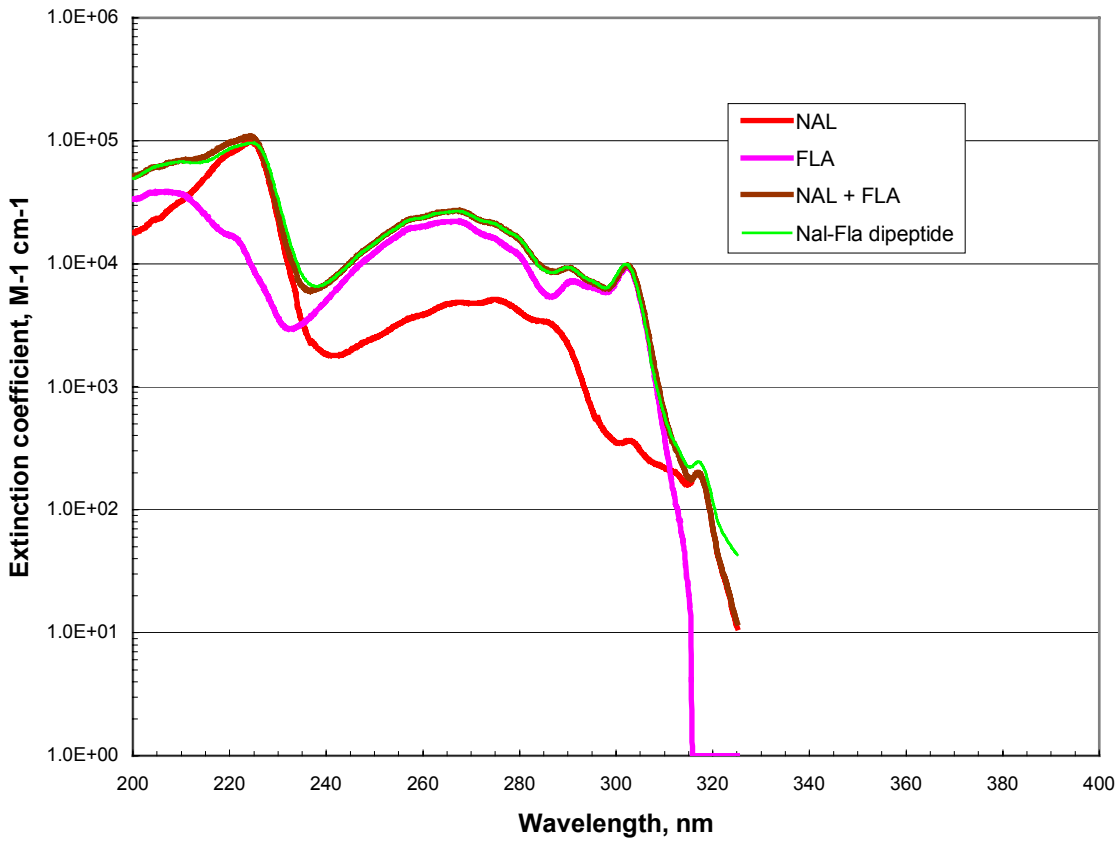

Figure 15**.** Extinction coefficient vs. wavelength for **Npa-Fla** dipeptide and model compounds.

was partitioned between the two chromophores in the dipeptides. These "excitation distributions" (ED) expressed as percentages of the total excitation for each wavelength, are shown in Table 2. The wavelengths were chosen to produce the maximum variation in absorption conditions.

Energy Distribution in the Singlet Manifold

Singlet energies (E_s) for the model compounds and dipeptides were determined from the fluorescence excitation and emission spectra. Figure 16 shows the **Fla** fluorescence excitation and emission spectra. Since **Bpa** essentially does not fluoresce ($\Phi_{fl} = 4 \times 10^{-6}$)[20], the literature value of 78.2 kcal/mol for 4-methyl benzophenone was used.[20] The literature values for **Fla** and **Npa** are very similar to the experimental values an indication that the amino acid contributes little to the electronic structure of the ground state. Thus, the literature value for **Bpa** can be taken as a reasonable estimate. Figure 17 is an analogous plot for **Npa**, except the area where the plots intersect has been enlarged to show the point of intersection.

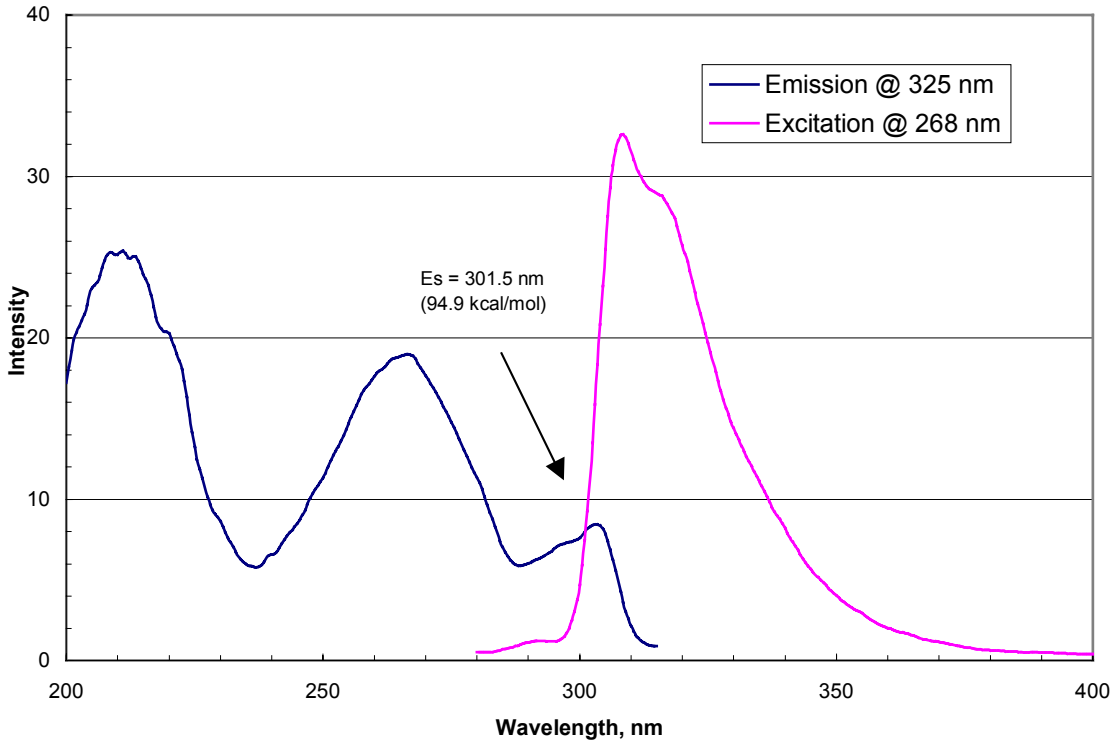

Figure 16. **Fla** emission and excitation fluorescence spectra.

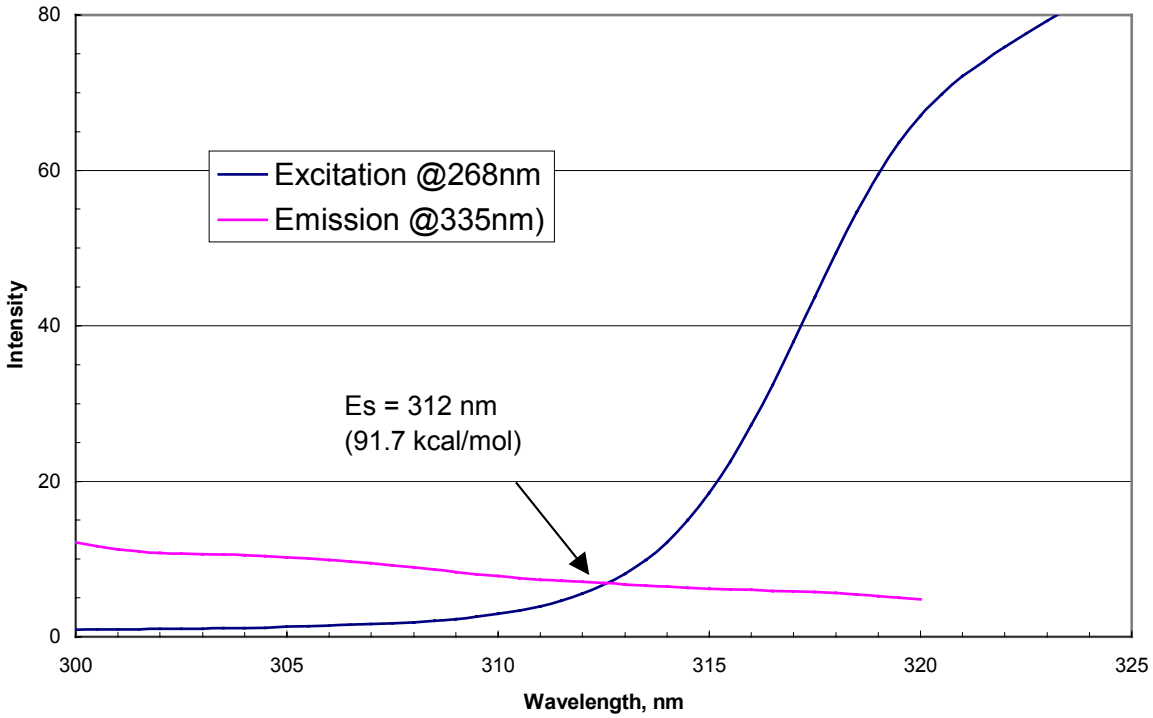

Figure 17. **Npa** emission and excitation fluorescence spectra.

While the dipeptide **Bpa-Fla** emission spectrum was similar in shape to **Fla** a significant difference was the reduced dipeptide fluorescence emission intensity. Figure 19 shows the fluorescence spectra of **Fla** and the **Bpa-Fla** dipeptide at the same excitation wavelength (260 nm) and ground state absorption value. The intensity was reduced to approximately 7% of the value of **Fla**.

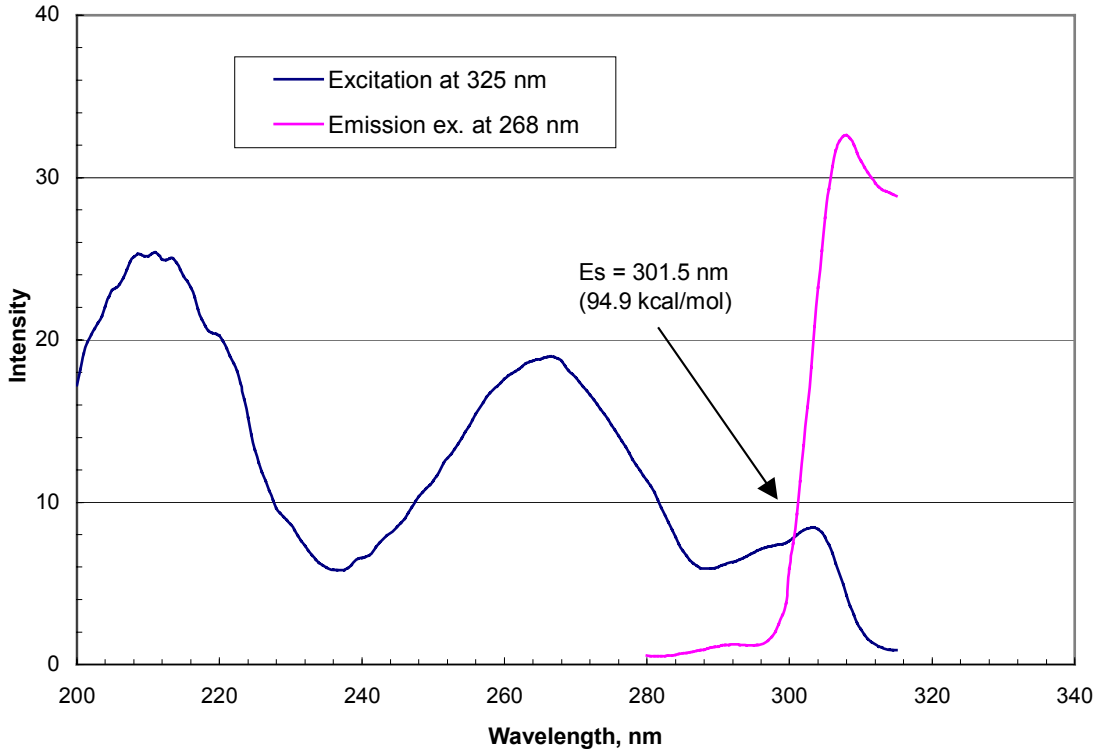

Figure 18. **Bpa-Fla** dipeptide emission and excitation fluorescence spectra.

Figure 20 shows the **Npa-Fla** dipeptide emission and excitation spectra. The singlet energy was evaluated as 93.3 kcal/mol. Since both **Npa** and **Fla** have similar singlet energies it was not possible to distinguish unambiguously between the two. In fact, the shape of the spectrum suggests a mixture of the two emission spectra. However, at the same time it is clear that the ratio of **Npa** to **Fla** emission observed in Figure 20 is not the same as would be expected from the ratio of initial excitation distributions. This is confirmed by Figure 21 which shows the emission spectrum of **Npa-Fla** overlaid with a composite spectrum constructed by adding **Npa** and **Fla** emission spectra in a intensity

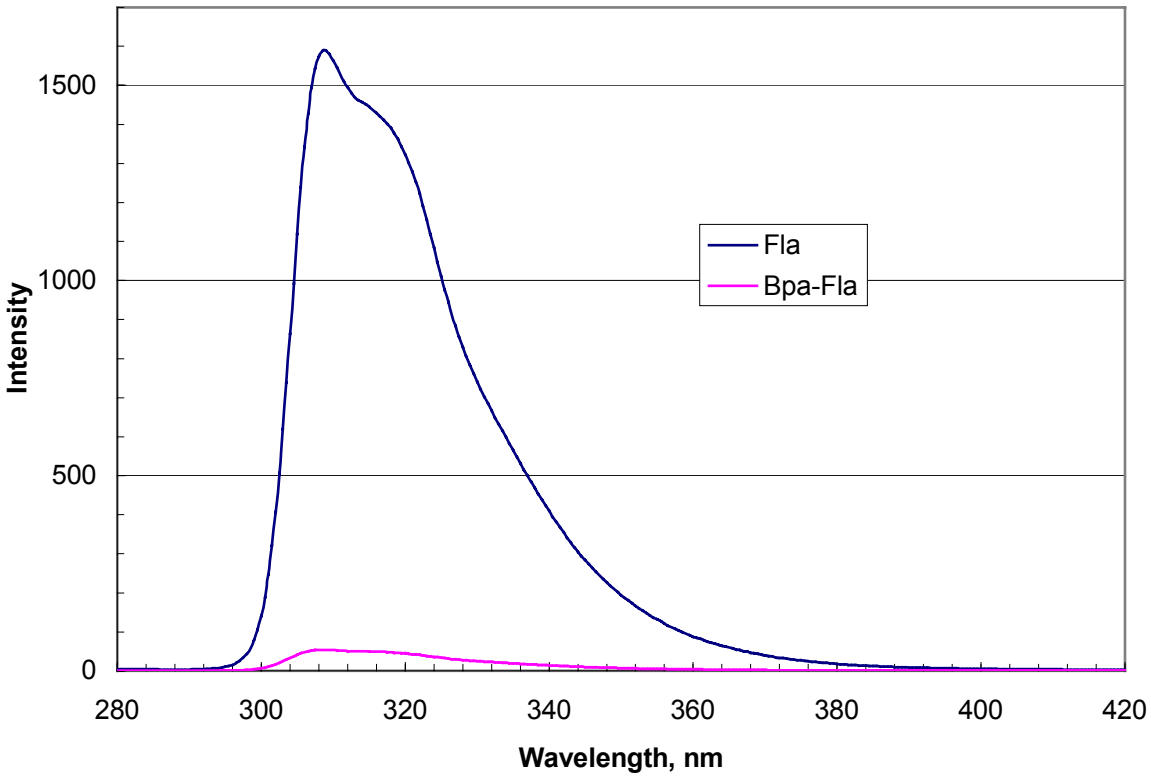

Figure 19. **Fla** and **Bpa-Fla** dipeptide fluorescence emission spectra, excitation at 260 nm.

ratio that provides a match with the experimental spectrum – 96.5% **Npa**:3.5% **Fla**. (Compare with the initial excitation distribution ratio 16% **Npa**: 84% **Fla**.) Similar attenuations are observed at all excitation wavelengths employed. (See Table 2.)

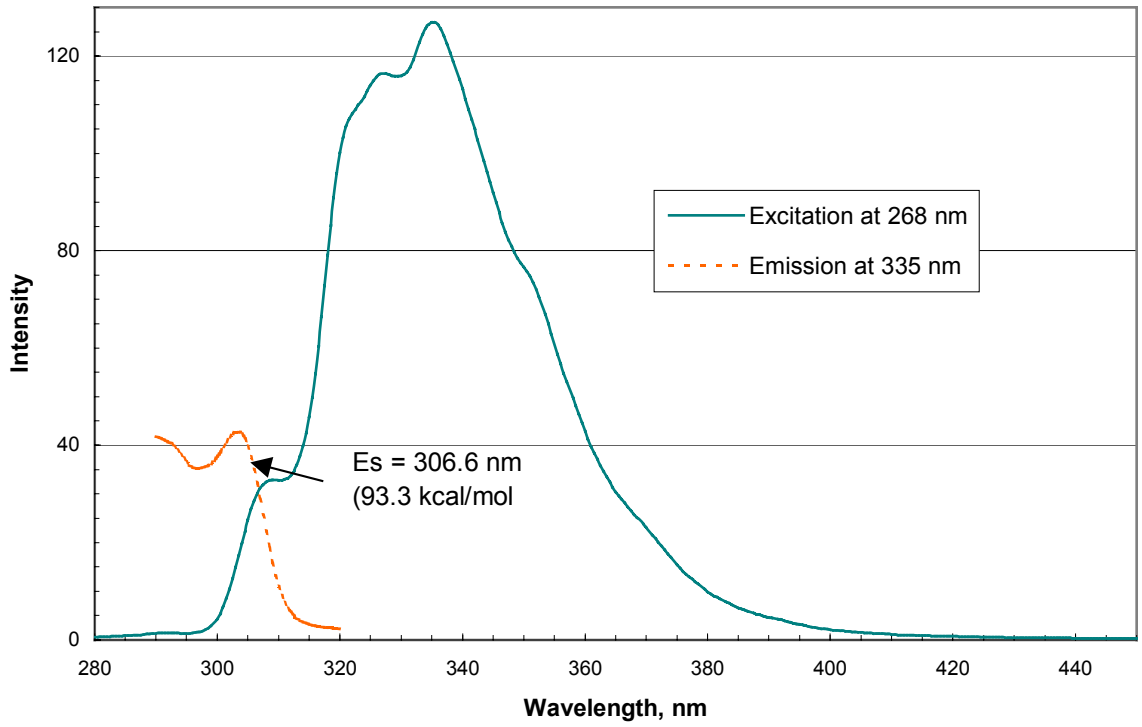

Figure 20. **Npa-Fla** dipeptide emission and excitation fluorescence spectra.

The attenuation of the **Fla** emission in the **Npa-Fla** and the **Bpa-Fla** dipeptides as compared to that expected from the initial excitation distribution is a good indicator for SSET from the fluorene moiety to the naphthalene (benzophenone) group, and allows an estimate of the **Fla**—>**Bpa** and **Fla**—>**Npa** energy transfer rate constant to be made. It should be noted that given the submillimolar concentrations of the dipeptides and the known short singlet lifetime of the fluorene chromophore,[20] energy transfer is an intramolecular process. The attenuation of emission was quantified by comparing the initial excitation distribution (ED value) for the **Fla** in each dipeptide with the final ED

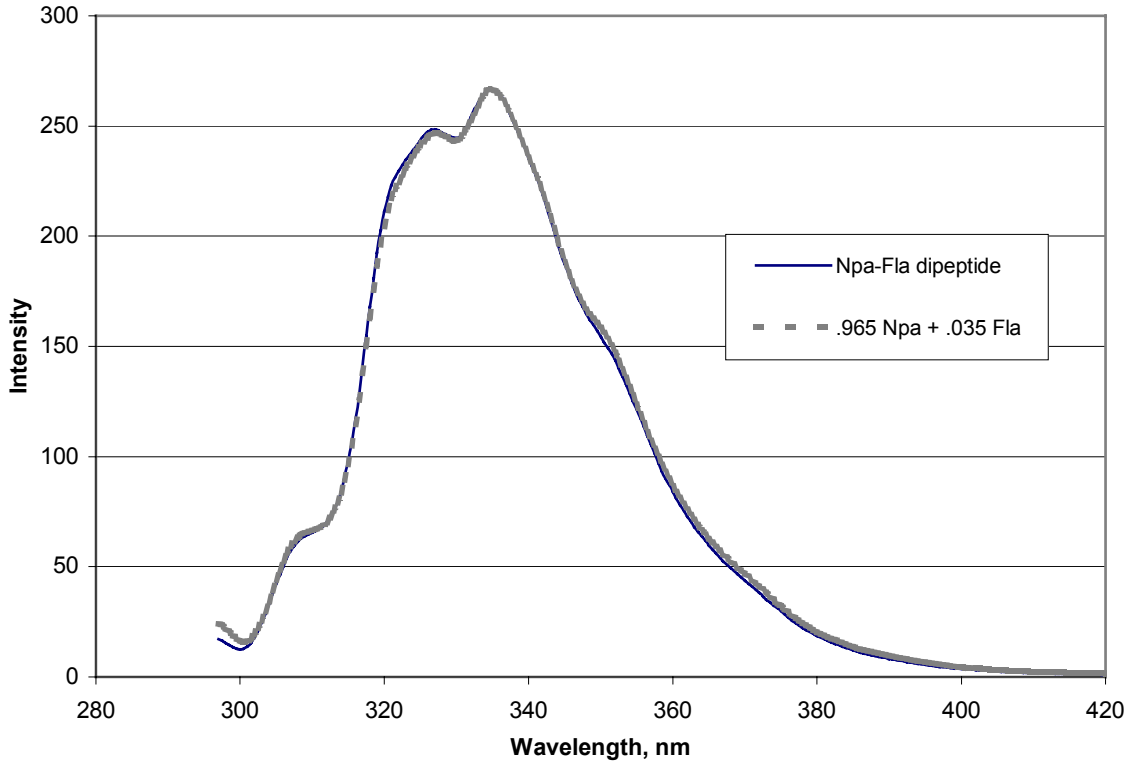

Figure 21. **Npa-Fla** fluorescence emission spectrum overlay with 96.5:3.5 **Npa:Fla** composite emission spectrum, excitation at 295 nm.

value as determined from the composite spectra or, in the case of **Bpa-Fla**, the **Fla** spectrum alone. The ratio of the two values $ED_{final}/ED_{initial}$ is equivalent to the ratio of the fluorescence quantum yields in the absence and the presence of the acceptor and is equal to the fluorescence emission efficiency (E_F). The SSET efficiency (E_{SSET}) was calculated using eq 7. The ED data in Table 2 indicate that as an average over the four excitation wavelengths, the SSET efficiencies for **Fla** in **Bpa-Fla** and **Npa-Fla** are 0.92 and 0.98 respectively. Using this value in eq 7 yields an estimate of the energy transfer rate constant, k_{SSET}.

$$E_F = \frac{\Phi^F_{dipeptide}}{\Phi^F_{Fla}} = \frac{ED_{Final}}{ED_{Initial}} = \frac{k_F/(k_{all}+k_{SSET})}{k_{SSET}/k_{all}} = \frac{k_{all}}{k_{all}+k_{SSET}} \quad (7)$$

In eq 7, k_F is the radiative rate constant for **Fla** and is assumed to be equal in both dipeptides and k_{all} is the sum of the rate constants for all intrachromophore deactivation processes including k_F, k_{IC}, and k_{ISC} and is equivalent to the rate constant obtained from the literature[20] for fluorene, 1 x 10^8 s^{-1}. Using this equation yields k_{SSET} = 4.9 x 10^9 s^{-1} for **Bpa-Fla** and 1.2 x 10^9 s^{-1} for **Npa-Fla.**

Table 2. Ground-state extinction coefficients and Energy Distribution (ED) values for **Npa, Bpa, Fla, Npa-Fla** and **Bpa-Fla.**

	Bpa	**Fla**	**Npa**	**Bpa-Fla**	**Npa-Fla**
ε_{295}	860	6440	650	7800	7230
ε_{260}	17540	20100	3860	39700	23650
ε_{235}	6960	3230	3380	10100	8140
ε_{220}	7440	17060	79070	25200	86210
ED Init./Final, %					
1) For Bpa-Fla	12/94	88/6	--	--	--
2) For Npa-Fla	--	91/3.5	9/96.5		
ED_{260}, %					
1) For Bpa-Fla	47/96.5	53/3.5	--	--	--
2) For Npa-Fla	--	84/2	16/98	--	--
ED_{235}, %					
1) For Bpa-Fla	68/93	32/3	--	--	--
2) For Npa-Fla	--	49/1	51/99	--	--
ED_{220}, %					
1) For Bpa-Fla	30/93	70/7	--	--	--
2) For Npa-Fla	--	18/1	84/99	--	--
k_{SSET} from fluor. data, s^{-1}				1.2×10^9	4.9×10^9
k_{SSET} from Hyperchem data, s^{-1}				7.0×10^8	5.1×10^9

Energy transfer rate parameters can be calculated using Förster theory (eq 8, 9) and compared with experimental values calculated as described above. This will give an indication as to the identity of the SSET mechanism operating in the dipeptide.

$$R_0^6 = \frac{9100(\ln 10)\Phi_d \kappa^2}{128\eta^4 \pi^5 N_A} J \tag{8}$$

$$E_{SSET} = \left[1 + (R/R_0)^6\right]^{-1} \tag{9}$$

In equation 8, κ^2 is a term that describes the relative orientation of the transition dipoles for the donor and acceptor moieties and in the case of freely rotating chromophores is usually assigned a value of 2/3, η is the refractive index of the solvent (for MeCN η = 1.34423), N_A is Avogadro's number, J is the spectral overlap integral and Φ_d is the fluorescence quantum yield of the donor. R and R_0 are the Förster distance and the critical Förster distance, respectively.

The fluorescence quantum yield for **Fla** was determined by measuring the fluorescence of fluorene (Φ_F = 0.68) [20] at the same concentration and excitation wavelength as **Fla** and calculating the ratio of the areas associated with the emission spectra, eq 10. Since the **Fla**: fluorene emission ratio = 0.85, (from figure 22), Φ_{Fla} is calculated as 0.58.

$$\Phi_{fluorene}/\ \Phi_{Fla} = A_{fluorene}/A_{Fla} \tag{10}$$

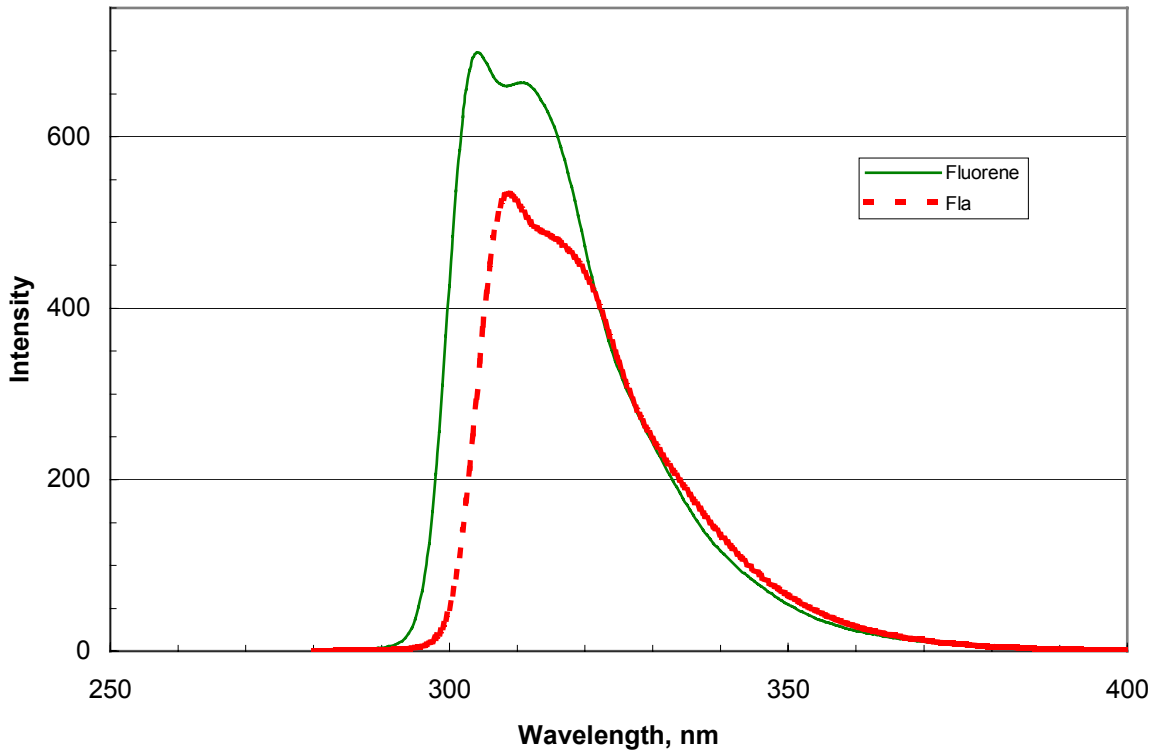

Figure 22. **Fla** and fluorene fluorescence spectra overlay, excitation at 268 nm.

The spectral overlap integral, *J* was determined empirically from the fluorescence emission and excitation data and was normalized so that complete overlap would correspond to a *J* value of 1.0. Figures 23 and 24 show the areas of overlap for the two dipeptides. The areas were calculated from the digital data, and found to be 1.435 x 10^{-16} L cm^3 mol^{-1} for **Bpa-Fla** and 1.711 x 10^{-16} L cm^3 mol^{-1} for **Npa-Fla**.

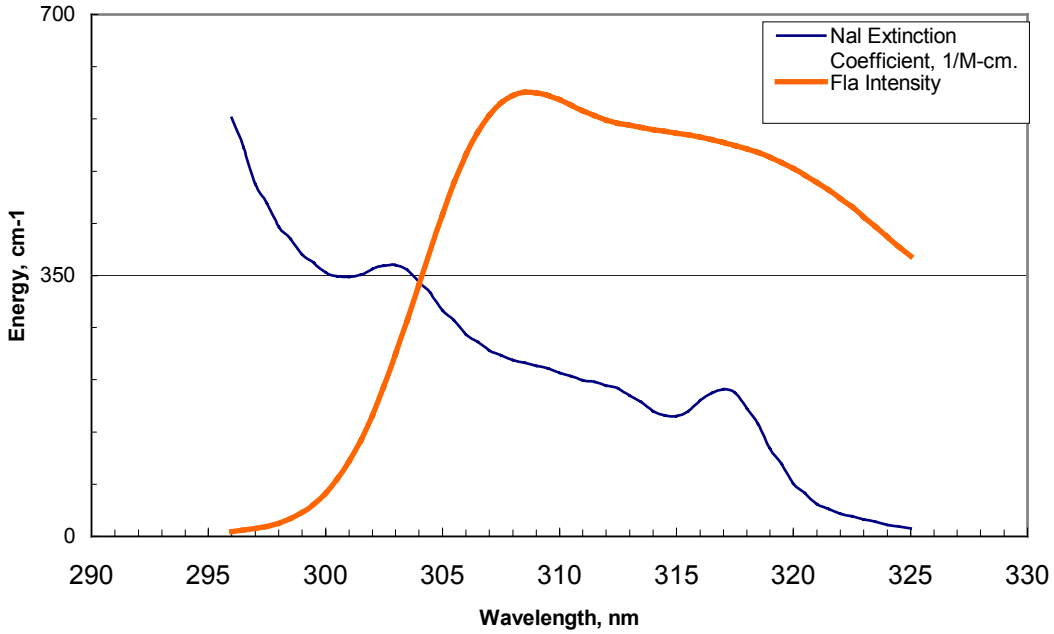

Figure 23. **Npa** and **Fla** UV absorbance and fluorescence emission spectral overlap plot.

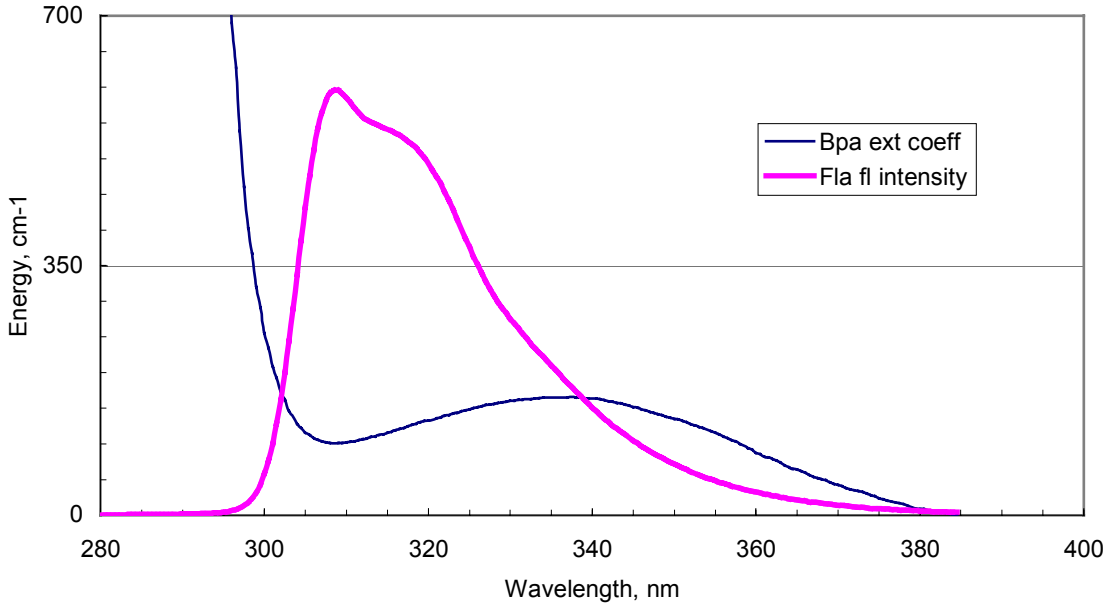

Figure 24. **Bpa** and **Fla** UV absorbance and fluorescence emission spectral overlap plot.

With the fluorescence quantum yield of **Fla**, R_0 was calculated as 16.2 Å. With R_0, R for the dipeptides was calculated with the efficiency equation, eq 9. The distance between **Bpa** and **Fla** in the dipeptide determined in this way was 9.14 Å, while for **Npa-Fla,** R = 8.69 Å.

Hyperchem MM3 molecular modeling

The R_{calc} values for the **Bpa-fla** and **Npa-Fla** dipeptides are substantially smaller than R_o reflecting the relatively efficient quenching of the donor fluorescence in each case. Molecular modeling and dynamics calculations for the dipeptides were carried out using HyperChem 5.02 (PC version, HyperCube, Inc.) to estimate the interchromophore separation for comparison with R_{calc}. (Separations calculated from these modeling studies are given as R_{model} in Table 3. The Hyperchem models of the two dipeptides and the 15-residue polypeptide are depicted in figures 25-27. Several conformations of each molecule were investigated and each was optimized to produce the minimum energy. The models shown were the optimized trans conformations. Interchromophoric distances were determined by averaging all the distances between each carbon in the aromatic rings (plus the carbonyl for benzophenone). Because the benzophenone singlet state acceptor is $n\pi^*$ in character and is therefore localized on the carbonyl group, the distance from the carbonyl group to the average fluorenyl carbon, 11.7 Å, was used for the efficiency calculations.

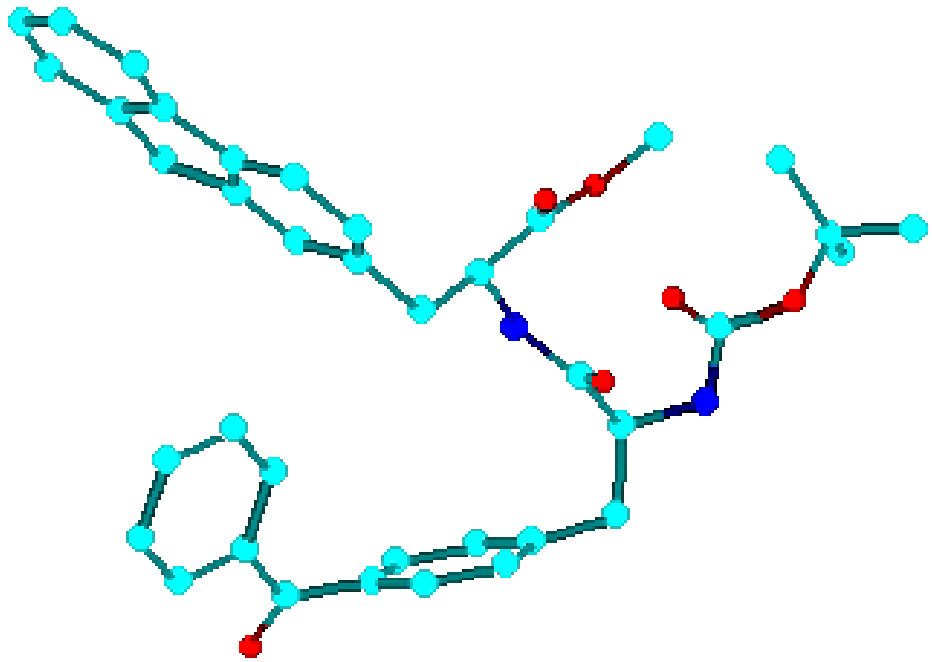

Figure 25. Hyperchem MM3 optimized model of **Bpa-Fla** dipeptide.

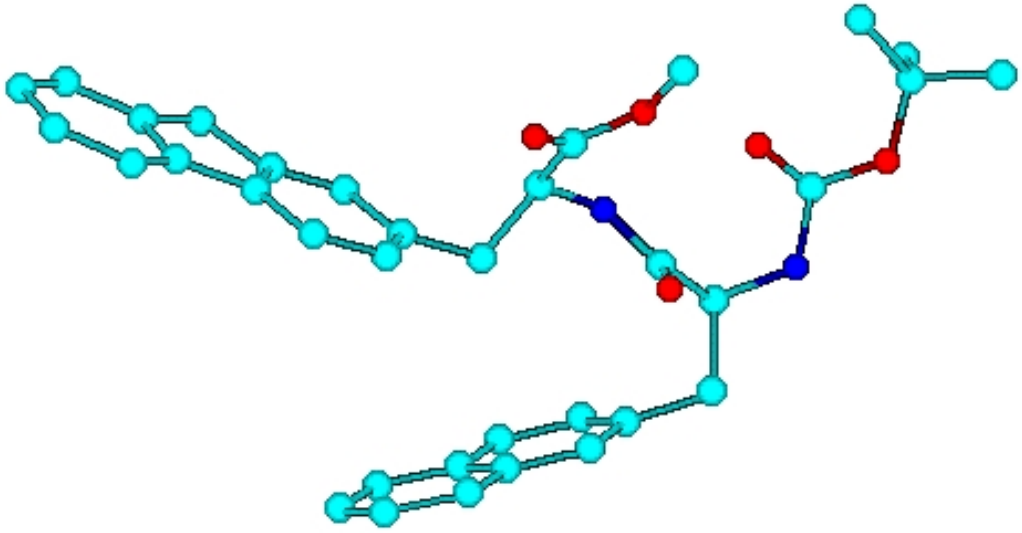

Figure 26. Hyperchem MM3 optimized model of **Npa-Fla** dipeptide.

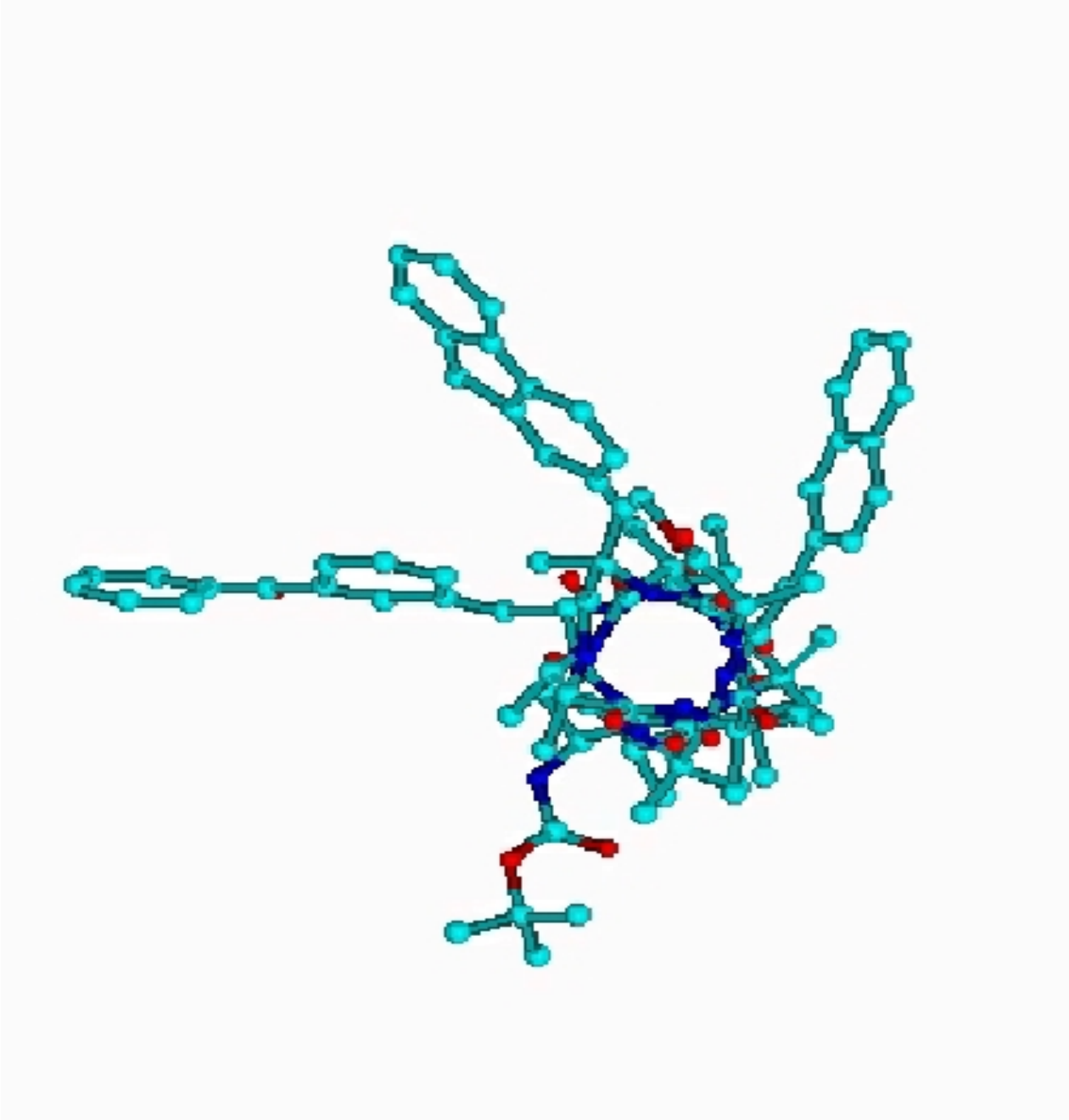

Figure 27. Hyperchem MM3 optimized model of trichromophore 15-residue polypeptide.

Singlet energy transfer rate constants were calculated from the fluorescence data with the inclusion of HyperChem modeling results. Rather than using the efficiencies to calculate

R, the R-values from the computer modeling were used to calculate efficiencies and the rate constants. Hyperchem R values for **Bpa-Fla** and **Npa-Fla** were 11.7 ± 3.1 and 10.6 ± 2.9Å, respectively. With these values, eq 9 calculations yielded **Bpa-Fla** $E_{SSET} = 0.88$ and **Npa-Fla** $E_{SSET} = 0.93$ and, from eq 7, $k_{SSET} = 7.0 \times 10^8\ s^{-1}$ and $5.1 \times 10^9\ s^{-1}$, for **Bpa-Fla** and **Npa-Fla** respectively. The magnitudes of these rates compare favorably to those calculated from the experimental data, giving further verification for the Förster-type SSET proposed.

Energy Distribution in the Triplet Manifold

Phosphorescence

Phosphorescence spectra of **Bpa-Fla** and **Npa-Fla** dipeptides and the three model compounds measured in 77 K 1:1 MeOH/EtOH glasses yielded the spectra and triplet energies shown in figures 28-32. The spectra for **Npa**, **Fla** and **Bpa** model compounds were similar to literature spectra for the parent aromatics.[20] The **Bpa-Fla** band shape was similar to **Fla**. However, the intensity of the fluorenyl emission in the dipeptide was nearly 7 times greater than in **Fla**.

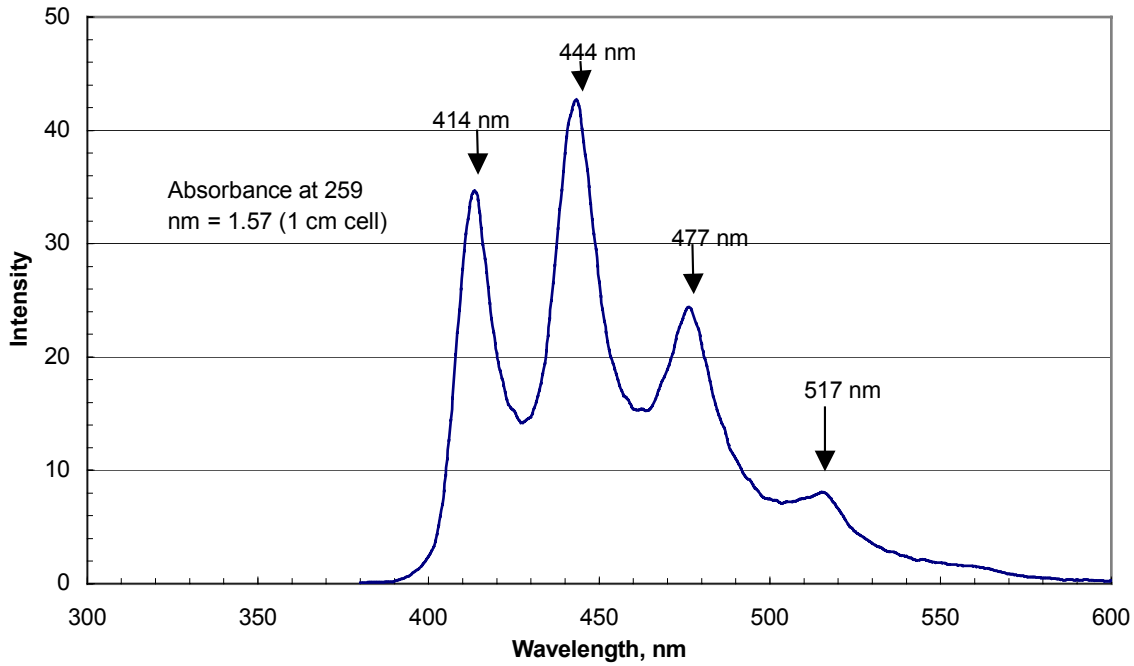

Figure 28. **Bpa** phosphorescence spectrum, excitation at 259 nm.

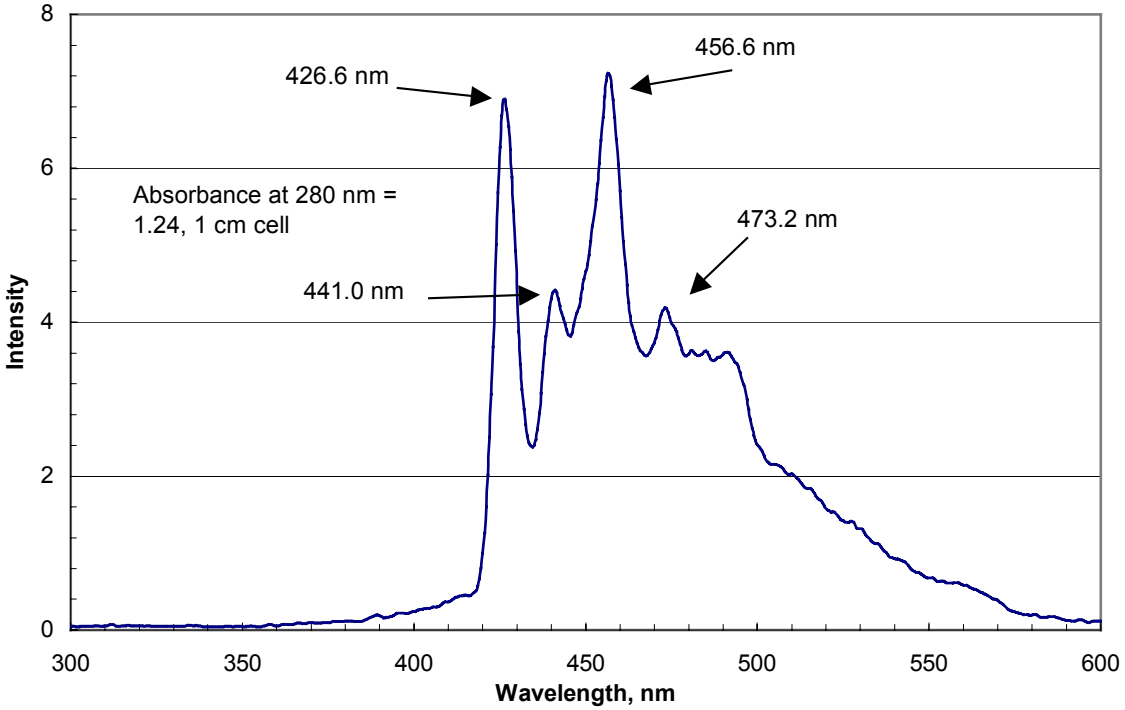

Figure 29. **Fla** phosphorescence spectrum, excitation at 280 nm.

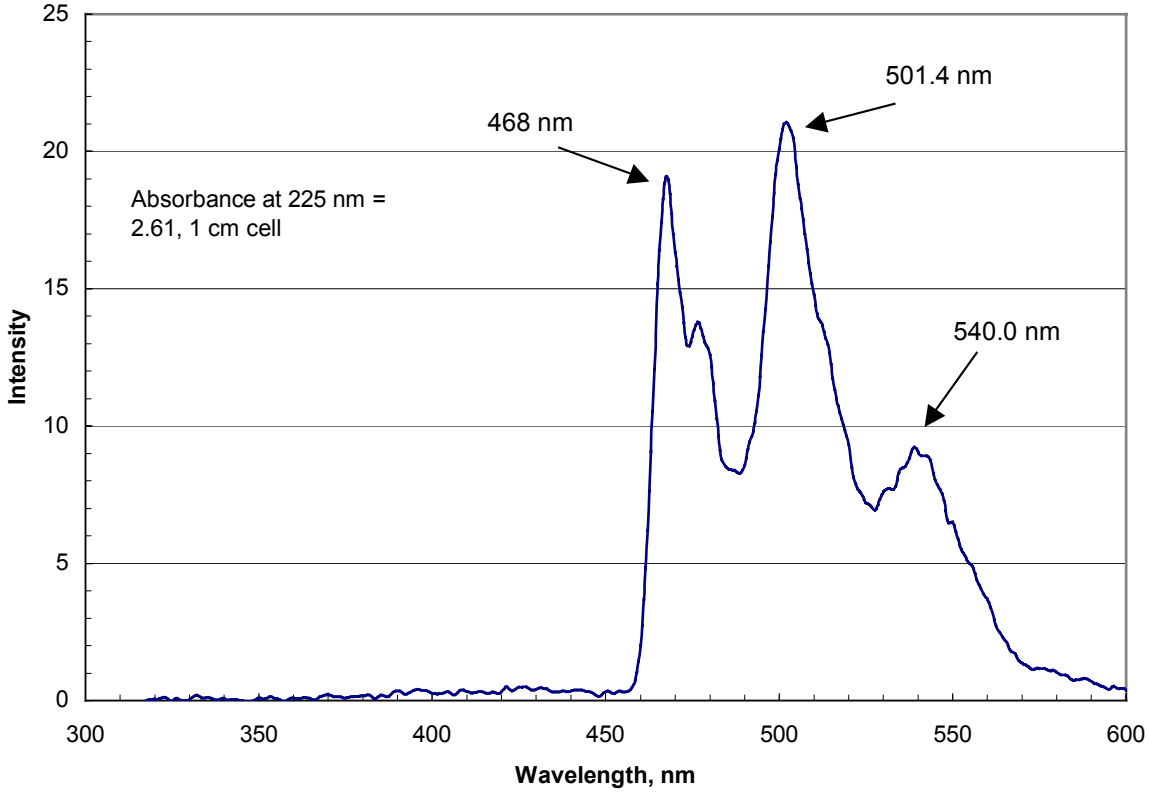

Figure 30**.** **Npa** phosphorescence spectrum, excitation at 225 nm.

The **Npa-Fla** band shape was similar to **Npa** but also included a band in the 400-450 nm range, which was identified as residual **Fla** emission. These phosphorescence results are strongly suggestive of TTET from the benzophenone to fluorene moiety in the case of **Bpa-Fla** and from the fluorene group to the naphthalene chromophore in **Npa-Fla**. Furthermore, since the 77 K matrix prevents efficient diffusion, the energy transfer is almost certainly intramolecular. While it is tempting to attempt to abstract TTET rate information from the phosphorescence intensities for the dipeptides and models, uncertainties generated by variable path lengths are too large to derive any meaningful values. However, based on the results we can assign an approximate value in the case of

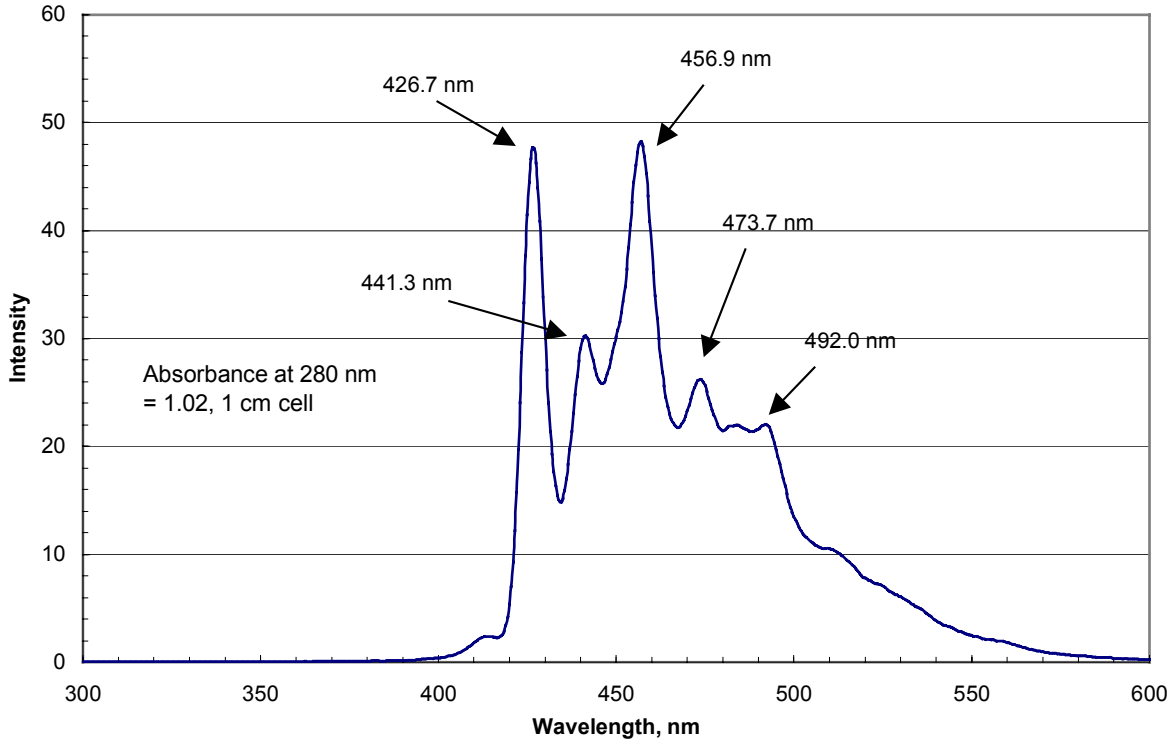

Figure 31**.** **Bpa-Fla** dipeptide phosphorescence spectrum, excitation at 280 nm.

Npa-Fla ($k_{TTET} \sim 7 \times 10^3\ s^{-1}$). This value is based on the phosphorescence lifetime of fluorene and our observation of at least some **Fla** phosphorescence in the dipeptide spectrum.

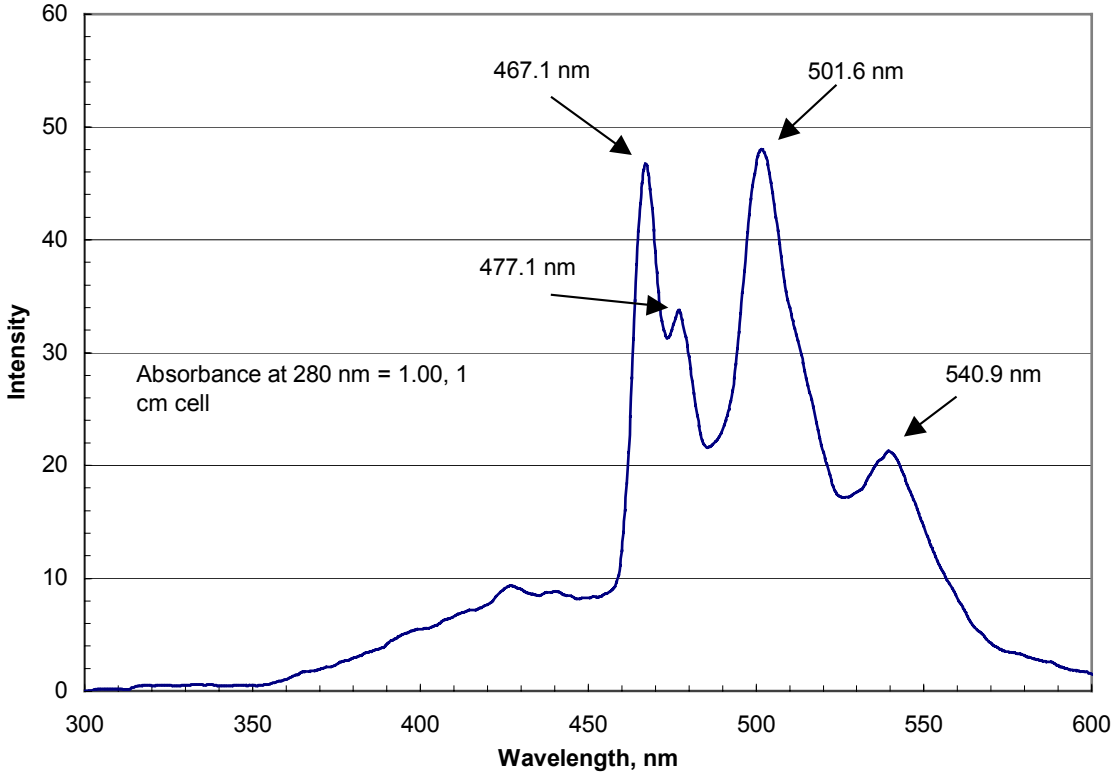

Figure 32**.** **Npa-Fla** phosphorescence spectrum, excitation at 280 nm.

Laser flash photolysis

Laser flash photolysis experiments were conducted on the **Npa-Fla** and **Bpa-Fla** dipeptides and the three model compounds. Kinetic traces for each model compound are shown in figures 33, 34 and 35 and verified that each exhibited triplet transients (as evidenced by O_2 quenching). **Bpa** was excited at 355 nm, while **Npa** and **Fla** were irradiated at 308 nm since the latter two compounds had no ground state absorption at 355 nm. As indicated in the transient absorption spectra, figures 36-38, the **Bpa** triplet state absorbs at λ_{max} = 520 nm, **Npa** at λ_{max} = 420 nm and **Fla** at λ_{max} = 380-390 nm,

comparable to literature values for each chromophore.[20] Table 3 shows the transient decay rates.

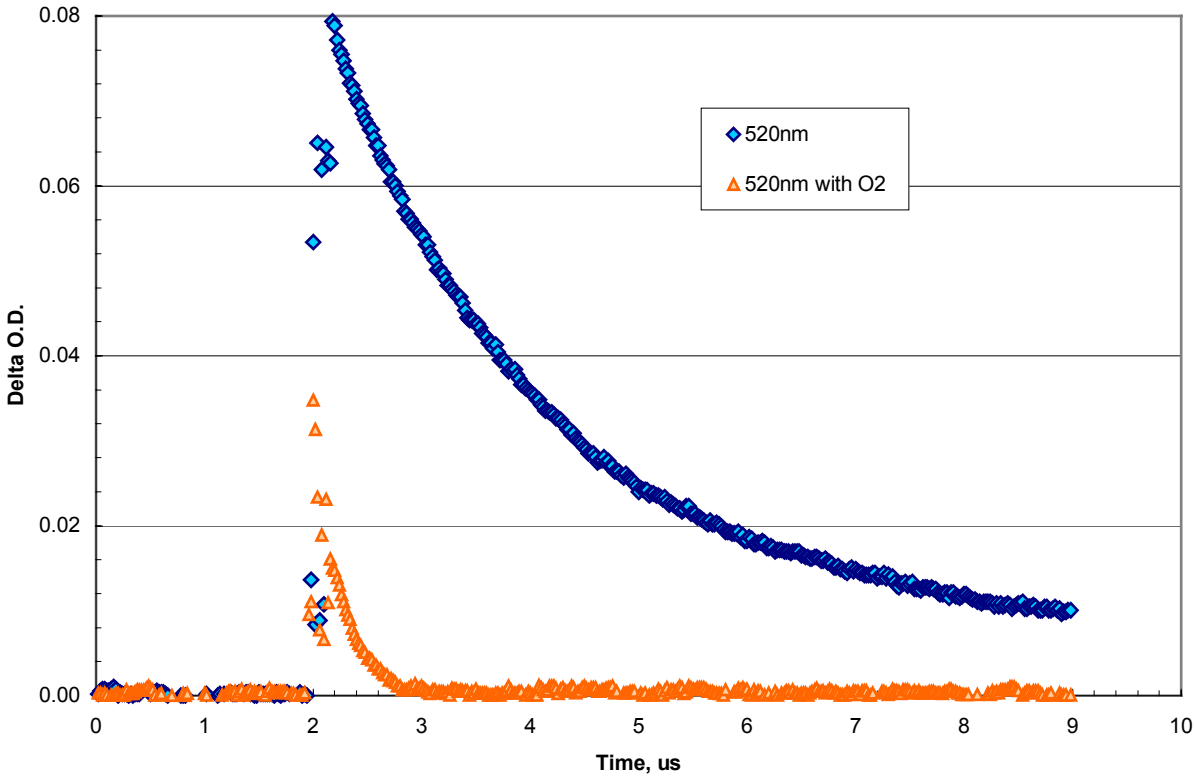

Figure 33. **Bpa** 520 nm transient decay spectrum, excitation with YAG laser at 355 nm, 32 mJ.

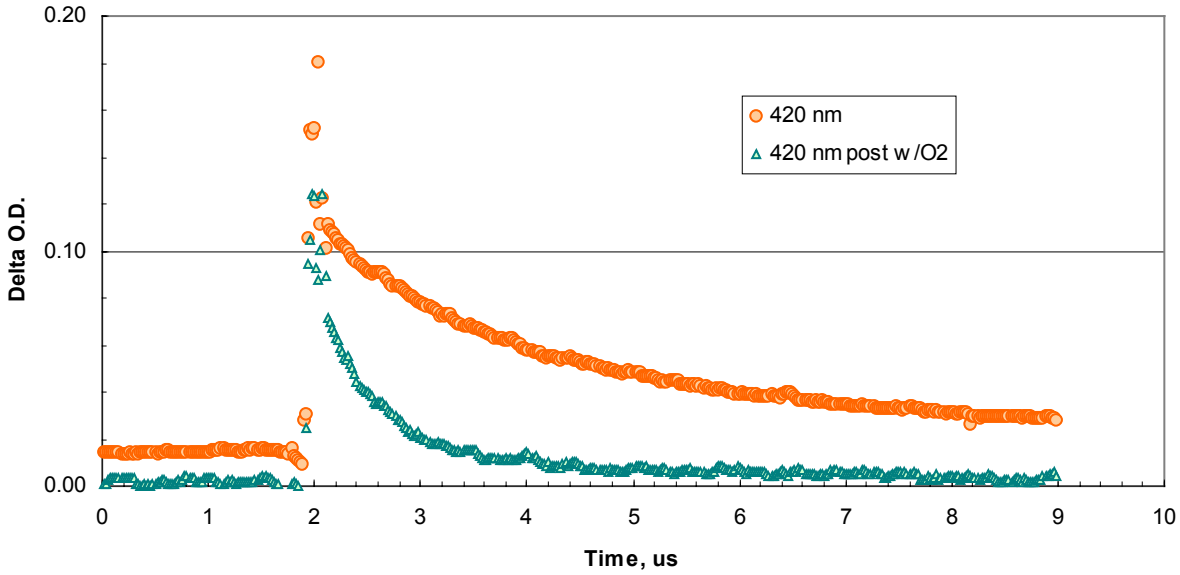

Figure 34**.** **Npa** 420 nm transient decay spectrum, excitation with Excimer laser at 308 nm, 36 mJ.

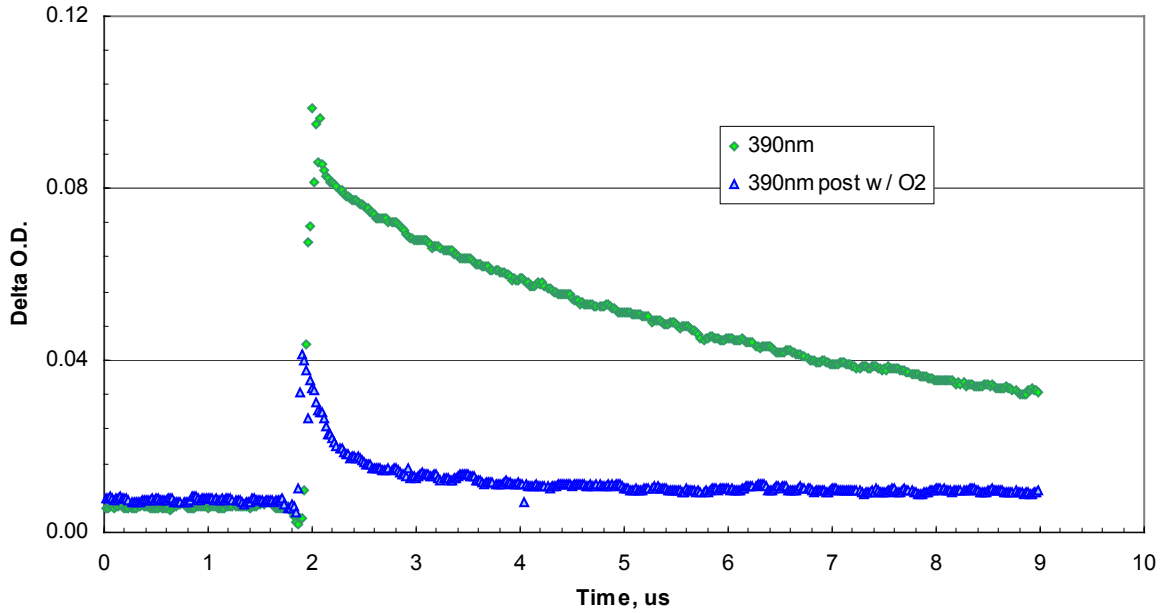

Figure 35. **Fla** 390 nm transient decay spectrum, excitation with Excimer laser at 308 nm, 32 mJ.

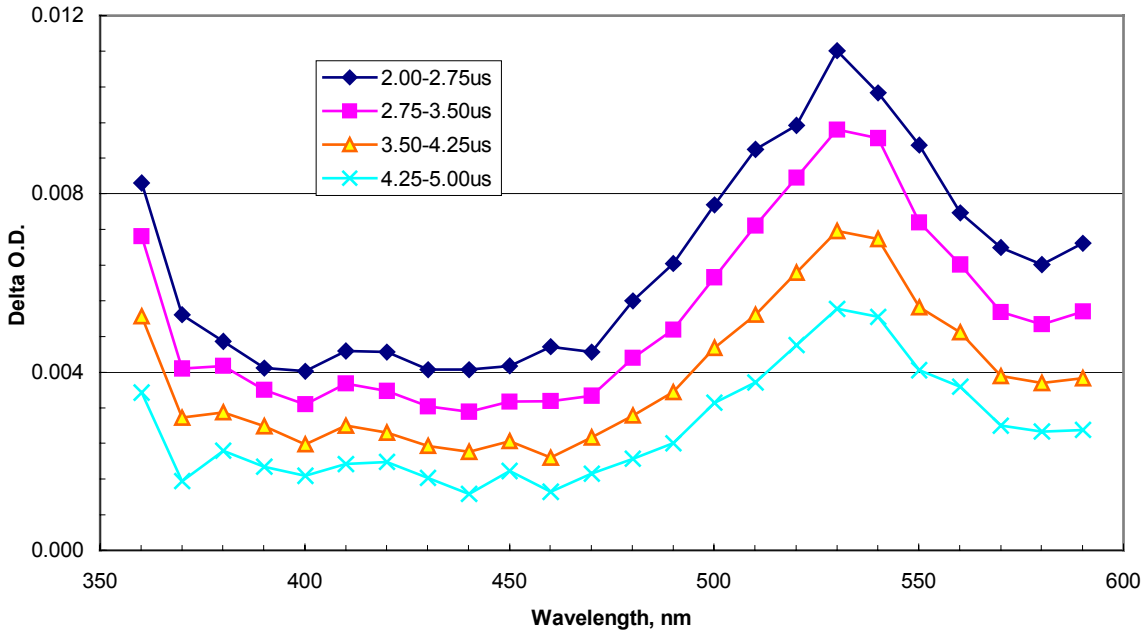

Figure 36. **Bpa** transient absorption spectra, excitation with YAG laser at 355 nm, 32 mJ.

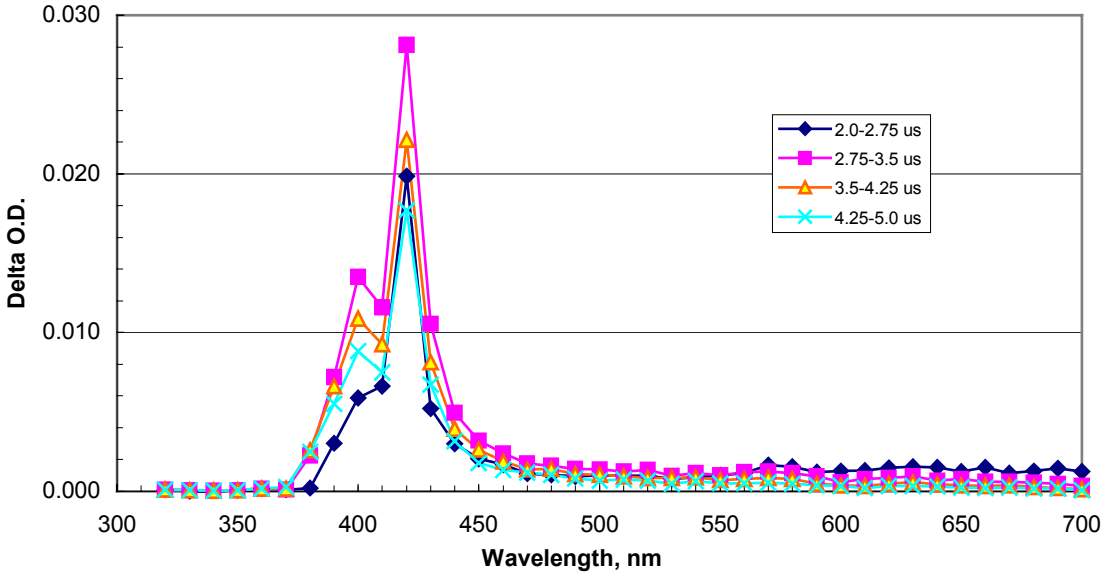

Figure 37. **Npa** transient absorption spectra, excitation with Excimer laser at 308 nm, 37 mJ.

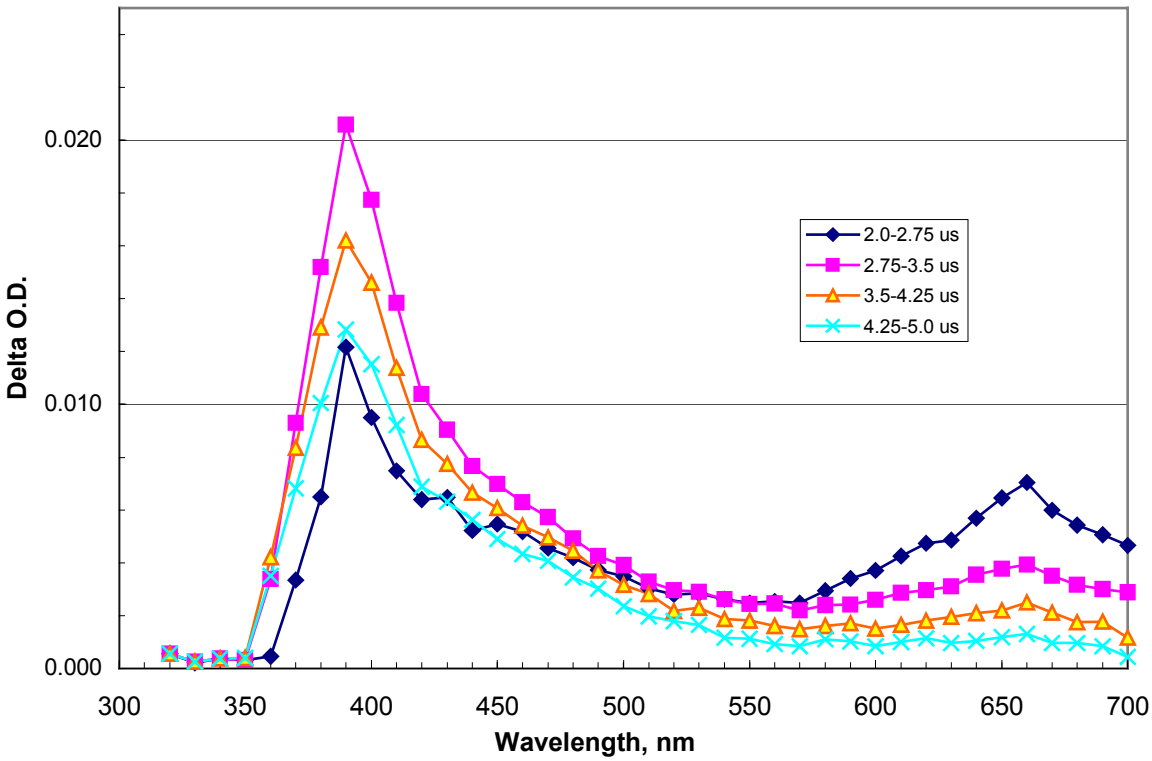

Figure 38. **Fla** transient absorption spectra, excitation with Excimer laser at 308 nm, 28 mJ.

Figures 39 and 40 show the kinetic traces for the **Bpa-Fla** dipeptide at 390nm, excited with the YAG laser at 355nm and the Excimer laser at 308nm. Both verify triplet transient absorption at 390 nm. The **Bpa-Fla** transient absorption spectra, figure 41 (excitation with YAG laser at 355 nm) and figure 42 (excitation with Excimer laser at 308 nm) show only the **Fla** absorption λ_{max} = 390 nm, i.e. no **Bpa** absorption was observed. These observations suggest that TTET occurs from the benzophenone group to the Fla group similar to the TTET behavior reported previously for a benzophenone-naphthalene dipeptide.[44] It should be noted that while the concentrations used in the laser

experiments are sufficiently high to make intermolecular TTET feasible, the fluorene triplet is produced within the duration of the laser pulse (10 ns), much too rapid for intermolecular transfer and indicative of an intramolecular process. These observations force the conclusion that $k_{TTET} > 10^8\ s^{-1}$, consistent with the phosphorescence results which showed a complete lack of benzophenone triplet present.

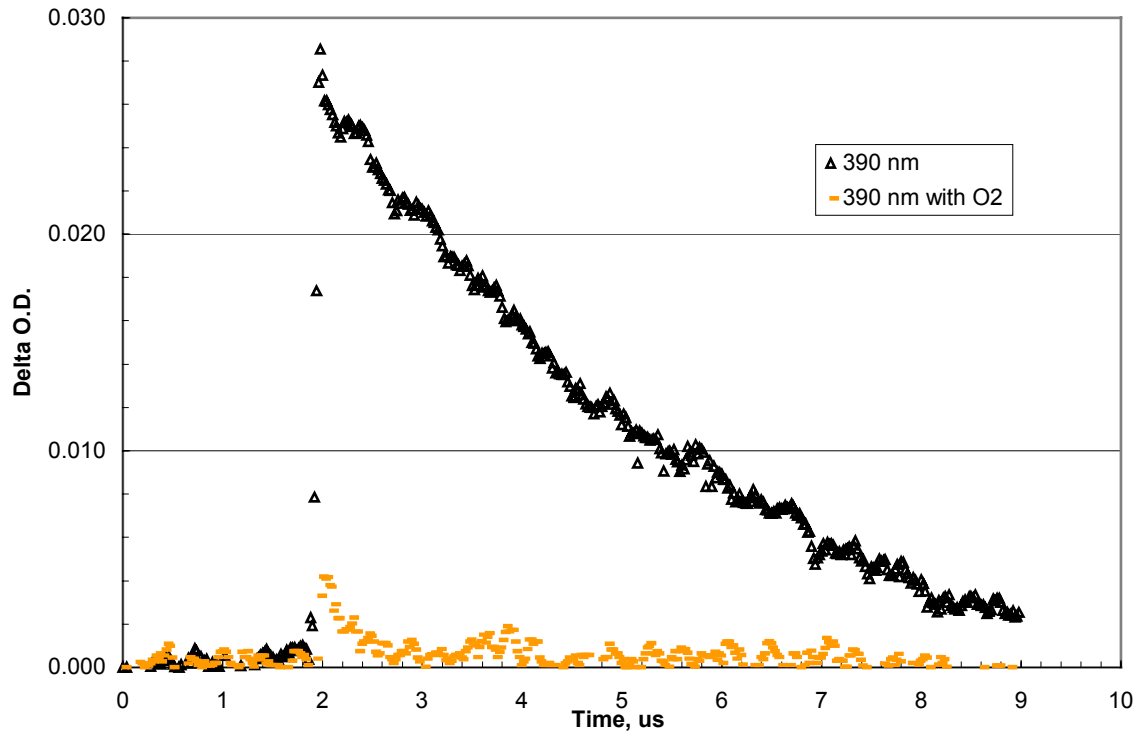

Figure 39. **Bpa-Fla** dipeptide 390 nm transient decay spectra, excitation with YAG laser at 355 nm, 16 mJ.

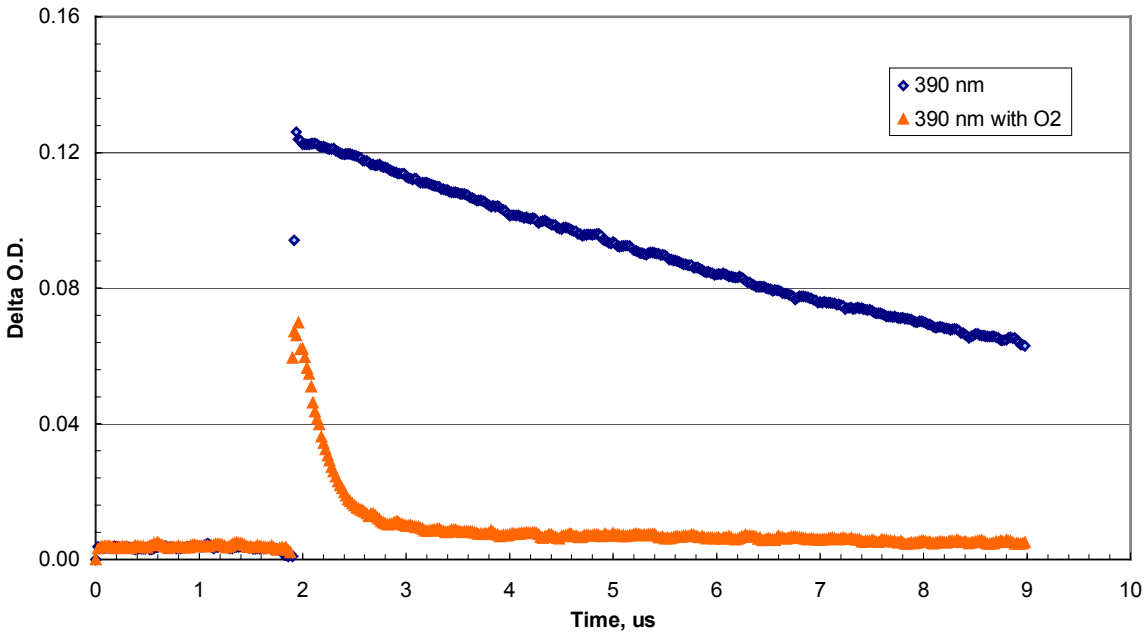

Figure 40. **Bpa-Fla** dipeptide 390 nm transient decay spectra, excitation with Excimer laser at 308 nm, 24 mJ.

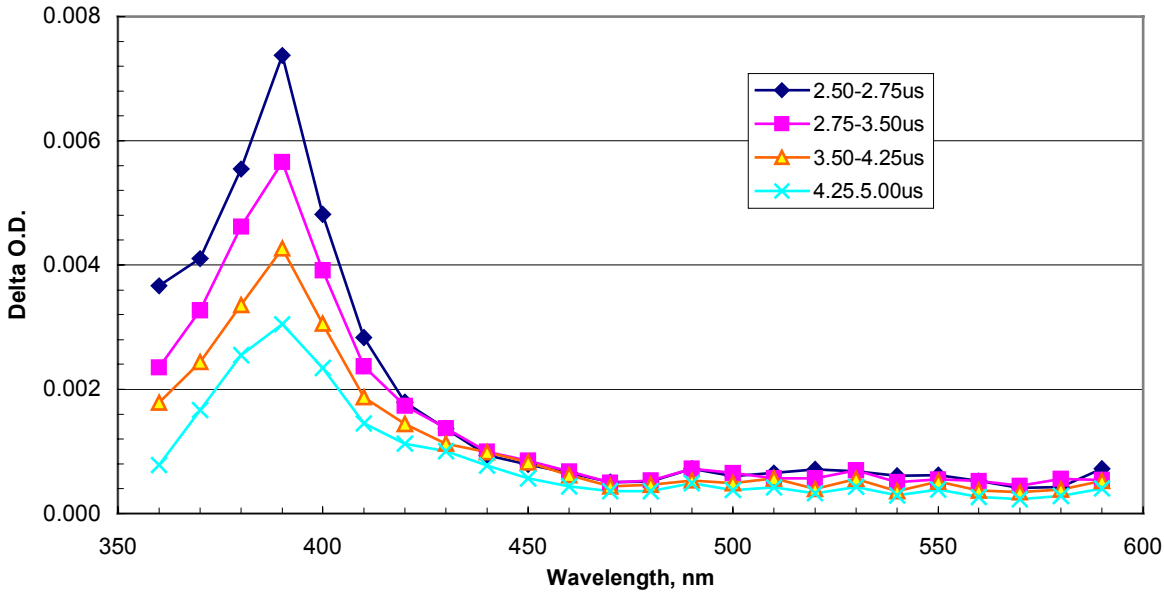

Figure 41. **Bpa-Fla** dipeptide transient absorption spectra, excitation with YAG laser at 355 nm, 24 mJ.

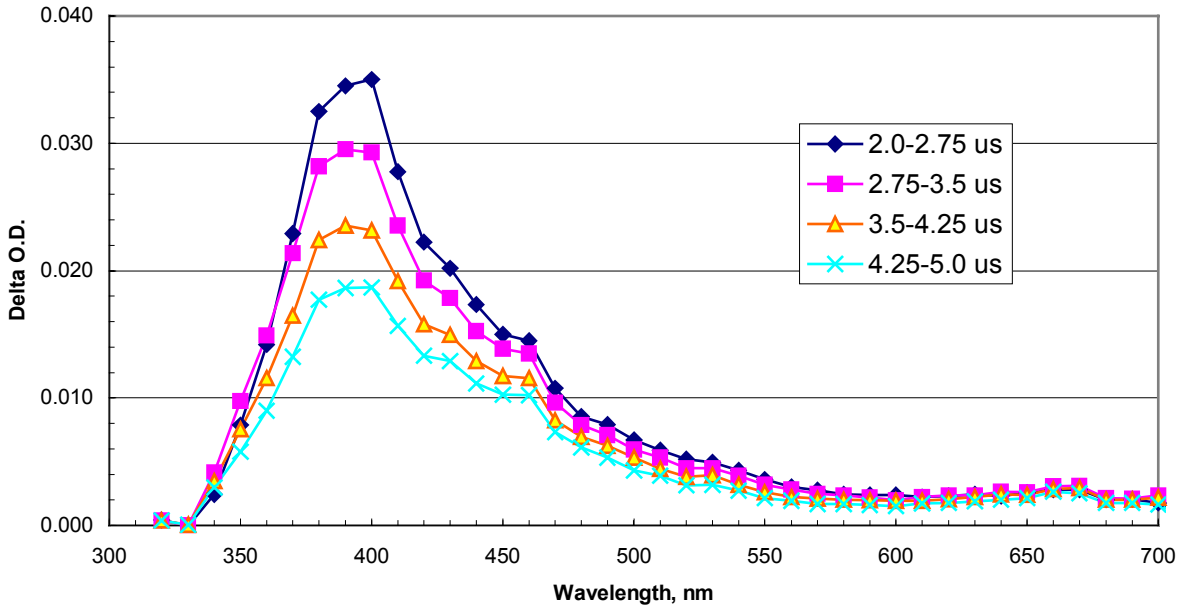

Figure 42**.** **Bpa-Fla** dipeptide transient absorption spectra, excitation with Excimer laser at 308 nm, 29 mJ.

For the **Npa-Fla** dipeptide, the transient absorption spectra showed peaks at both 390 and 420 nm (figure 43, kinetics shown in figure 44). The **Npa-Fla** dipeptide transient absorption spectrum in figure 43 was very similar to the **Npa** spectrum. However, given that both the naphthalene and fluorene triplets have peaks at 390 nm, we compared the ratio of the 390:420 T-T absorption in **Npa** to that obtained for the dipeptide. If the fluorene triplet was contributing to the dipeptide signal at 390, the peak height ratios should differ. However, no difference was observed, leading us to conclude that only naphthalene triplet is present. This implies that TTET is efficient and quantitative ($k_{TTET} > 10^8\ s^{-1}$). The efficient TTET observed is inconsistent with the phosphorescence results given above. We suggest that the origin of this difference lies in the greater rotational

mobility allowed in room-temperature liquid solutions compared with low-temperature glasses. The low-temperature matrices may freeze out or restrict motion of the chromophores and thereby prevent them from achieving conformations that provide the orbital overlap required for efficient exchange energy transfer. The effect of relative chromophore conformation on transfer efficiency has been reported in the past.[45] Good orbital overlap may be furnished by small interchromophore distances as well as conformations that involve stacking of the aromatic π-systems of the chromophores. However, such conformations may not be achieved at low temperature. In room temperature liquid solution, relatively unhindered rotational motion will allow the chromophores to sample a wide variety of conformations possessing both good and poor overlap. As long as the rate of interconversion between the conformers is competitive with the TTET rate, more rapid transfer can be expected at room temperature. Such an explanation has been invoked to explain the dependence of SSET rates on conformation in bichromophoric peptides containing protoporphyrin and naphthalene and TTET rates in bichromophoric peptides containing benzophenone and naphthalene chromophores.[18, 44]

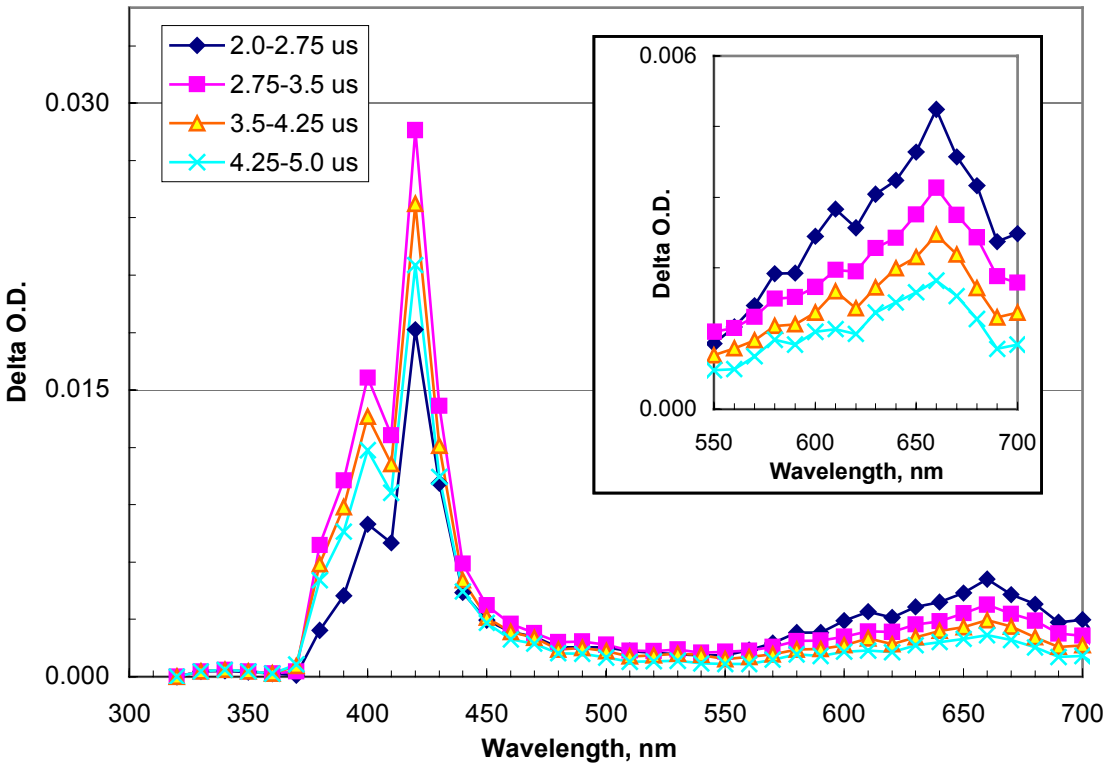

Figure 43. **Npa-Fla** transient absorption spectra, excitation with Excimer laser at 308 nm, 37 mJ.

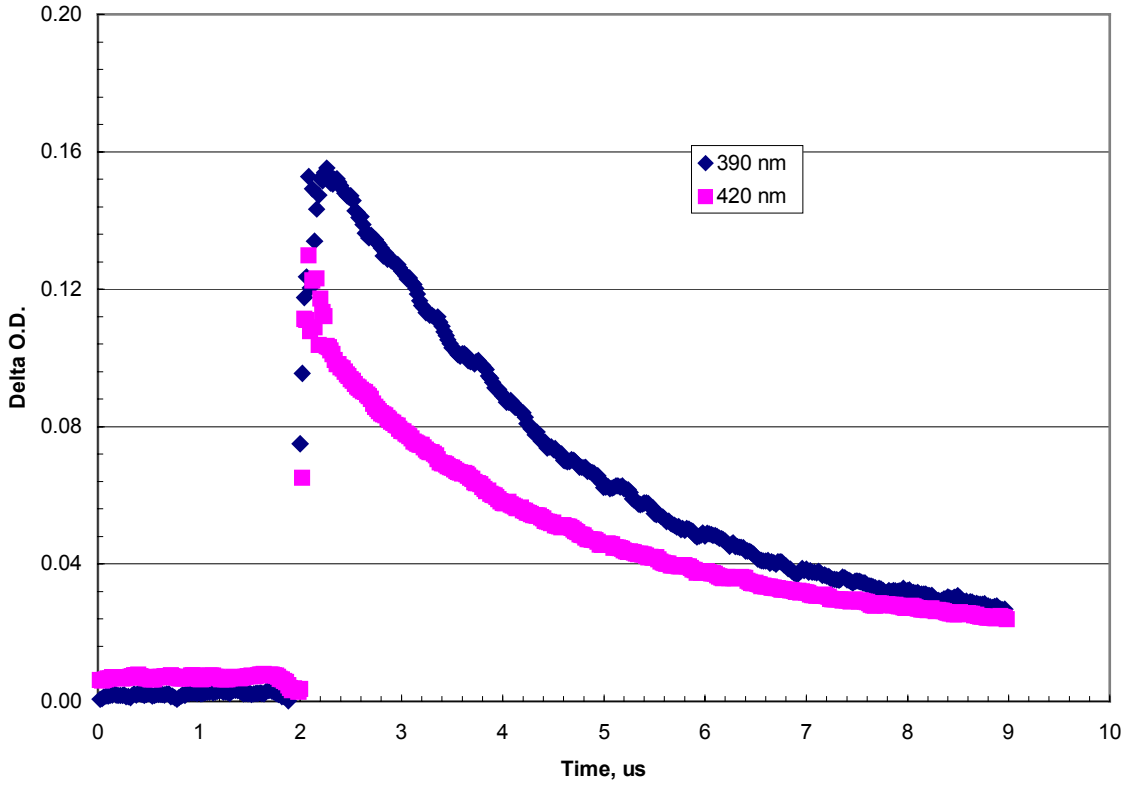

Figure 44. **Npa-Fla** dipeptide 390 nm and 420 nm transient decay spectra, excitation with Excimer laser at 308 nm, 37 mJ.

Laser-induced chemical reactions

Transient absorption spectra of **Fla**, **Bpa-Fla** and **Npa-Fla** (figures 38, 42 and 43) exhibited peaks at 440 and 660 nm that we felt warranted further investigation. These two peaks were not evident in the transient absorption spectra of **Npa** and **Bpa**, and therefore the experiments focused on **Fla** and the dipeptides. Apart from the usual photophysical processes occurring following excitation, e.g., ISC, IC, fluorescence, etc., pulsed laser irradiation can lead to multiphoton pathways, including photoionization to

yield cation radicals. In fact, a comparison of the transient absorption spectra obtained for **Npa-Fla** and **Fla** itself with known fluorene cation radical spectra[58] shows a distinct similarity (see figure 45).

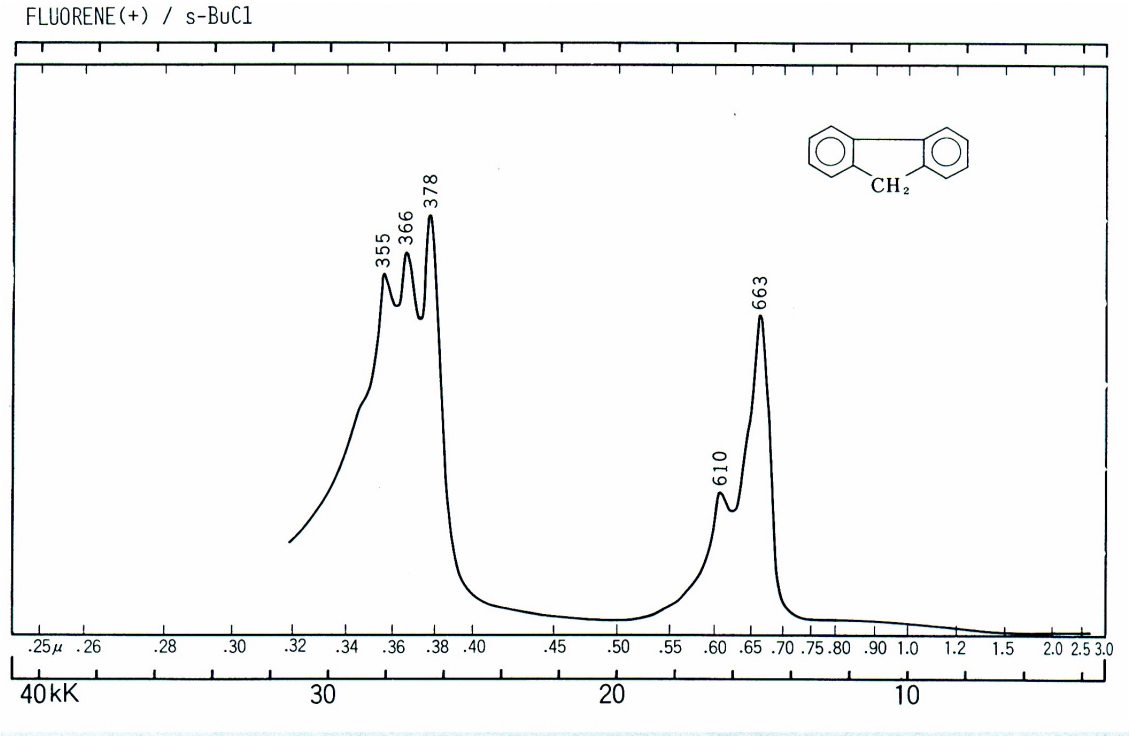

Figure 45**.** Fluorene in s-butyl chloride, cation radical UV spectrum.[58]

To verify this, a new sample of **Npa-Fla** dipeptide was prepared with 2-propanol as the solvent. 2-propanol is less polar than acetonitrile and will not stabilize the cation radical-electron pair as well as acetonitrile. In addition, acetonitrile undergoes irreversible reaction with the electron. Both of these factors make recombination of cation and electron more likely in 2-propanol. The transient absorption spectra, figure 46, show a 660 nm absorption band. However, the ΔOD is smaller than for the dipeptide in N_2-saturated MeCN. In addition, the lifetime at 660 nm is considerably shorter than in MeCN, probably reflecting the nucleophilic quenching of the cation radical by 2-

propanol. Lifetimes for **Fla**, **Nal-Fla** and **Bpa-Fla** in N_2-saturated MeCN at 660 nm were 2.7 µs, 7.8 µs and 9.7 µs respectively while the transient lifetime for **Nal-Fla** in N_2-saturated 2-propanol was 0.57µs.

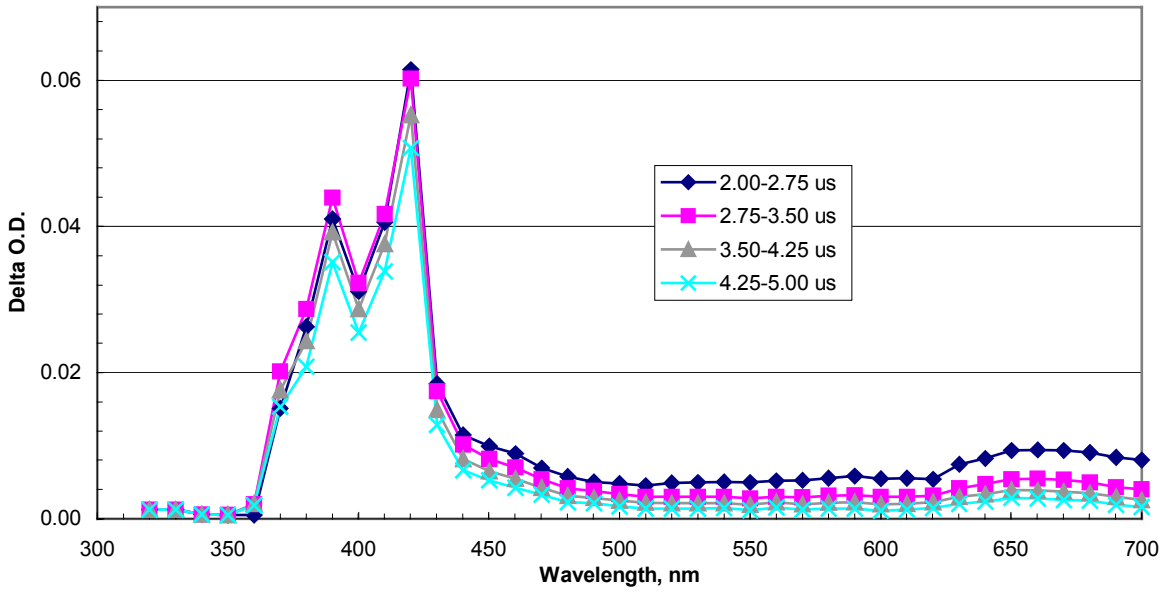

Figure 46. **Npa-Fla** dipeptide in 2-propanol, transient absorption spectra, excitation with Excimer laser at 308 nm, 16 mJ.

To further elucidate the cation radical properties, LFP experiments were conducted on **Fla** and **Npa-Fla** dipeptide in O_2-saturated $MeCl_2$ and MeCN. Like MeCN, $MeCl_2$ undergoes irreversible reaction with electrons, thereby preventing recombination and increasing cation radical yields. Experiments were conducted in O_2-saturated solutions in order to quench any triplet transient that may interfere with the cation radical absorptions. However, these experiments failed due to the rapid (approximately 40 laser pulses) decomposition of the **Fla** moiety and the buildup of a new product that produces a transient absorbing at 440 nm.

The transient absorption spectra in O_2-saturated $MeCl_2$ and MeCN, figures 47 and 48, now show only a 440 nm band due to a new transient with a lifetime of 0.5 μs in O_2-saturated solvent. Furthermore, with 2 minutes of degassing with N_2, the lifetime increased to 2.0 μs. (To illustrate that there is only one transient present, decays are shown at both 440 nm and at 390 nm, the latter being the λ_{max} for **Fla** triplet. The decays are identical.) The same 440 nm band is produced by the dipeptides in O_2-saturated solvents, figures 51 and 52.

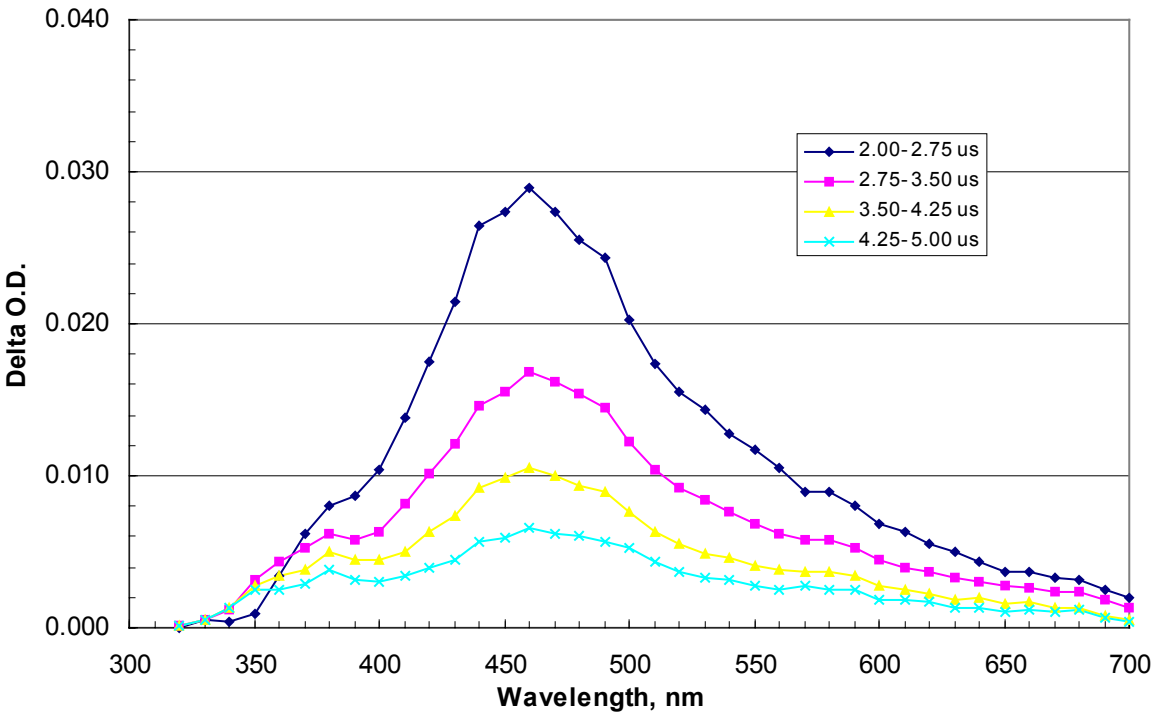

Figure 47. **Fla** dipeptide transient absorption spectra in O_2 sat. $MeCl_2$, excitation with Excimer laser at 308 nm, 44 mJ.

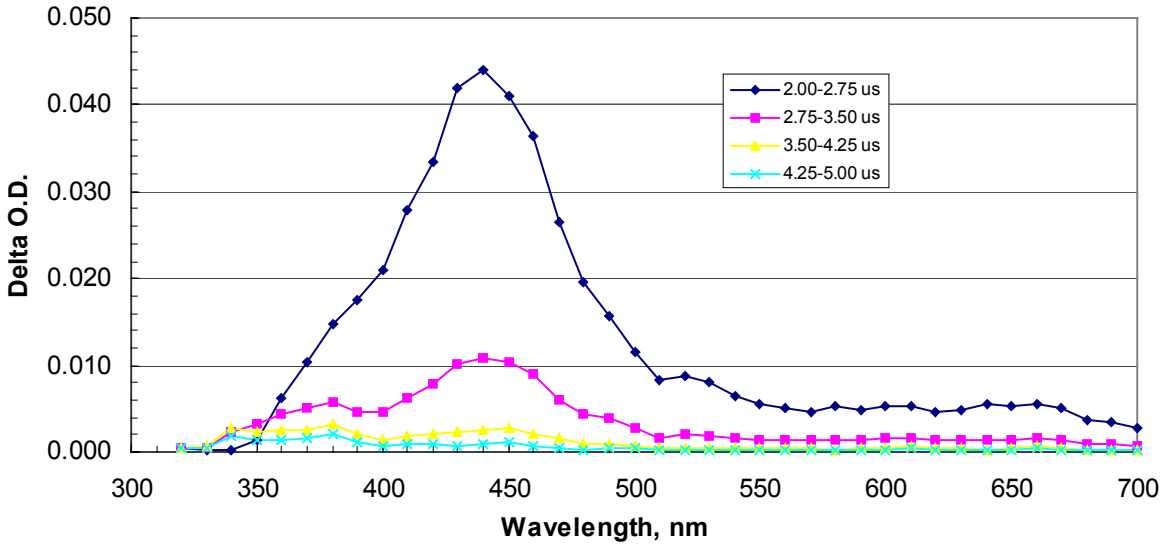

Figure 48. **Fla** transient absorption spectra in O_2 sat. MeCN, excitation with Excimer laser at 308 nm, 44mJ.

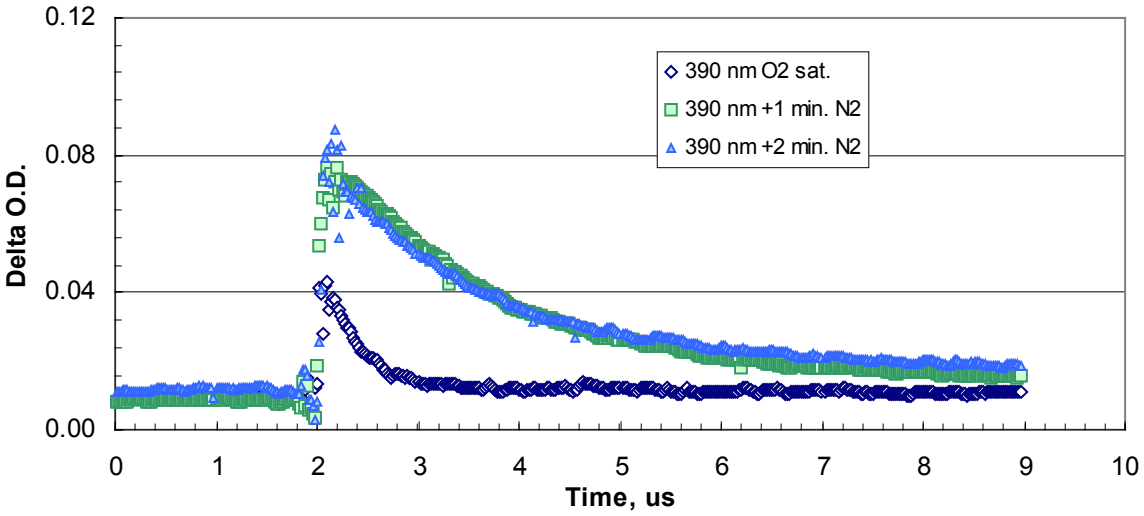

Figure 49. **Fla** 390 nm transient decay spectra in O_2 sat. MeCN and added N_2, excitation with Excimer laser at 308 nm, 37 mJ.

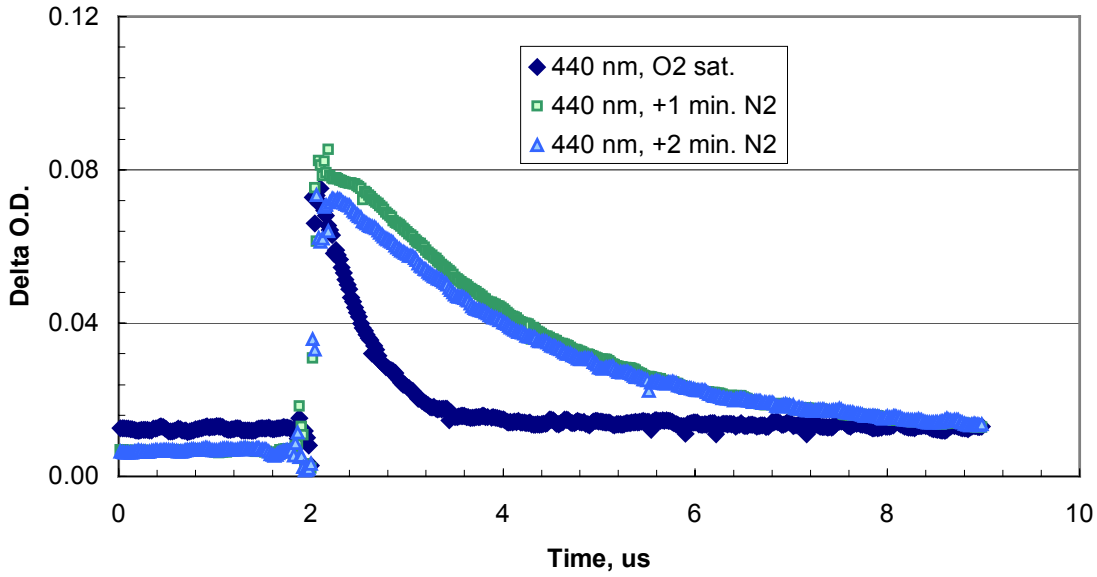

Figure 50. **Fla** 440 nm transient decay spectra in O_2 sat. MeCN and added N_2, excitation with Excimer laser at 308 nm, 37 mJ.

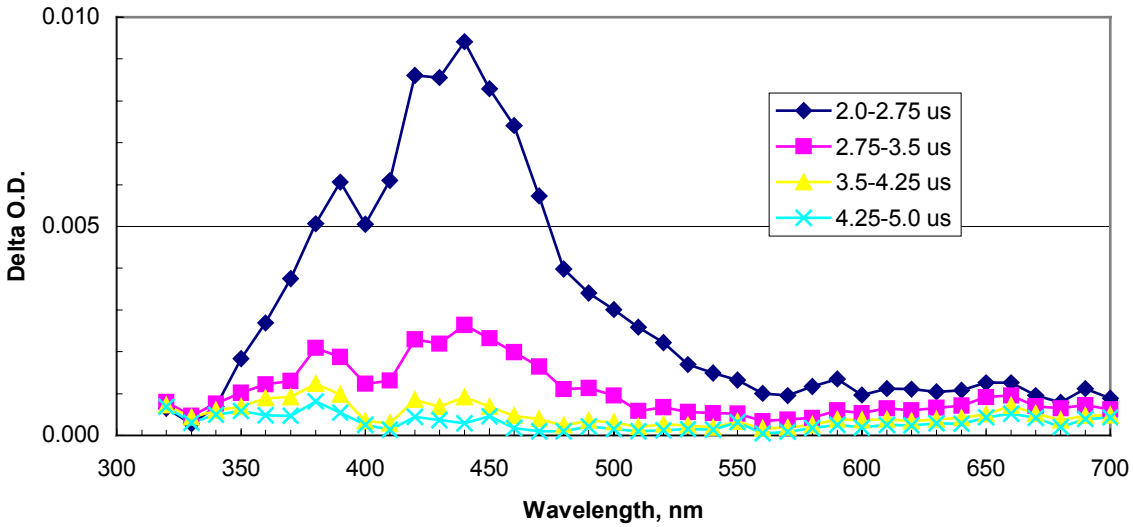

Figure 51. **Bpa-Fla** transient absorption spectra in O_2 sat. MeCN, excitation with Excimer laser at 308 nm, 29mJ.

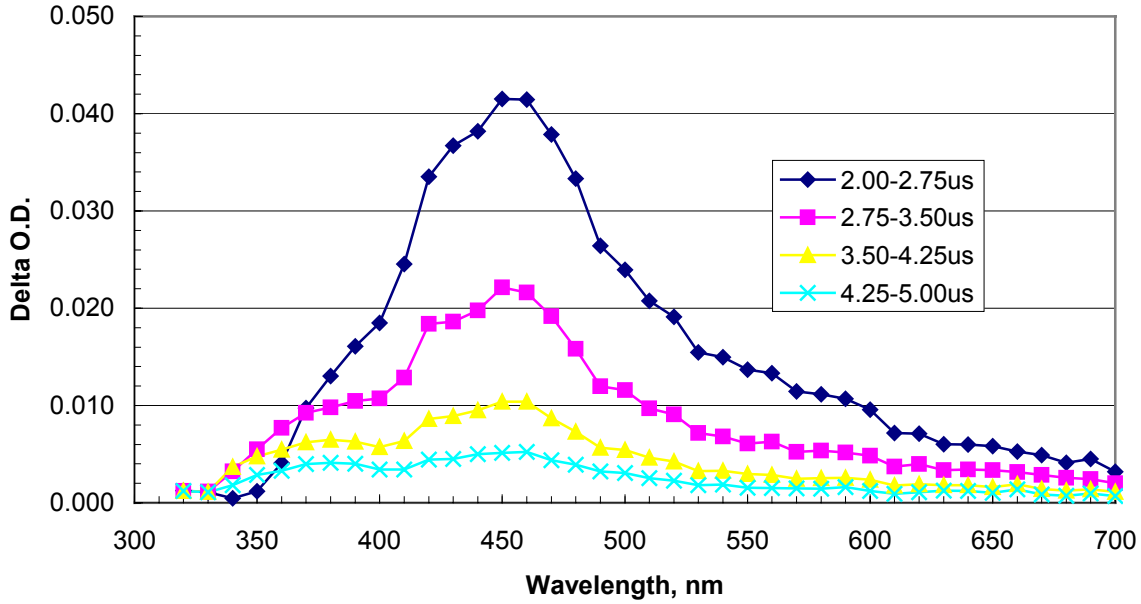

Figure 52. **Npa-Fla** transient absorption spectra in O_2 sat. $MeCl_2$, excitation with Excimer laser at 308 nm, 26 mJ.

This new transient is almost certainly due to the re-excitation of a photoproduct to produce an excited state or some other reactive species. The band position of this species is reminiscent of transients derived from fluorenone and the literature supports the suggestion that the fluorene chromophores could be photooxidizing to fluorenone.[46] The question remains as to the identity of the transient.

While the fluorenone radical anion has been reported to possess an absorption band in the 440 nm region[46], the same authors failed to note any sensitivity of this species to oxygen, contrary to our own observations. On the other hand, the fluorenone triplet state certainly absorbs at 440 nm and shows the same sensitivity to O_2 as we observed. We conclude

that fluorenone is produced in our system by a sequence of events initiated by photoionization followed by deprotonation at the fluorene 9-position and addition of O_2 to the resultant neutral radical.[46]

We note with some surprise the apparent high efficiency of this photoreaction. Essentially none of the original starting material remains after only a few tens of laser pulses. Supporting this degradation are UV absorption spectra of **Fla** before and after laser flash photolysis in O_2 and N_2-saturated MeCN, which showed substantial degradation due to irradiation, figure 53. TLC of the irradiated sample shows no **Fla** but it does indicate a new as yet unidentified product.

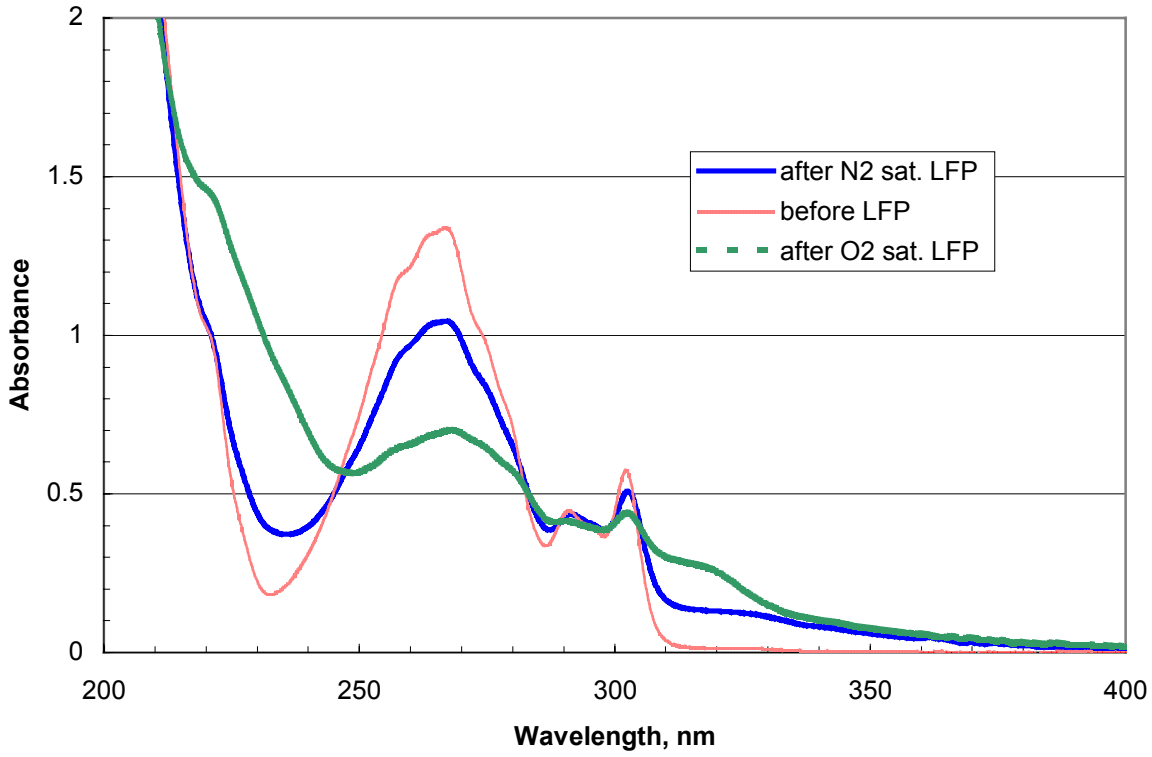

Figure 53. **Fla** UV absorption spectra before and after laser flash photolysis in O_2 and N_2 sat. MeCN.

Summary of photochemistry experiments

A summary of the photochemistry results is provided in table 3.

Table 3. Summary of photochemical analyses.

	Bpa	Fla	Fluorene	Npa	Bpa-Fla	Npa-Fla
E_S, kcal/mol	78.2[3]	94.3[2]	94.9[1]	91.7[2]	94.9[2]	93.3[2]
E_T, kcal/mol	69.2[2]	67.1[2]	67.9[1]	61.2[2]	67.1[2]	61.3[2]
λ_{TT}, nm	520[2]	390[2]	390[1]	420[2]	390[2]	420[2]
Φ_{fl}	0	.58[2]	.68[1]	.31[2]		
Φ_{ph}	.84[1]	.07[1]	.07[1]	.039[1]		
R_{0calc}, Å					16.2[2]	16.2[2]
R_{calc}, Å					9.14[2]	8.69[2]
R_{model}, Å					11.7 ±3.1	10.6 ±2.9
Eff. SSET	.943[2]	.965[2]				
τ, μs ex at 308nm		4.7 at 390 nm[2]		2.9 at 420 nm	10.0 at 390 nm[2]	1.86 at 390 nm[2] 2.55 at 420 nm[2]
τ, μs ex at 355nm	2.2 at 520 nm[2]				4.4 at390nm[2]	
J, L cm^3 mol^{-1}					1.435E-16[2]	1.711E-16[2]

1. Handbook[18]
2. Experimental
3. Handbook value for 4-methyl benzophenone[18]

Conclusions

N- and C-protected 3-(2-fluorenyl)-L-alanine (**Fla**) and the two dipeptides formed by combining **Fla** and either N-Boc-3-(2-naphthyl)-L-alanine (**Npa**) or N-Boc-3[(4'-benzoyl)-phenyl]-L-alanine (**Bpa**) were synthesized and characterized, first for chemical purity then for photophysical properties in order to ascertain their suitability for potential application in nanoscale devices. The devices envisioned would incorporate a polypeptide scaffold where TTET is accomplished via intramolecular processes between chromophore moieties.

The synthesis of **Fla** and chiral separation of the L and D isomers using cross-linked enzyme crystals (CLECs) of Subtilisin protease[34] were accomplished using a modified Sorenson procedure.[26-28] The C-protected **Fla** methyl ester was synthesized and then coupled to **Bpa** or **Npa.** The N-protected fluorenylmethoxycarbonyl (Fmoc) **Fla** derivative was synthesized for the 15-residue peptide.

UV absorption, fluorescence, phosphorescence and laser flash photolysis analyses of the single chromophore model compounds and bichromophoric peptides show that efficient SSET and TTET occur in the dipeptides and that SSET occurs via a Förster mechanism. Fluorescence excitation and emission results were used to calculate Förster diameters of 9.1 Å and 8.7 Å for the **Bpa-Fla** and the **Npa-Fla** dipeptides respectively. These values compare favorably with the Hyperchem MM+ values of 11.7 ± 3.1 and 10.6 ± 2.9. Phosphorescence and laser flash photolysis of the dipeptides demonstrate near complete TTET from **Bpa** to **Fla** and **Fla** to **Npa** in the dipeptides. If interchromophore distances

in the analogous 15-residue trichromophoric polypeptide are consistent with modeling results, efficient through-space TTET should result.

Energy level diagrams, figures 54 and 55, summarize the energy transfer properties of the two dipeptides.

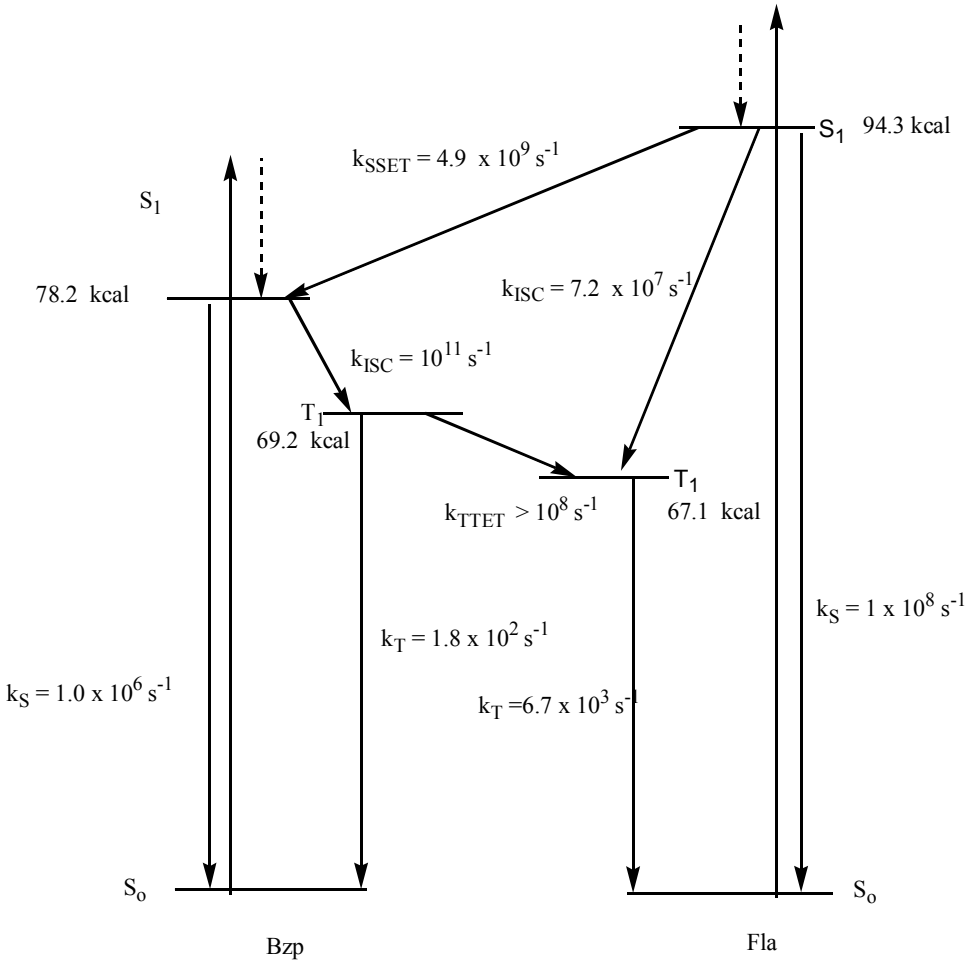

Figure 54**.** Energy level diagram for **Bpa-Fla** dipeptide showing energy transfer rates.

The k_F (fluorescence) and k_P (phosphorescence) values were obtained from literature for benzophenone, fluorene and naphthalene.[20] k_{ISC} rates were derived from the fluorescence quantum yield values, Φ_{FL}, using Ermolaev's rule, equations 11 and 12.

$$\Phi_{FL} + \Phi_{ISC} = 1 \tag{11}$$

$$\Phi_{ISC} = \frac{k_{ISC}}{k_{FL} + k_{IC} + k_{ISC}} \qquad \text{Assume } k_{IC} = 0 \tag{12}$$

TTET rates were estimated from LFP transient absorption spectra. The lower limit of the lifetime measurements is 10 ns, providing $k_{TTET} > 10^8\ s^{-1}$.

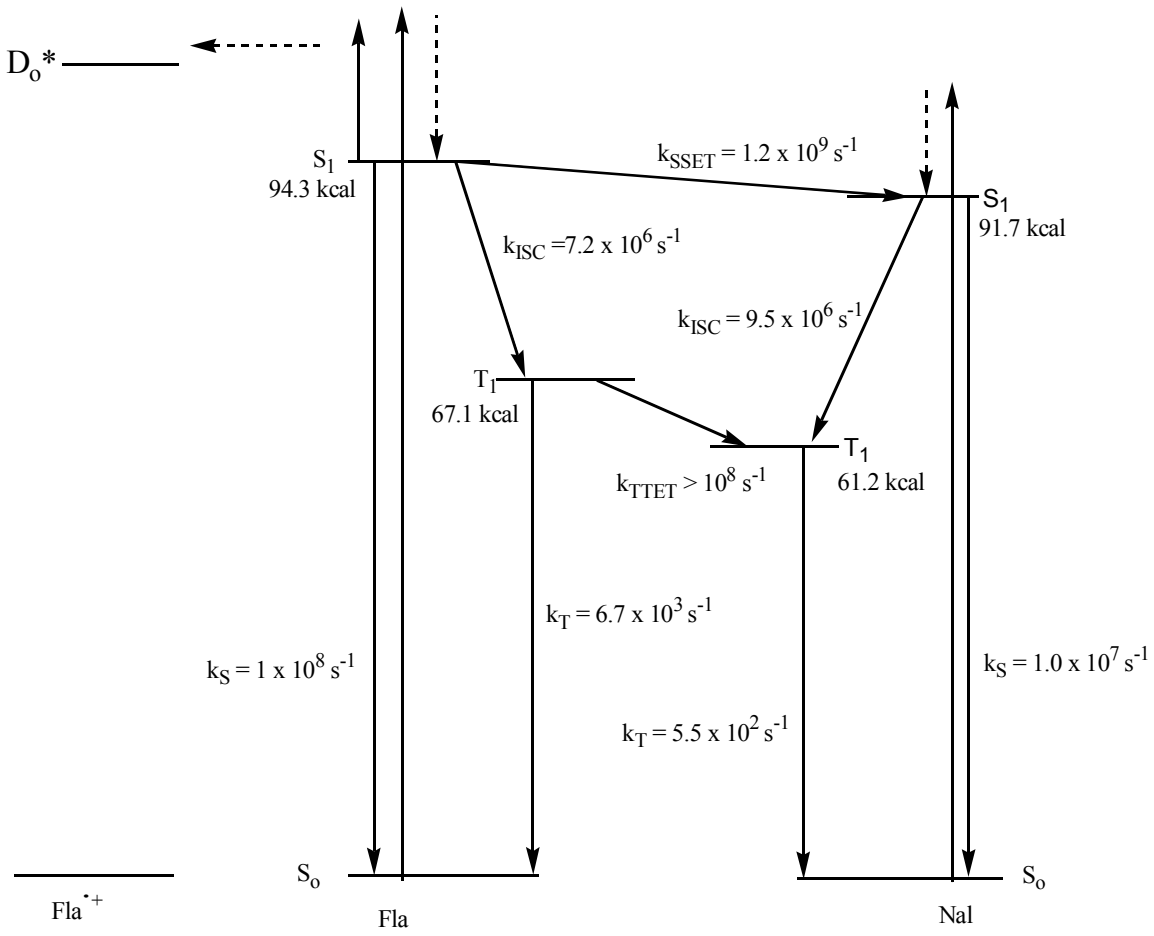

Figure 55. Jablonski diagram for **Npa-Fla** dipeptide showing energy transfer rates.

Laser flash photolysis transient absorption spectra at 308 nm show evidence of a fluorene cation radical[58]and, in O_2 saturated solvents, show photochemical reaction products from the **Fla**, **Npa-Fla** dipeptide and, to a lesser extent, with **Bpa-Fla**. The cation radical is likely produced by a two-photon process.

References

1. Wagner, R.W.; Lindsay, J.S. *J. Am. Chem. Soc.* **1994**, *116*, 9759.
2. Ren, Y.; Wang, Z.; Zhu, H.; Weininger, S.J.; McGimpsey, W.G. *J. Am. Chem. Soc.* **1995**, *117*, 4367.
3. Tan, Z.; Kote, R.; Samaniego, W.N.; Weininger, S.J.; McGimpsey, W.G. *J. Phys. Chem. A* **1999**, *103*, 7612.
4. Kroon, J.; Oliver, A.M.; Paddon-Row, M.N.; Verhoeven, J.W. *J. Am. Chem. Soc.* **1990**, *112*, 4868.
5. Chen, L.; Qi, N.; Houmam, A.; Wayner, D.D.M.; Weininger, S.J.; McGimpsey, W.G. *J. Phys. Chem. A* **1999**, *103*, 9167.
6. Closs, G.L.; Johnson, M.D.; Miller, J.R.; Piotrowiak, P.J. *J. Am. Chem. Soc.* **1989**, *111*, 3751.
7. Jordan, K.D.; Paddon-Row, M.N. *Chem. Rev.* **1992**, *92*, 395.
8. Morrison, H.; Wu, Z.Z. *J. Am. Chem. Soc.* **1992**, *114*, 4119.
9. McGimpsey, W.G.; Samaniego, W.N.; Chen, L.; Wang, F. *J. Phys. Chem. A* **1998**, *45*, 8679.
10. Hisada, K.; Tsuchida, A.; Ito, S.; Yamamoto, M. *J. Phys. Chem. B* **1998**, *102*, 2640.
11. Castellan, a.; Kessab, L.; Grelier, S.; Nourmamode, A. *J. Chem. Soc. Perkin Trans.* **1993**, 953.
12. Galoppini, E.; Fox, M.A. *J. Am. Chem. Soc.* **1996**, *118*, 2299.
13. McCafferty, D.G.; Friesen, D.A.; Danielson, E.; Wall, C.G.; Saderholm, J.; Erickson, B.W.; Meyer, T.J. *Proc. Natl. Acad. Sci. US* **1996**, *93*, 8200.
14. Sisido, M. *Macromolecules* **1989**, *22*, 4367.

15. Egusa, S.; Sisido, M.; Imanishi, Y. *Bull. Chem. Soc. Jpn.* **1986**, *59*, 3175.

16. Eis, P.S.; Lakowicz, J.R. *Biochemistry* **1993**, *32*, 7981.

17. Pispisa, B.; Venanzi, M.; Palleschi, A.; Zanotti, G. *Macromolecules* **1994**, *27*, 7800.

18. Pispisa, B.; Palleschi, A.; Venanzi, M.; Zanotti, G. *J. Phys. Chem.* **1996**, *100*, 6835.

19. Private communication with Prof. W.G. McGimpsey.

20. Murov, S.L.; Carmichel, I.; Hug, G.L. *Handbook of Photochemistry Second Ed.* , Marcel Dekker Inc., 1993.

21. Turro, N.J. *Modern Molecular Photochemistry*; University Science Books: Sausalito, CA, 1991.

22. Barltrop, J.A.; Coyle, J.D. *Excited States in Organic Chemistry*; John Wiley & Sons: New York, 1975, Chaps. 2-6.

23. Michl, J. *Electronic Aspects of Organic Photochemistry*; John Wiley & Sons: New York, 1990, Chap. 2.

24. Wang, Z.; Weininger, S.J.; Mcgimpsey, W.G. *J. Phys. Chem.* **1993**, *97*, 374.

25. Wang, Z. Thesis, **1994**, Worcester Polytechnic Insititute.

26. Sorensen, S.P.L. *Z. Physiol. Chem*. **1905**, *44*, 448.

27. Snyder, H.R.; Shekleton, J.F.; Lewis, C.D. *J. Am. Chem. Soc.* **1945**, *67*, 310.

28. Morrison, D.C. *J. Org. Chem.* **1958**, *24*, 463.

29. Nestor, J.J.; Ho, T.L.; Simpson, R.A.; Horner, B.L.; Jones, G.H.; McRae, G.I.; Vickery, B.H. *J. Med. Chem.* **1982**, *25*, 795.

30. Bosshard, H.R.; Berger, A. *Helvetica Chimica Acta* **1973**, *56*, 1838.

31. Leanna, M.R.; Morton, H.E. *Tetrahedron* **1993**, *34*, 4485.

32. Wong, C.-H.; Chen, S.-T.; Hennen, W.J.; Bibbs, J.A.; Wang, Y.-F.; Liu, J.L.; Pantoliano, M.W.; Whitlow, M.; Bryan, P.N. *J. Am. Chem. Soc.* **1990**, *112*, 945.

33. Imperiali, B.; Prins, T.J.; Fisher, S.L. *J. Org. Chem.* **1993**, 58, 1613.

34. Wang, Y.-F.; Yakovlevsky, K.; Zhang, B.; Margolin, A.L. *J. Org. Chem.* **1997**, *62*, 3488.

35. Carpino, L.A.; Han, G.Y. *J. Org. Chem.* **1972**, *37*, 3404.

36. Chen, F.M.; Benoiton, N.L. *Can. J. Chem*. **1987,** *65*, 1224.

37. Kremminger, P.; Undheim, K. *Tetrahedron* **1997**, *53*, 6925.

38. Falck-Pedersen, M.L.; Undheim, K. *Tetrahedron* **1996**, *52*, 7761.

39. Salvador, L.A.; Elofsson, M.; Kihlberg, J. *Tetrahedron* **1995**, *51*, 5643.

40. Williams, B.J.; Curtis, N.R.; McKnight, A.T.; Maguire, J.J.; Young, S.C.; Veber, D.F.; Baker, R. *J. Med. Chem.* **1993**, *36*, 2.

41. Ten Kortenaar, P.B.W.; Van Dijk, B.G.; Peeters, J.M.; Raabex, B.J.; Adams, P.J.H.M.; Tesser, G.I. *Int. J. Peptide Res.* **1986**, 398.

42. Carpino, L.A. *Acc. Chem. Res.* **1987**, *20*, 401.

43. Henklein, P.; Heyne, H.-U.; Halatsch, W.-R.; Niedrich, H. *Synthesis* **1987**, 167.

44. McGimpsey, W.G.; Chen, L.; Carraway, R.; Samaniego, W.N. *J. Phys. Chem. A* **1999**, *103*, 6082

45. Chang, D.S.; Filipescue, N. *J. Am. Chem. Soc.* **1972**, 94, 4171.

46. Barbas, J.T.; Sigman, M.E.; Arce, R.; Dabestani, R. *J. Photochem. Photobiol. A: Chem.* **1997**, 109, 229.

47. Davidson, R.S.; Santhanam, M. *J. Chem. Soc. Perkin II*, **1972**, 2355.

48. Bolin, D.R. *U.S. Patent* 4,822,890 (1986) Hoffmann-Laroche Inc.; NJ, **1989**.

49. Lamouri, A.; Heymans, F.; Tavet, F.; Dive, G.; Batt, J.-P.; Blavet, N.; Braquet, P.; Godfroid, J.-J. *J. Med. Chem.* **1993**, 36, .

50. Easton, C.J.; Harper, J.B. *Tetrahedron* **1998**, *39*, 5269.

51. Bommarius, A.S.; Drauz, K.D.; Günther, K.; Knaup, G.; Schwarm, M. *Tetrahedron* **1997**, *8*, 3197.

52. Chenault, H.K.; Dahmer, J.; Whitesides, G.M. *J. Am. Chem. Soc.* **1989**, *111*, 6354.

53. Tüchsen, E.; Ottesen, M. *Carlsberg Res. Commun*. **1977**, *42*, 407.

54. Paquet, A. *Can. J. Chem.* **1982**, *60*, 976.

55. Sigler, G.F.; Fuller, W.D.; Chaturvedi, N.C.; Goodman, M.; Verlander, M. *Biopolymers* **1983**, *22*, 2157.

56. de L. Milton, R.C.; Becker, E.; Milton, S.C.F.; Baxter, J.E.H.; Elsworth, J.F. *Int. J. Pept. Protein Res.* **1987**, 30*,* 431.

57. Carraway, R., U. Massachusetts Med. Center, Worcester, MA. **1999,** *Private Communication*.

58. Shida, T. *Electronic Absorption Spectra of Radical Ions* Elsevier, **1988**.

59. Podlech, J.; Seebach, D. *Agnew. Chem. Int. Ed. Engl.* **1995**, *34*, 471.

60. Seebach, D.; Overhand, M.; Kühnle, Martinoni, B. *Helv. Chem. Acta* **1996**, *79*, 913.

61. Marshall, E. *Science*, **1999**, *285*, 31.

62. Collier, C.P.; Wong, E.W.; Belohradsky, M.; Raymo, F.M.; Stoddart, J.F.; Kuekes, P.J.; Williams, R.S.; Heath, J.R. *Science* **1999**, *285*, 391.

Appendix A – NMR Spectra

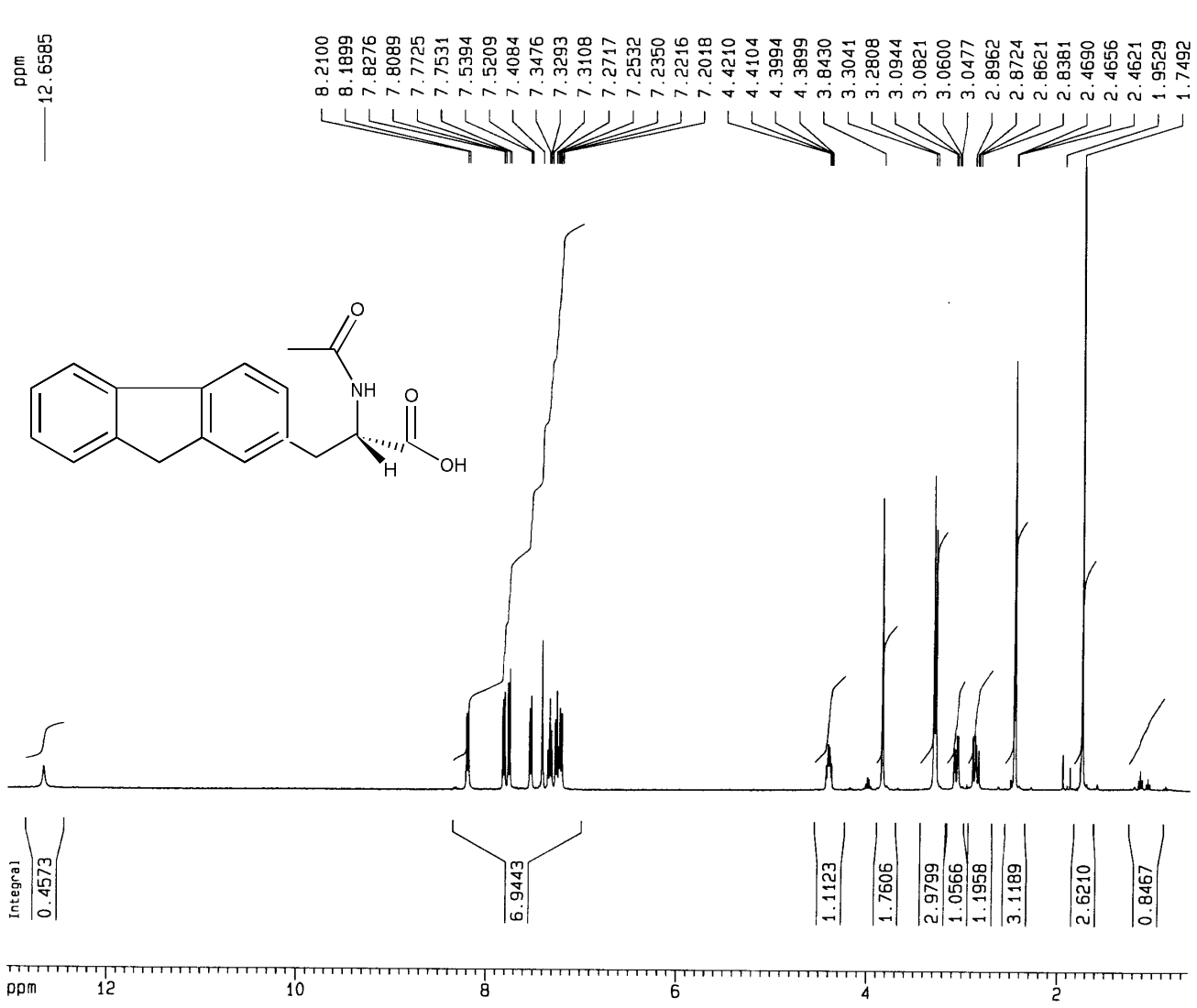

Current Data Parameters

NAME	DCF-48-L-acid
EXPNO	21
PROCNO	1

F2 - Acquisition Parameters

Date_	990407
Time	14.44
INSTRUM	spect
PROBHD	5 mm BBO BB-1
PULPROG	zg30
TD	32768
SOLVENT	DMSO
NS	16
DS	2
SWH	8223.685 Hz
FIDRES	0.250967 Hz
AQ	1.9923444 sec
RG	574.7
DW	60.800 usec
DE	6.00 usec
TE	300.0 K
D1	1.00000000 sec
P1	8.70 usec
SFO1	400.1324710 MHz
NUC1	1H
PL1	0.00 dB

F2 - Processing parameters

SI	16384
SF	400.1300167 MHz
WDW	EM
SSB	0
LB	0.50 Hz
GB	0
PC	1.00

1D NMR plot parameters

CX	20.00 cm
F1P	13.034 ppm
F1	5215.24 Hz
F2P	0.625 ppm
F2	250.22 Hz
PPMCM	0.62043 ppm/cm
HZCM	248.25098 Hz/cm

Current Data Parameters

NAME	DCF50-D-ester
EXPNO	21
PROCNO	1

F2 - Acquisition Parameters

Date_	990323
Time	9.49
INSTRUM	spect
PROBHD	5 mm BBO BB-1
PULPROG	zg30
TD	32768
SOLVENT	DMSO
NS	16
DS	2
SWH	8223.685 Hz
FIDRES	0.250967 Hz
AQ	1.9923444 sec
RG	406.4
DW	60.800 usec
DE	6.00 usec
TE	300.0 K
D1	1.00000000 sec
P1	8.70 usec
SFO1	400.1324710 MHz
NUC1	1H
PL1	0.00 dB

F2 - Processing parameters

SI	16384
SF	400.1300167 MHz
WDW	EM
SSB	0
LB	0.50 Hz
GB	0
PC	1.00

1D NMR plot parameters

CX	20.00 cm
F1P	11.000 ppm
F1	4401.43 Hz
F2P	-1.000 ppm
F2	-400.13 Hz
PPMCM	0.60000 ppm/cm
HZCM	240.07800 Hz/cm

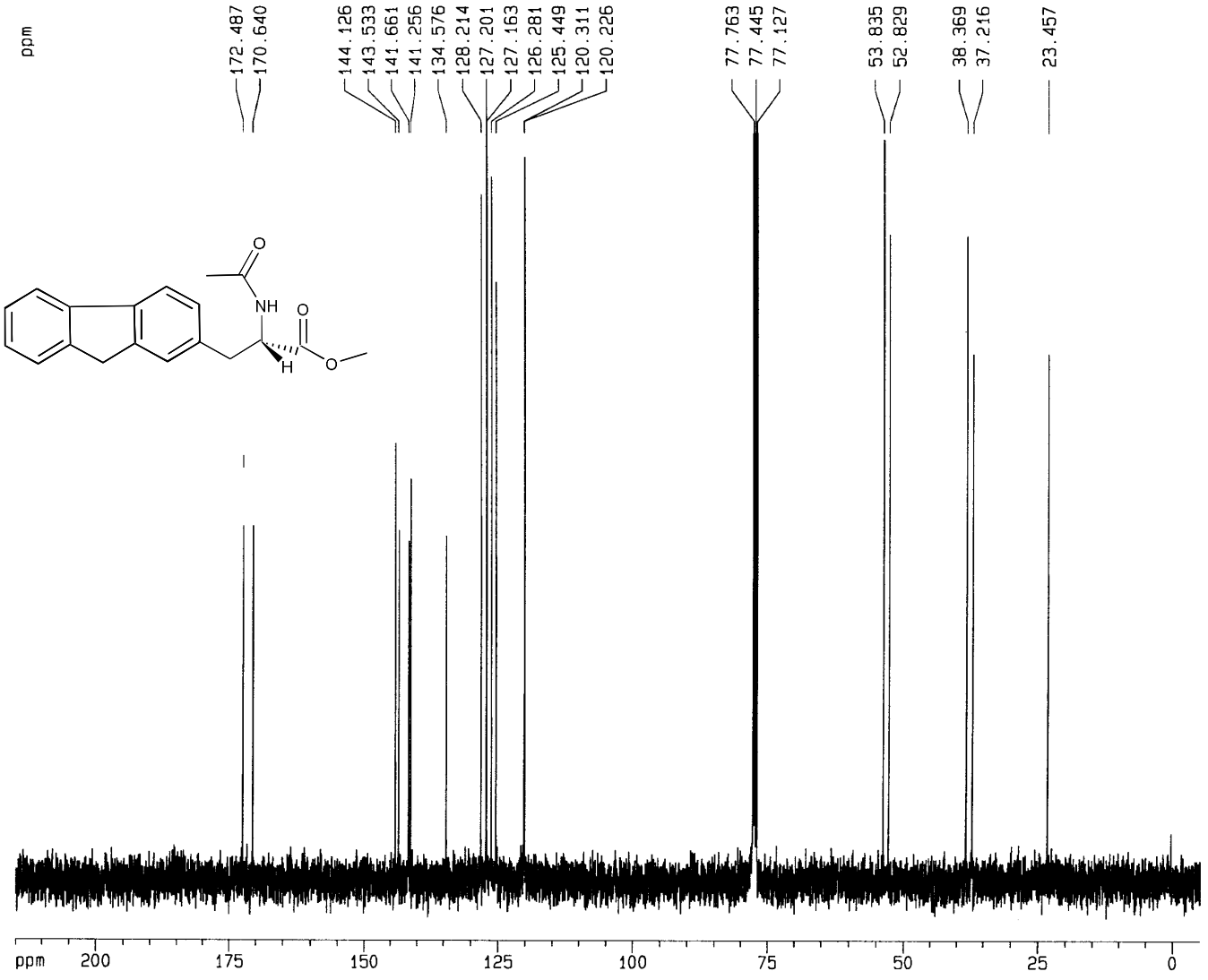

Current Data Parameters

NAME	DCF18
EXPNO	21
PROCNO	1

F2 - Acquisition Parameters

Date_	990125
Time	14.57
INSTRUM	spect
PROBHD	5 mm BBO BB-1
PULPROG	zgpg30
TD	65536
SOLVENT	CDCl3
NS	512
DS	2
SWH	31847.133 Hz
FIDRES	0.485949 Hz
AQ	1.0289652 sec
RG	8192
DW	15.700 usec
DE	6.00 usec
TE	300.0 K
d11	0.03000000 sec
d12	0.00002000 sec
PL13	20.00 dB
D1	2.00000000 sec
CPDPRG2	waltz16
PCPD2	80.00 usec
SFO2	400.1316005 MHz
NUC2	1H
PL2	0.00 dB
PL12	20.00 dB
P1	9.00 usec
SFO1	100.6254358 MHz
NUC1	13C
PL1	-1.00 dB

F2 - Processing parameters

SI	32768
SF	100.6127290 MHz
WDW	EM
SSB	0
LB	1.00 Hz
GB	0
PC	1.40

1D NMR plot parameters

CX	20.00 cm
F1P	215.000 ppm
F1	21631.74 Hz
F2P	-5.000 ppm
F2	-503.06 Hz
PPMCM	11.00000 ppm/cm
HZCM	1106.73999 Hz/cm

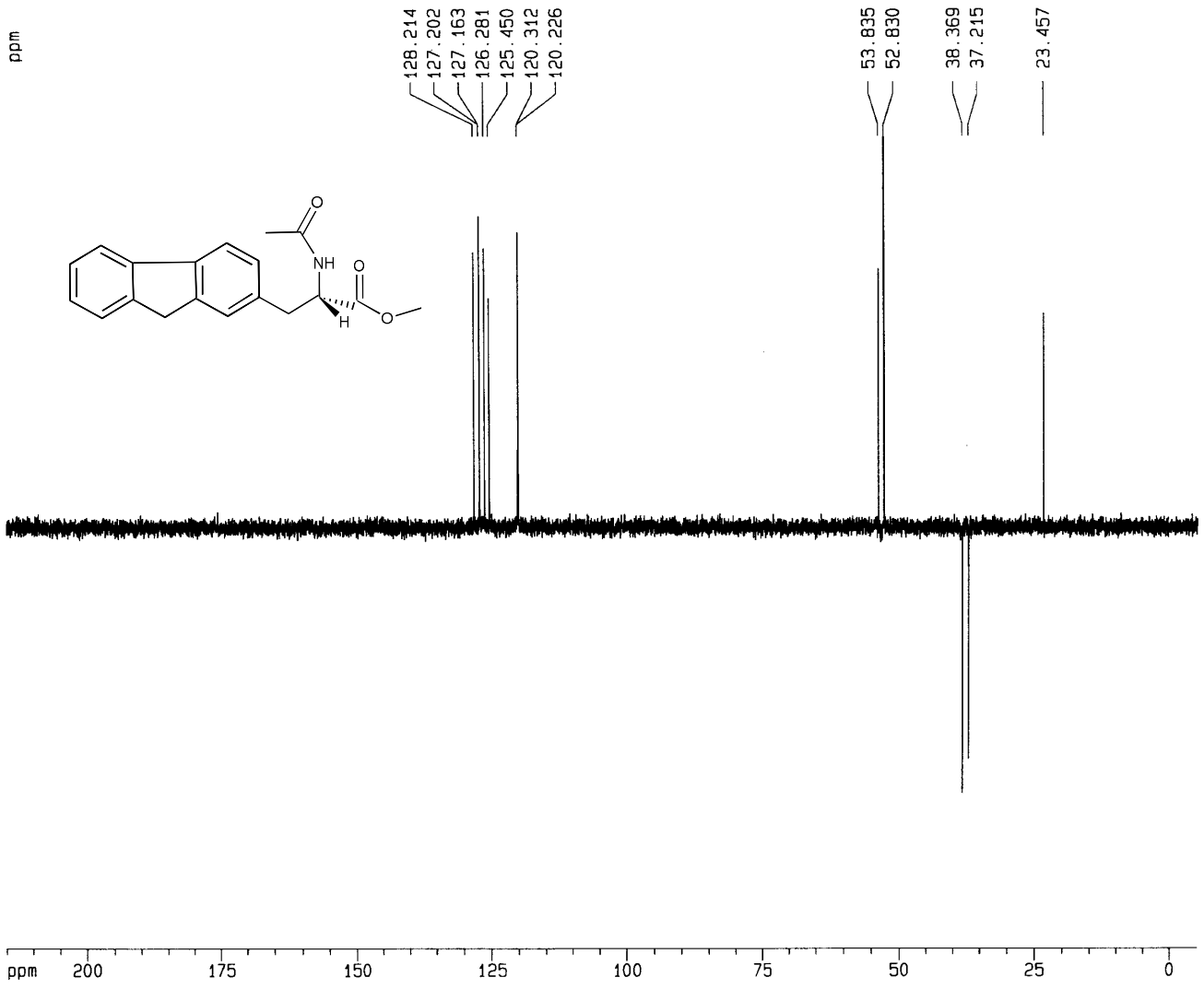

Current Data Parameters

NAME	DCF18
EXPNO	22
PROCNO	1

F2 - Acquisition Parameters

Date_	990125
Time	15.16
INSTRUM	spect
PROBHD	5 mm BBO BB-1
PULPROG	dept135
TD	65536
SOLVENT	CDCl3
NS	256
DS	4
SWH	31847.133 Hz
FIDRES	0.485949 Hz
AQ	1.0289652 sec
RG	16384
DW	15.700 usec
DE	6.00 usec
TE	300.0 K
P1	9.00 usec
p2	18.00 usec
P3	8.70 usec
p4	17.40 usec
CNST2	145.0000000
d2	0.00344828 sec
d12	0.00002000 sec
DELTA	0.00001146 sec
D1	2.00000000 sec
PL2	0.00 dB
SFO2	400.1316005 MHz
NUC2	1H
SFO1	100.6254358 MHz
NUC1	13C
PL1	-1.00 dB
PL12	20.00 dB
CPDPRG2	waltz16
PCPD2	80.00 usec

F2 - Processing parameters

SI	32768
SF	100.6127290 MHz
WDW	EM
SSB	0
LB	1.00 Hz
GB	0
PC	1.40

1D NMR plot parameters

CX	20.00 cm
F1P	215.000 ppm
F1	21631.74 Hz
F2P	-5.000 ppm
F2	-503.06 Hz
PPMCM	11.00000 ppm/cm
HZCM	1106.73999 Hz/cm

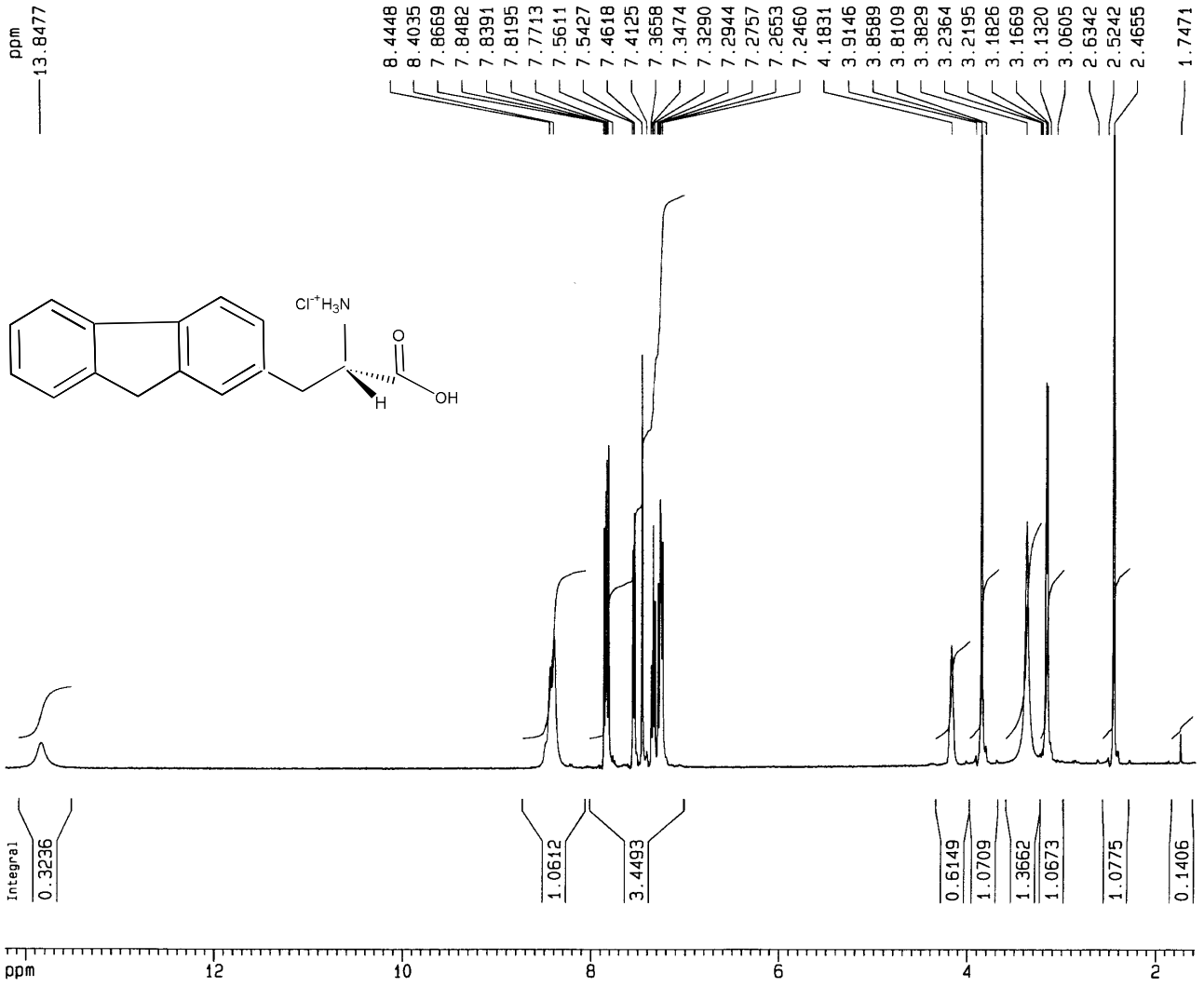

Current Data Parameters

NAME	DCF62
EXPNO	21
PROCNO	1

F2 - Acquisition Parameters

Date_	990414
Time	14.09
INSTRUM	spect
PROBHD	5 mm BBO BB-1
PULPROG	zg30
TD	32768
SOLVENT	DMSO
NS	16
DS	2
SWH	8223.685 Hz
FIDRES	0.250967 Hz
AQ	1.9923444 sec
RG	574.7
DW	60.800 usec
DE	6.00 usec
TE	300.0 K
D1	1.00000000 sec
P1	8.70 usec
SFO1	400.1324710 MHz
NUC1	1H
PL1	0.00 dB

F2 - Processing parameters

SI	16384
SF	400.1300167 MHz
WDW	EM
SSB	0
LB	0.50 Hz
GB	0
PC	1.00

1D NMR plot parameters

CX	20.00 cm
F1P	14.226 ppm
F1	5692.33 Hz
F2P	1.586 ppm
F2	634.77 Hz
PPMCM	0.63199 ppm/cm
HZCM	252.87828 Hz/cm

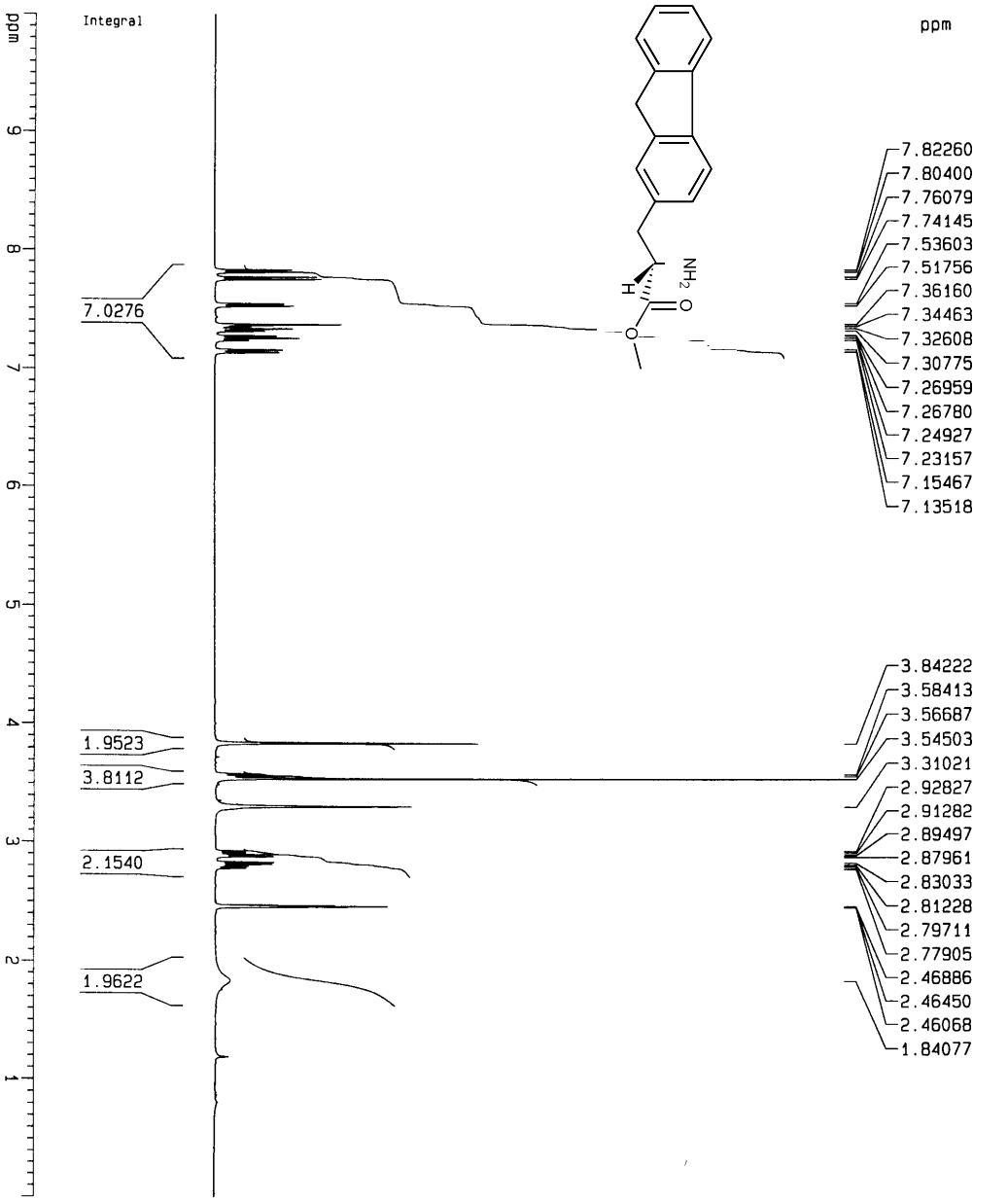

Current Data Parameters
NAME DCF73-proton
EXPNO 23
PROCNO 1

F2 - Acquisition Parameters
Date_ 990610
Time 17.34
INSTRUM spect
PROBHD 5 mm BBO BB-1
PULPROG zg30
TD 32768
SOLVENT DMSO
NS 16
DS 2
SWH 8223.685 Hz
FIDRES 0.250967 Hz
AQ 1.9923444 sec
RG 406.4
DW 60.800 usec
DE 6.00 usec
TE 300.0 K
D1 1.00000000 sec
P1 8.70 usec
SFO1 400.1324710 MHz
NUC1 1H
PL1 0.00 dB

F2 - Processing parameters
SI 16384
SF 400.1300167 MHz
WDW EM
SSB 0
LB 0.50 Hz
GB 0
PC 1.00

1D NMR plot parameters
CX 20.00 cm
F1P 10.000 ppm
F1 4001.30 Hz
F2P 0.000 ppm
F2 0.00 Hz
PPMCM 0.50000 ppm/cm
HZCM 200.06500 Hz/cm

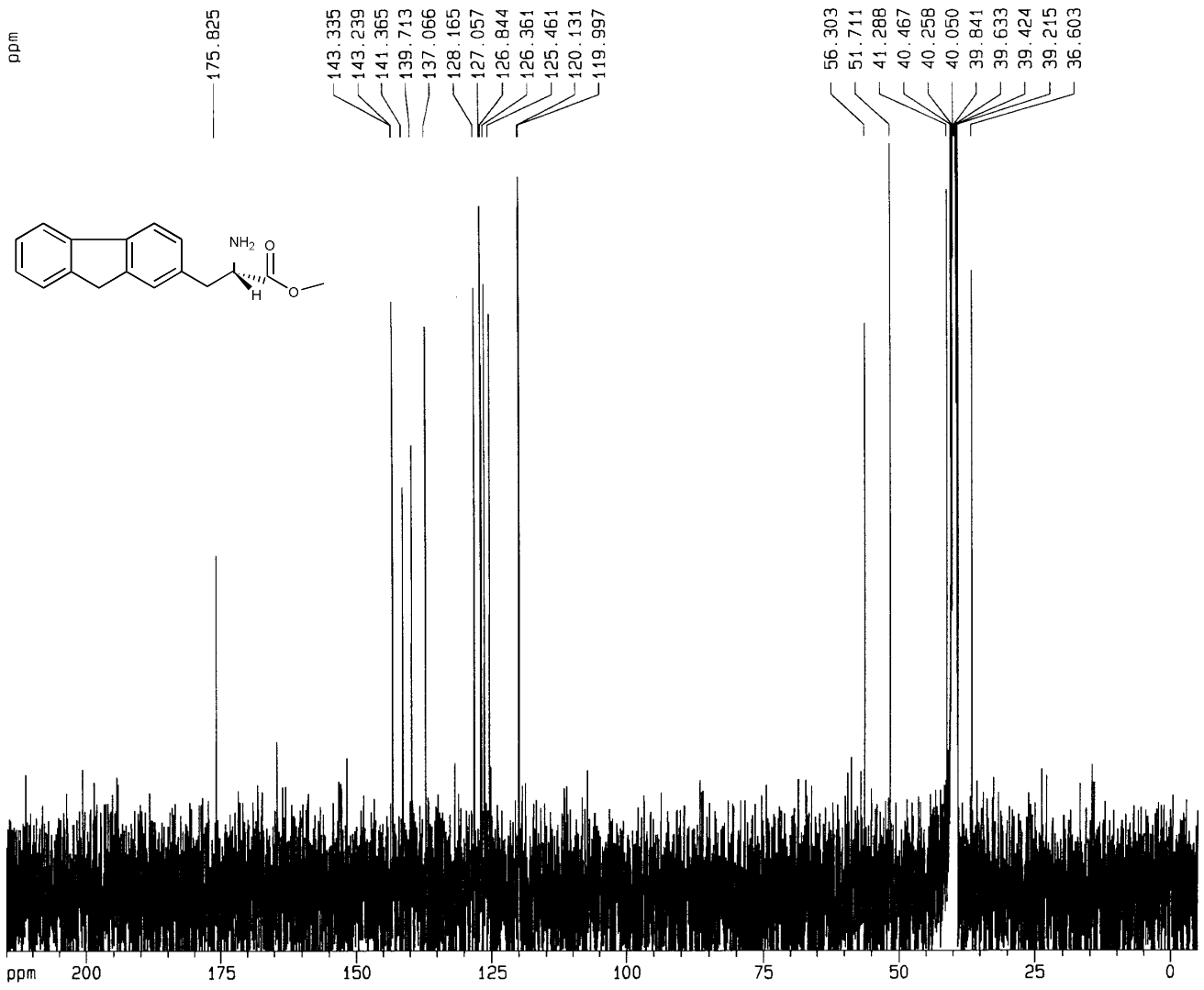

Current Data Parameters

NAME	DCF73
EXPNO	22
PROCNO	1

F2 - Acquisition Parameters

Date_	990609
Time	9.13
INSTRUM	spect
PROBHD	5 mm BBO BB-1
PULPROG	zgpg30
TD	65536
SOLVENT	DMSO
NS	512
DS	2
SWH	31847.133 Hz
FIDRES	0.485949 Hz
AQ	1.0289652 sec
RG	16384
DW	15.700 usec
DE	6.00 usec
TE	300.0 K
d11	0.03000000 sec
d12	0.00002000 sec
PL13	20.00 dB
D1	2.00000000 sec
CPDPRG2	waltz16
PCPD2	80.00 usec
SFO2	400.1316005 MHz
NUC2	1H
PL2	0.00 dB
PL12	20.00 dB
P1	9.00 usec
SFO1	100.6254358 MHz
NUC1	13C
PL1	-1.00 dB

F2 - Processing parameters

SI	32768
SF	100.6127793 MHz
WDW	EM
SSB	0
LB	1.00 Hz
GB	0
PC	1.40

1D NMR plot parameters

CX	20.00 cm
F1P	215.000 ppm
F1	21631.75 Hz
F2P	-5.000 ppm
F2	-503.06 Hz
PPMCM	11.00000 ppm/cm
HZCM	1106.74060 Hz/cm

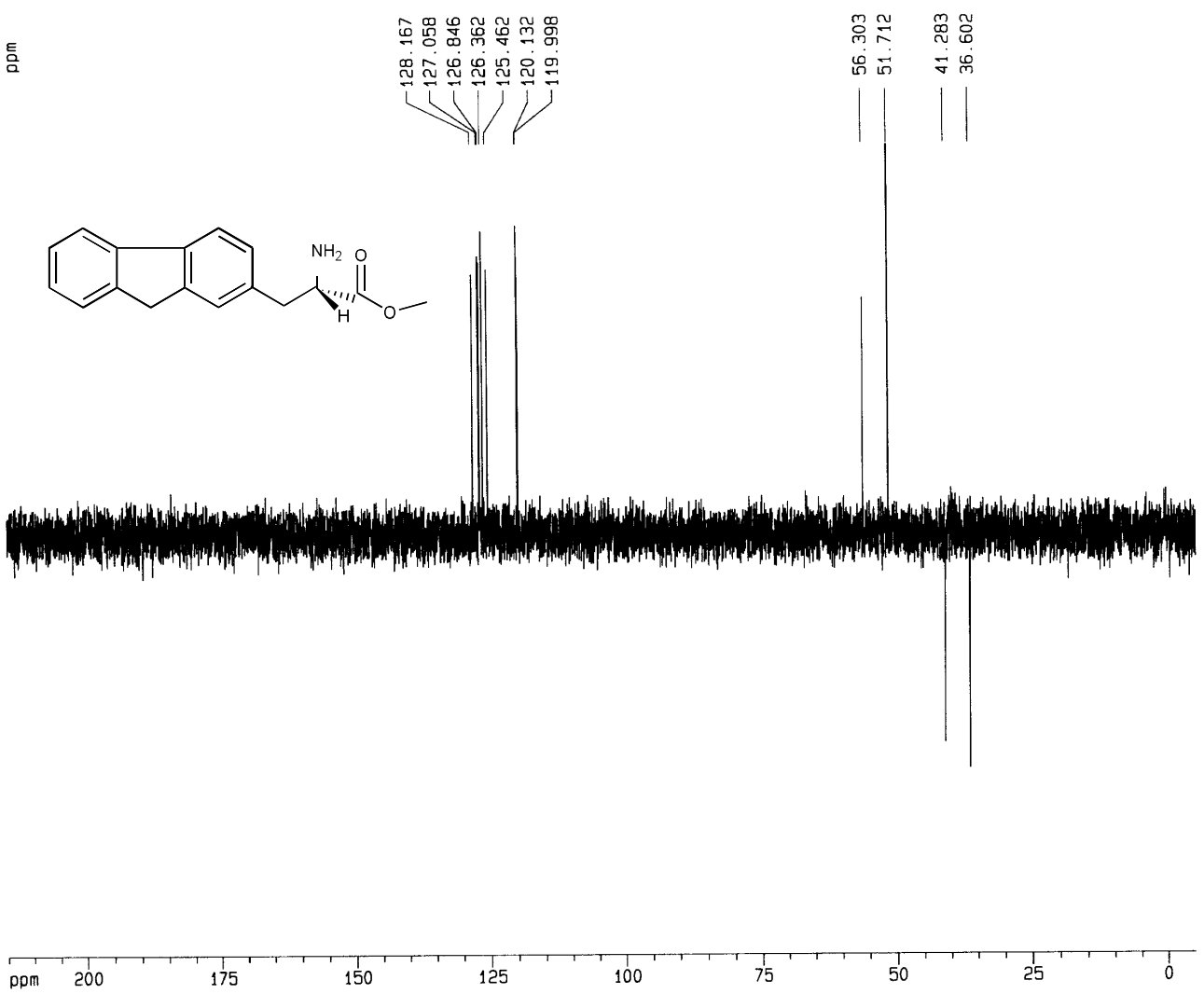

Current Data Parameters

NAME	DCF73
EXPNO	23
PROCNO	1

F2 - Acquisition Parameters

Date_	990609
Time	9.30
INSTRUM	spect
PROBHD	5 mm BBO BB-1
PULPROG	dept135
TD	65536
SOLVENT	DMSO
NS	256
DS	4
SWH	31847.133 Hz
FIDRES	0.485949 Hz
AQ	1.0289652 sec
RG	8192
DW	15.700 usec
DE	6.00 usec
TE	300.0 K
P1	9.00 usec
p2	18.00 usec
P3	8.70 usec
p4	17.40 usec
CNST2	145.0000000
d2	0.00344828 sec
d12	0.00002000 sec
DELTA	0.00001146 sec
D1	2.00000000 sec
PL2	0.00 dB
SFO2	400.1316005 MHz
NUC2	1H
SFO1	100.6254358 MHz
NUC1	13C
PL1	-1.00 dB
PL12	20.00 dB
CPDPRG2	waltz16
PCPD2	80.00 usec

F2 - Processing parameters

SI	32768
SF	100.6127793 MHz
WDW	EM
SSB	0
LB	1.00 Hz
GB	0
PC	1.40

1D NMR plot parameters

CX	20.00 cm
F1P	215.000 ppm
F1	21631.75 Hz
F2P	-5.000 ppm
F2	-503.06 Hz
PPMCM	11.00000 ppm/cm
HZCM	1106.74060 Hz/cm

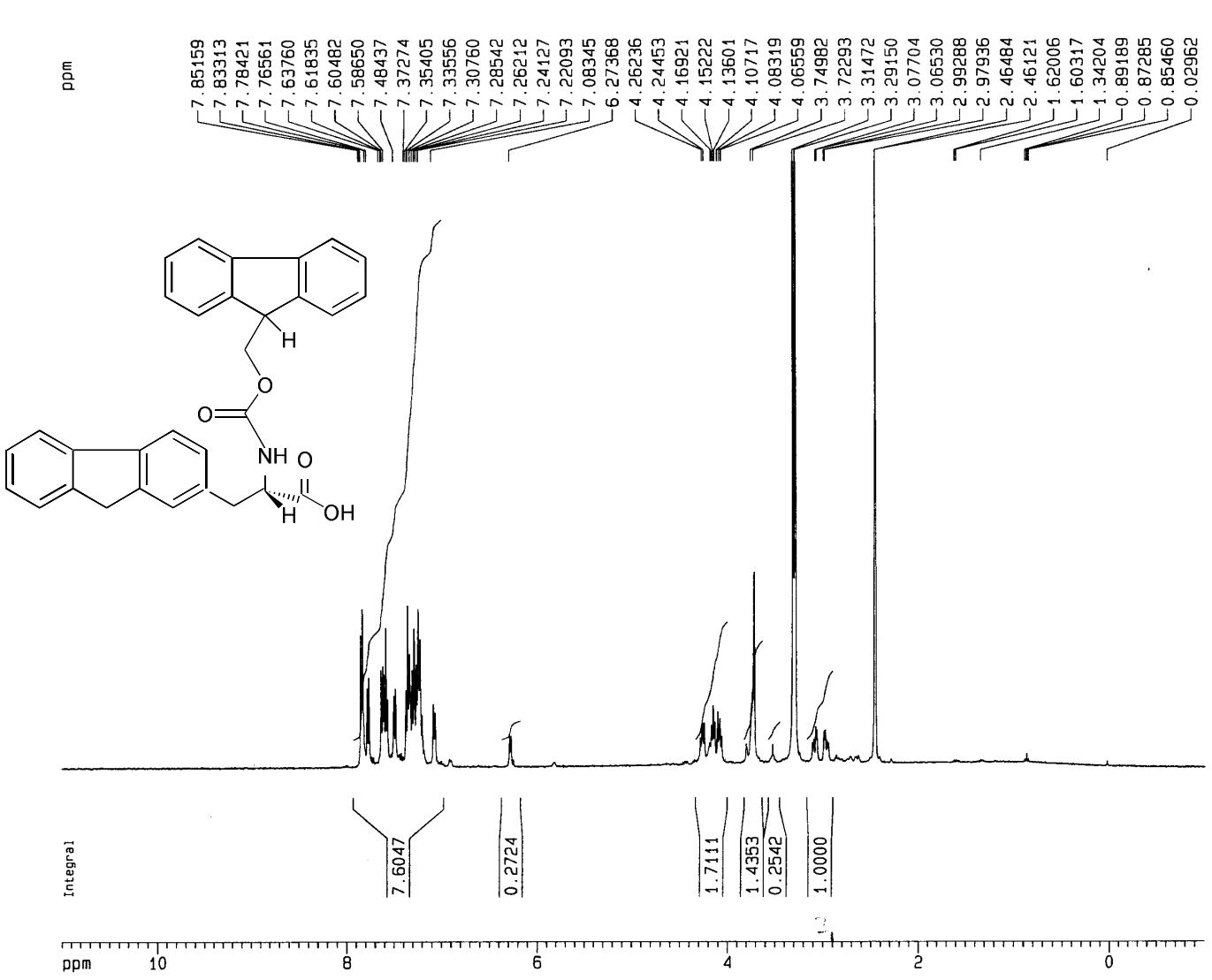

Current Data Parameters

NAME	DCF63-dry
EXPNO	21
PROCNO	1

F2 - Acquisition Parameters

Date_	990419
Time	15.43
INSTRUM	spect
PROBHD	5 mm BBO BB-1
PULPROG	zg30
TD	32768
SOLVENT	DMSO
NS	16
DS	2
SWH	8223.685 Hz
FIDRES	0.250967 Hz
AQ	1.9923444 sec
RG	512
DW	60.800 usec
DE	6.00 usec
TE	300.0 K
D1	1.00000000 sec
P1	8.70 usec
SFO1	400.1324710 MHz
NUC1	1H
PL1	0.00 dB

F2 - Processing parameters

SI	16384
SF	400.1300167 MHz
WDW	EM
SSB	0
LB	0.50 Hz
GB	0
PC	1.00

1D NMR plot parameters

CX	20.00 cm
F1P	11.000 ppm
F1	4401.43 Hz
F2P	-1.000 ppm
F2	-400.13 Hz
PPMCM	0.60000 ppm/cm
HZCM	240.07800 Hz/cm

Current Data Parameters

NAME	DCF70
EXPNO	21
PROCNO	1

F2 - Acquisition Parameters

Date_	990602
Time	8.30
INSTRUM	spect
PROBHD	5 mm BBO BB-1
PULPROG	zg30
TD	32768
SOLVENT	CDCl3
NS	16
DS	2
SWH	8223.685 Hz
FIDRES	0.250967 Hz
AQ	1.9923444 sec
RG	57
DW	60.800 usec
DE	6.00 usec
TE	300.0 K
D1	1.00000000 sec
P1	8.70 usec
SFO1	400.1324710 MHz
NUC1	1H
PL1	0.00 dB

F2 - Processing parameters

SI	16384
SF	400.1300167 MHz
WDW	EM
SSB	0
LB	0.50 Hz
GB	0
PC	1.00

1D NMR plot parameters

CX	20.00 cm
F1P	11.000 ppm
F1	4401.43 Hz
F2P	-1.000 ppm
F2	-400.13 Hz
PPMCM	0.60000 ppm/cm
HZCM	240.07800 Hz/cm

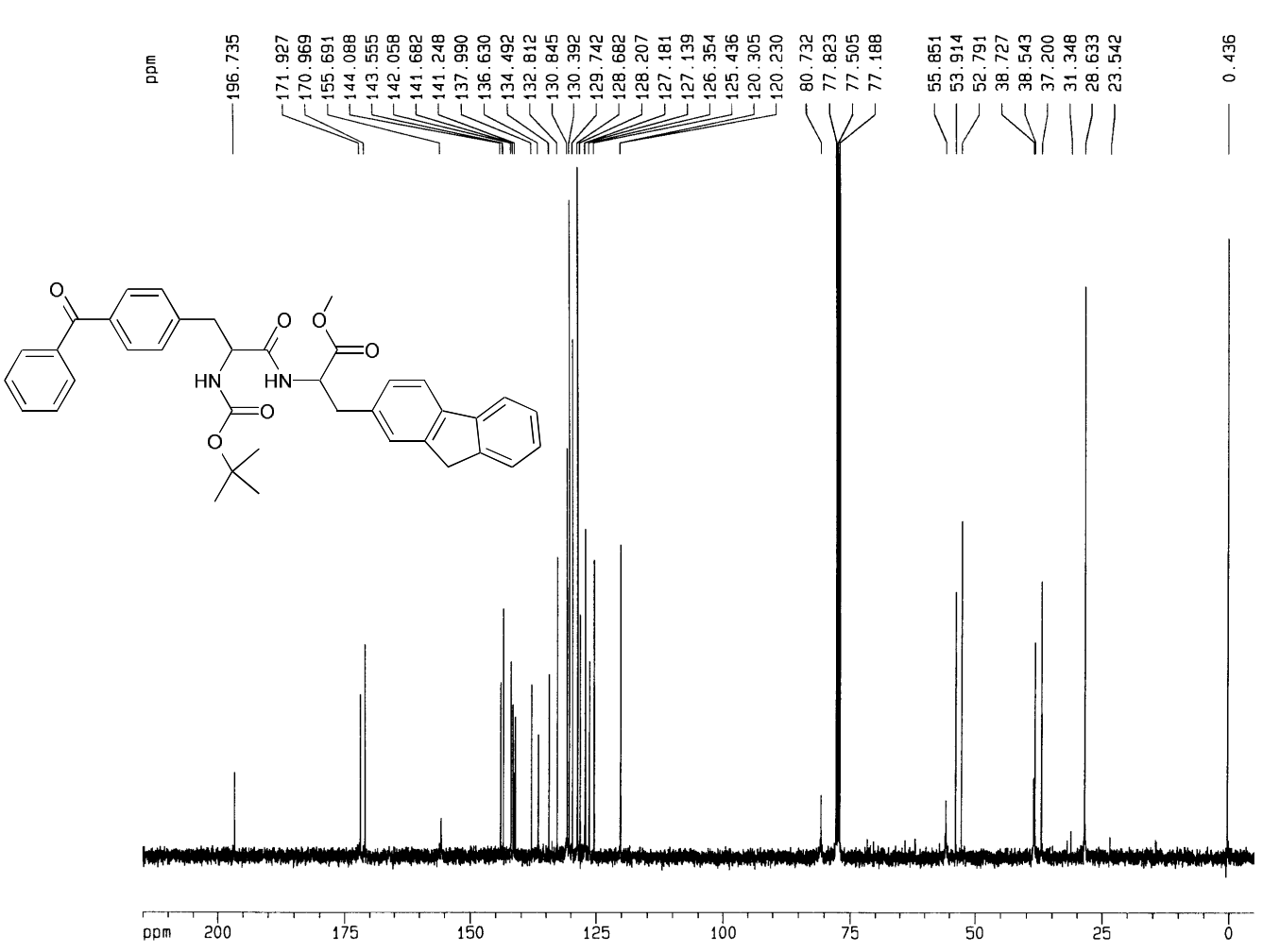


```
Current Data Parameters
NAME                  DCF70-c13
EXPNO                        21
PROCNO                        1

F2 - Acquisition Parameters
Date_                     990602
Time                       19.24
INSTRUM                    spect
PROBHD     5 mm BBO BB-1
PULPROG                  zgpg30
TD                        65536
SOLVENT                   CDCl3
NS                          512
DS                            2
SWH                  31647.133 Hz
FIDRES                0.485949 Hz
AQ                    1.0289652 sec
RG                        32768
DW                       15.700 usec
DE                        6.00 usec
TE                       300.0 K
d11                   0.03000000 sec
d12                   0.00002000 sec
PL13                     20.00 dB
D1                    2.00000000 sec
CPDPRG2                 waltz16
PCPD2                     80.00 usec
SFO2                400.1316005 MHz
NUC2                        1H
PL2                       0.00 dB
PL12                     20.00 dB
P1                        9.00 usec
SFO1                100.6254358 MHz
NUC1                        13C
PL1                      -1.00 dB

F2 - Processing parameters
SI                        32768
SF                  100.6127290 MHz
WDW                         EM
SSB                          0
LB                        1.00 Hz
GB                           0
PC                        1.40

1D NMR plot parameters
CX                       20.00 cm
F1P                     215.000 ppm
F1                    21631.74 Hz
F2P                      -5.000 ppm
F2                     -503.06 Hz
PPMCM                 11.00000 ppm/cm
HZCM                1106.73999 Hz/cm
```

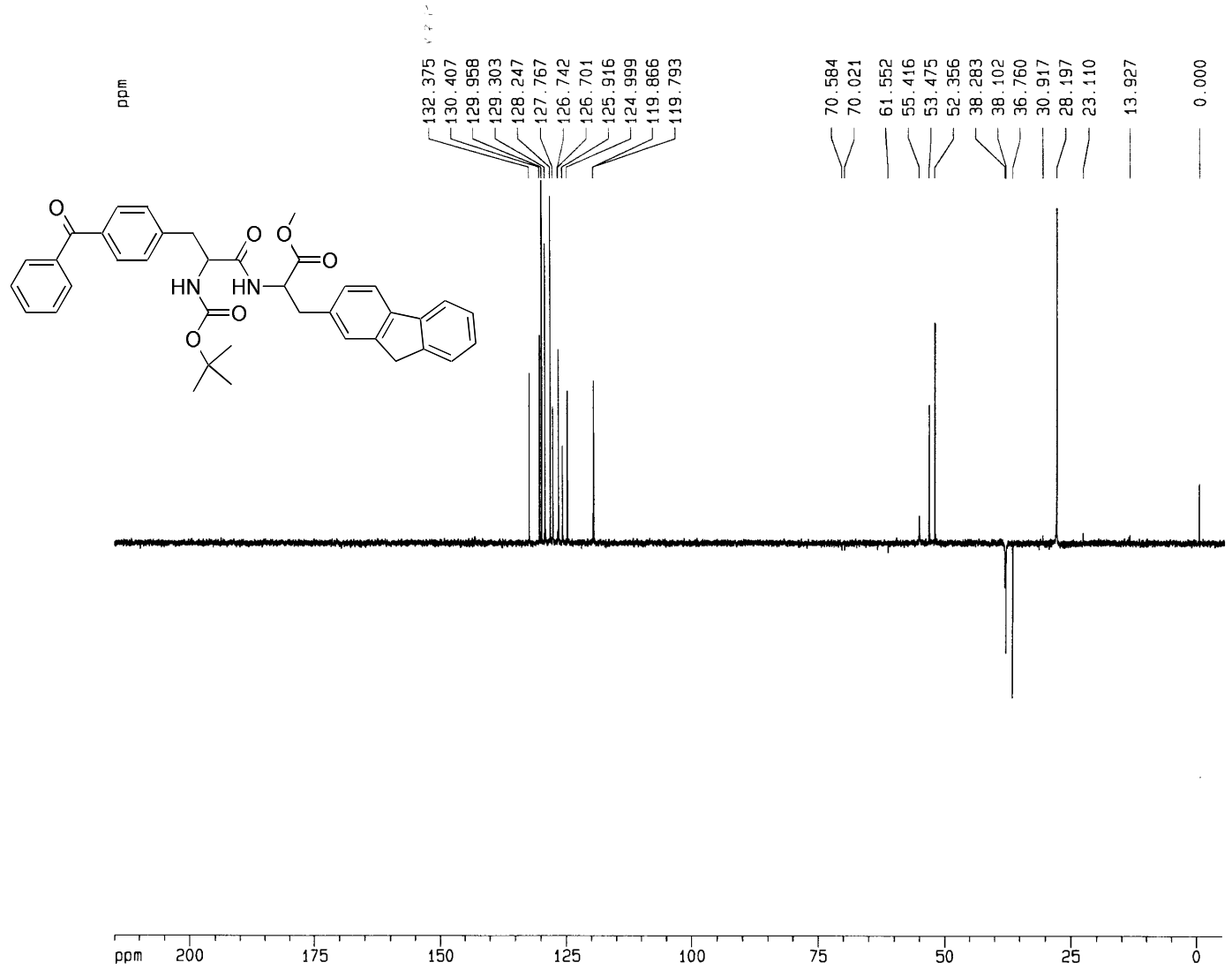

Current Data Parameters
NAME DCF70-dept135-4
EXPNO 21
PROCNO 1

F2 - Acquisition Parameters
Date_ 990603
Time 8.19
INSTRUM spect
PROBHD 5 mm BBO BB-1
PULPROG dept135
TD 65536
SOLVENT CDCl3
NS 256
DS 4
SWH 31847.133 Hz
FIDRES 0.485949 Hz
AQ 1.0289652 sec
RG 16384
DW 15.700 usec
DE 6.00 usec
TE 300.0 K
P1 9.00 usec
p2 18.00 usec
P3 8.70 usec
p4 17.40 usec
CNST2 145.0000000
d2 0.00344828 sec
d12 0.00002000 sec
DELTA 0.00001146 sec
D1 2.00000000 sec
PL2 0.00 dB
SFO2 400.1316005 MHz
NUC2 1H
SFO1 100.6254358 MHz
NUC1 13C
PL1 -1.00 dB
PL12 20.00 dB
CPDPRG2 waltz16
PCPD2 80.00 usec

F2 - Processing parameters
SI 32768
SF 100.6127713 MHz
WDW EM
SSB 0
LB 1.00 Hz
GB 0
PC 1.40

1D NMR plot parameters
CX 20.00 cm
F1P 215.000 ppm
F1 21631.75 Hz
F2P -5.000 ppm
F2 -503.06 Hz
PPMCM 11.00000 ppm/cm
HZCM 1106.74048 Hz/cm

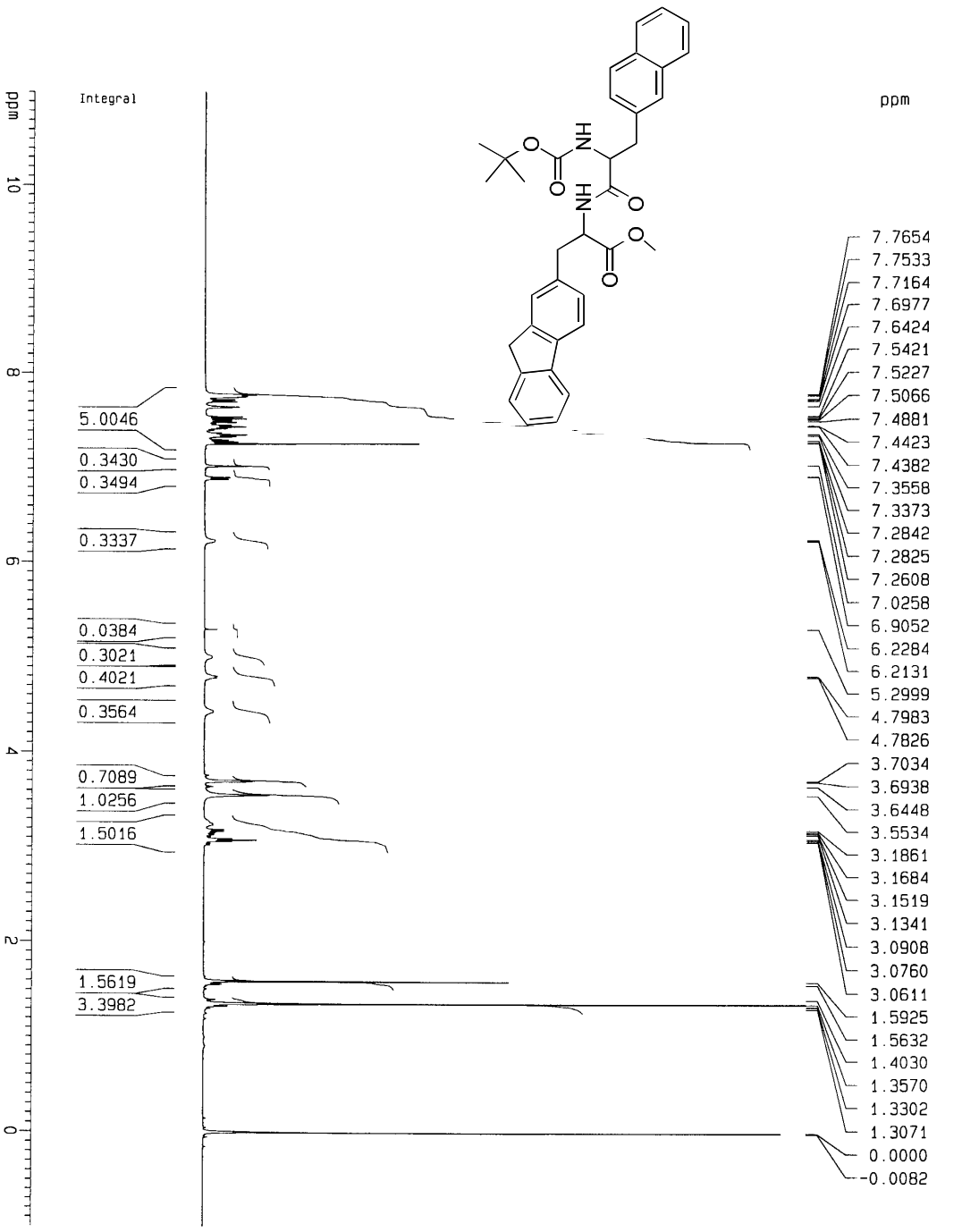

Current Data Parameters
NAME DCF74
EXPNO 32
PROCNO 1

F2 - Acquisition Parameters
Date_ 990729
Time 8.55
INSTRUM spect
PROBHD 5 mm BBO BB-1
PULPROG zg30
TD 32768
SOLVENT CDCl3
NS 16
DS 2
SWH 8223.685 Hz
FIDRES 0.250967 Hz
AQ 1.9923444 sec
RG 512
DW 60.800 usec
DE 6.00 usec
TE 300.0 K
D1 1.00000000 sec
P1 8.70 usec
SFO1 400.1324710 MHz
NUC1 1H
PL1 0.00 dB

F2 - Processing parameters
SI 16384
SF 400.1300089 MHz
WDW EM
SSB 0
LB 0.50 Hz
GB 0
PC 1.00

1D NMR plot parameters
CX 20.00 cm
F1P 11.000 ppm
F1 4401.43 Hz
F2P -1.000 ppm
F2 -400.13 Hz
PPMCM 0.60000 ppm/cm
HZCM 240.07800 Hz/cm

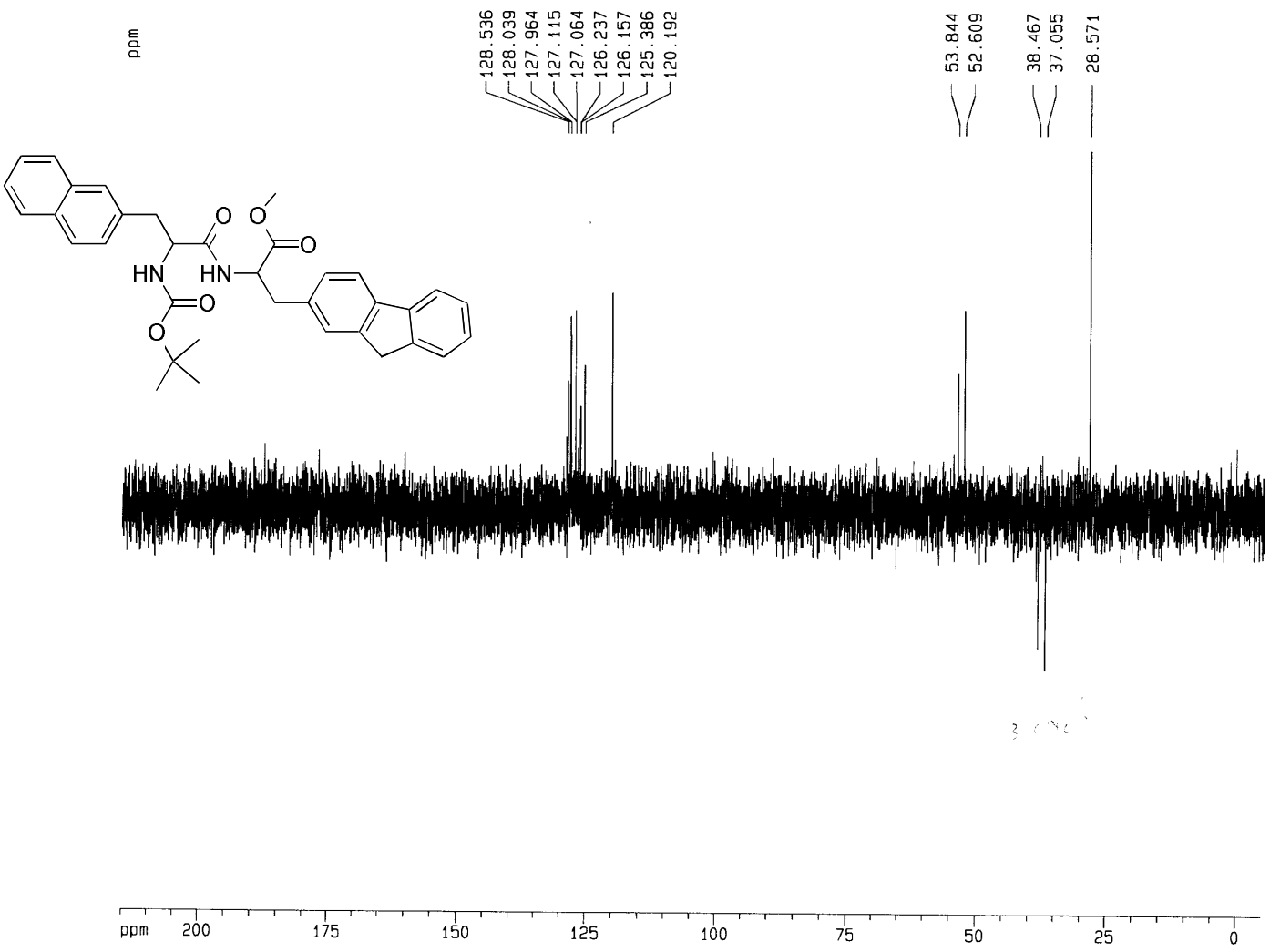

Current Data Parameters

NAME	DCF74
EXPNO	33
PROCNO	1

F2 - Acquisition Parameters

Date_	990729
Time	9.12
INSTRUM	spect
PROBHD	5 mm BBO BB-1
PULPROG	dept135
TD	65536
SOLVENT	CDCl3
NS	256
DS	4
SWH	31847.133 Hz
FIDRES	0.485949 Hz
AQ	1.0289652 sec
RG	8192
DW	15.700 usec
DE	6.00 usec
TE	300.0 K
P1	9.00 usec
p2	18.00 usec
P3	8.70 usec
p4	17.40 usec
CNST2	145.0000000
d2	0.00344828 sec
d12	0.00002000 sec
DELTA	0.00001146 sec
D1	2.00000000 sec
PL2	0.00 dB
SFO2	400.1316005 MHz
NUC2	1H
SFO1	100.6254358 MHz
NUC1	13C
PL1	-1.00 dB
PL12	20.00 dB
CPDPRG2	waltz16
PCPD2	80.00 usec

F2 - Processing parameters

SI	32768
SF	100.6127290 MHz
WDW	EM
SSB	0
LB	1.00 Hz
GB	0
PC	1.40

1D NMR plot parameters

CX	20.00 cm
F1P	215.000 ppm
F1	21631.74 Hz
F2P	-5.000 ppm
F2	-503.06 Hz
PPMCM	11.00000 ppm/cm
HZCM	1106.73999 Hz/cm